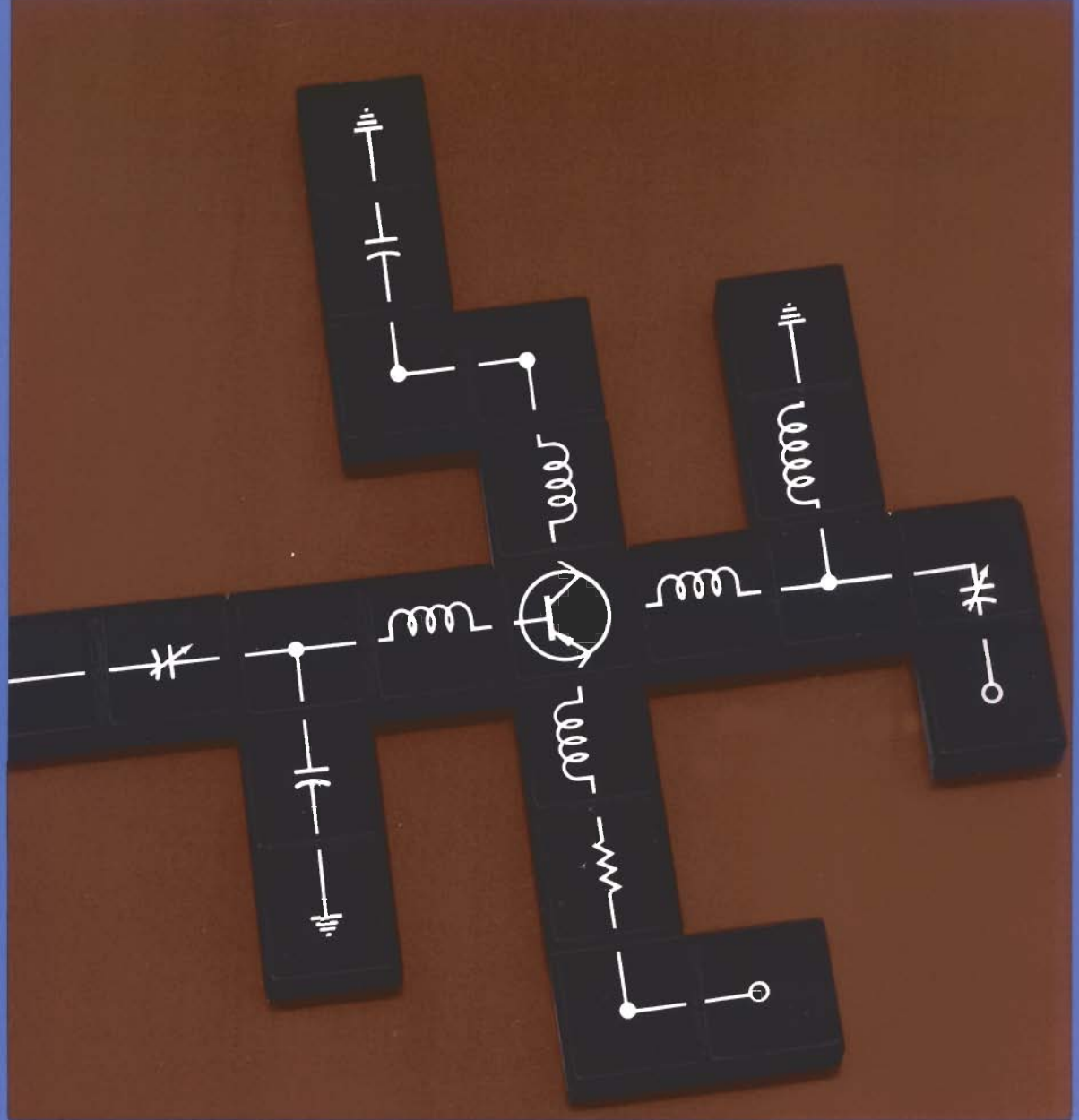




Newnes

RF Circuit Design

Chris Bowick



RF CIRCUIT DESIGN

Chris Bowick is presently employed as the Product Engineering Manager For Headend Products with Scientific Atlanta Video Communications Division located in Norcross, Georgia. His responsibilities include design and product development of satellite earth station receivers and headend equipment for use in the cable tv industry. Previously, he was associated with Rockwell International, Collins Avionics Division, where he was a design engineer on aircraft navigation equipment. His design experience also includes vhf receiver, hf synthesizer, and broadband amplifier design, and millimeter-wave radiometer design.

Mr. Bowick holds a BEE degree from Georgia Tech and, in his spare time, is working toward his MSEE at Georgia Tech, with emphasis on rf circuit design. He is the author of several articles in various hobby magazines. His hobbies include flying, ham radio (WB4UHY), and raquetball.

RF CIRCUIT DESIGN

by

Chris Bowick



Newnes is an imprint of Elsevier Science.

Copyright © 1982 by Chris Bowick

All rights reserved.

No part of this publication may be reproduced, stored in a retrieval system, or transmitted in any form or by any means, electronic, mechanical, photocopying, recording, or otherwise, without the prior written permission of the publisher.

Permissions may be sought directly from Elsevier's Science & Technology Rights Department in Oxford, UK: phone: (+44) 1865 843830, fax: (+44) 1865 853333, e-mail: permissions@elsevier.co.uk. You may also complete your request on-line via the Elsevier Science homepage (<http://www.elsevier.com>), by selecting 'Customer Support' and then 'Obtaining Permissions'.

- ∞ This book is printed on acid-free paper.

Library of Congress Cataloging-in-Publication Data

Bowick, Chris.

RF circuit design / by Chris Bowick

p. cm.

Originally published: Indianapolis : H.W. Sams, 1982

Includes bibliographical references and index.

ISBN 0-7506-9946-9 (pbk. : alk. paper)

1. Radio circuits Design and construction. 2. Radio Frequency.

I. Title.

TK6553.B633 1997

96-51612

621.384'12-dc20

CIP

The publisher offers special discounts on bulk orders of this book.

For information, please contact:

Manager of Special Sales

Elsevier Science

200 Wheeler Road

Burlington, MA 01803

Tel: 781-313-4700

Fax: 781-313-4802

For information on all Newnes publications available, contact our World Wide Web homepage at <http://www.newnespress.com>

15 14 13 12 11 10

Printed in the United States of America

PREFACE

RF Circuit Design is written for those who desire a practical approach to the design of rf amplifiers, impedance matching networks, and filters. It is totally *user oriented*. If you are an individual who has little rf circuit design experience, you can use this book as a catalog of circuits, using component values designed for your application. On the other hand, if you are interested in the theory behind the rf circuitry being designed, you can use the more detailed information that is provided for in-depth study.

An expert in the rf circuit design field will find this book to be an *excellent reference manual*, containing most of the commonly used circuit-design formulas that are needed. However, an electrical engineering student will find this book to be a valuable bridge between classroom studies and the real world. And, finally, if you are an experimenter or ham, who is interested in designing your own equipment, *RF Circuit Design* will provide numerous examples to guide you every step of the way.

Chapter 1 begins with some basics about components and how they behave at rf frequencies; how capacitors become inductors, inductors become capacitors, and wires become inductors, capacitors, and resistors. Toroids are introduced and toroidal inductor design is covered in detail.

Chapter 2 presents a review of resonant circuits and their properties including a discussion of Q, passband ripple, bandwidth, and coupling. You learn how to design single and multiresonator circuits, at the loaded Q you desire. An understanding of resonant circuits naturally leads to filters and their design. So, Chapter 3 presents complete design procedures for multiple-pole Butterworth, Chebyshev, and Bessel filters including low-pass, high-pass, bandpass, and bandstop designs. Within minutes after reading Chapter 3, you will be able to design multiple-pole filters to meet your specifications. Filter design was never easier.

Next, Chapter 4 covers impedance matching of both real and complex impedances. This is done both numerically and with the aid of the Smith Chart. Mathematics are kept to a bare minimum. Both high-Q and low-Q matching networks are covered in depth.

Transistor behavior at rf frequencies is discussed in Chapter 5. Input impedance, output impedance, feedback capacitance, and their variation over frequency are outlined. Transistor data sheets are explained in detail, and Y and S parameters are introduced.

Chapter 6 details complete cookbook design procedures for rf small-signal amplifiers, using both Y and S parameters. Transistor biasing, stability, impedance matching, and neutralization techniques are covered in detail, complete with practical examples. Constant-gain circles and stability circles, as plotted on a Smith Chart, are introduced while rf amplifier design procedures for minimum noise figure are also explained.

The subject of Chapter 7 is rf power amplifiers. This chapter describes the differences between small- and large-signal amplifiers, and provides step-by-step procedures for designing the latter. Design sections that discuss coaxial-feedline impedance matching and broadband transformers are included.

Appendix A is a math tutorial on complex number manipulation with emphasis on their relationship to complex impedances. This appendix is recommended reading for those who are not familiar with complex number arithmetic. Then, Appendix B presents a systems approach to low-noise design by examining the Noise Figure parameter and its relationship to circuit design and total systems design. Finally, in Appendix C, a bibliography of technical papers and books related to rf circuit design is given so that you, the reader, can further increase your understanding of rf design procedures.

CHRIS BOWICK

ACKNOWLEDGMENTS

The author wishes to gratefully acknowledge the contributions made by various individuals to the completion of this project. First, and foremost, a special thanks goes to my wife, Maureen, who not only typed the entire manuscript *at least* twice, but also performed duties both as an editor and as the author's principal source of encouragement throughout the project. Needless to say, without her help, this book would have never been completed.

Additional thanks go to the following individuals and companies for their contributions in the form of information and data sheets: Bill Amidon and Jim Cox of Amidon Associates, Dave Stewart of Piezo Technology, Irving Kadesh of Piconics, Brian Price of Indiana General, Richard Parker of Fair-Rite Products, Jack Goodman of Sprague-Goodman Electronics, Phillip Smith of Analog Instruments, Lothar Stern of Motorola, and Larry Ward of Microwave Associates.

To my wife, Maureen, and daughter, Zoe . . .

CONTENTS

CHAPTER 1

COMPONENTS	11
Wire — Resistors — Capacitors — Inductors — Toroids — Toroidal Inductor Design — Practical Winding Hints	

CHAPTER 2

RESONANT CIRCUITS	31
Some Definitions — Resonance (Lossless Components) — Loaded Q — Insertion Loss — Impedance Transformation — Coupling of Resonant Circuits	

CHAPTER 3

FILTER DESIGN	44
Background — Modern Filter Design — Normalization and the Low-Pass Prototype — Filter Types — Frequency and Impedance Scaling — High-Pass Filter Design — The Dual Network — Bandpass Filter Design — Summary of the Bandpass Filter Design Procedure — Band-Rejection Filter Design — The Effects of Finite Q	

CHAPTER 4

IMPEDANCE MATCHING	66
Background — The L Network — Dealing With Complex Loads — Three-Element Matching — Low-Q or Wideband Matching Networks — The Smith Chart — Impedance Matching on the Smith Chart — Summary	

CHAPTER 5

THE TRANSISTOR AT RADIO FREQUENCIES	98
The Transistor Equivalent Circuit — Y Parameters — S Parameters — Understanding Rf Transistor Data Sheets — Summary	

CHAPTER 6

SMALL-SIGNAL RF AMPLIFIER DESIGN	117
Transistor Biasing — Design Using Y Parameters — Design Using S Parameters	

CHAPTER 7

RF POWER AMPLIFIERS	150
Rf Power Transistor Characteristics — Transistor Biasing — Power Amplifier Design — Matching to Coaxial Feedlines — Automatic Shutdown Circuitry — Broadband Transformers — Practical Winding Hints — Summary	

APPENDIX A

VECTOR ALGEBRA	164
--------------------------	-----

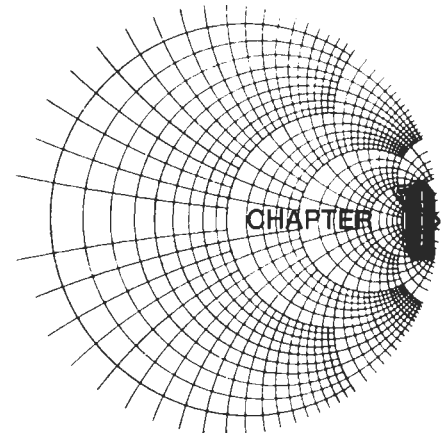
APPENDIX B

NOISE CALCULATIONS	167
Types of Noise — Noise Figure — Receiver Systems Calculations	

APPENDIX C

BIBLIOGRAPHY	170
Technical Papers — Books	

INDEX	172
-----------------	-----



COMPONENTS

Components, those bits and pieces which make up a radio frequency (rf) circuit, seem at times to be taken for granted. A capacitor is, after all, a capacitor—isn't it? A 1-megohm resistor presents an impedance of at least 1 megohm—doesn't it? The reactance of an inductor always increases with frequency, right? Well, as we shall see later in this discussion, things aren't always as they seem. Capacitors at certain frequencies may not be capacitors at all, but may look inductive, while inductors may look like capacitors, and resistors may tend to be a little of both.

In this chapter, we will discuss the properties of resistors, capacitors, and inductors at radio frequencies as they relate to circuit design. But, first, let's take a look at the most simple component of any system and examine its problems at radio frequencies.

WIRE

Wire in an rf circuit can take many forms. Wire-wound resistors, inductors, and axial- and radial-leaded capacitors all use a wire of some size and length either in their leads, or in the actual body of the component, or both. Wire is also used in many interconnect applications in the lower rf spectrum. The behavior of a wire in the rf spectrum depends to a large extent on the wire's diameter and length. Table 1-1 lists, in the American Wire Gauge (AWG) system, each gauge of wire, its corresponding diameter, and other characteristics of interest to the rf circuit designer. In the AWG system, the diameter of a wire will roughly double every six wire gauges. Thus, if the last six

gauges and their corresponding diameters are memorized from the chart, all other wire diameters can be determined without the aid of a chart (Example 1-1).

Skin Effect

A conductor, at low frequencies, utilizes its entire cross-sectional area as a transport medium for charge carriers. As the frequency is increased, an increased magnetic field at the center of the conductor presents an impedance to the charge carriers, thus decreasing the current density at the center of the conductor and increasing the current density around its perimeter. This increased current density near the edge of the conductor is known as *skin effect*. It occurs in all conductors including resistor leads, capacitor leads, and inductor leads.

The depth into the conductor at which the charge-carrier current density falls to $1/e$, or 37% of its value along the surface, is known as the *skin depth* and is a function of the frequency and the permeability and conductivity of the medium. Thus, different conductors, such as silver, aluminum, and copper, all have different skin depths.

The net result of skin effect is an effective decrease in the cross-sectional area of the conductor and, therefore, a net increase in the ac resistance of the wire as shown in Fig. 1-1. For copper, the skin depth is approximately 0.85 cm at 60 Hz and 0.007 cm at 1 MHz. Or, to state it another way: 63% of the rf current flowing in a copper wire will flow within a distance of 0.007 cm of the outer edge of the wire.

Straight-Wire Inductors

In the medium surrounding any current-carrying conductor, there exists a magnetic field. If the current in the conductor is an alternating current, this magnetic field is alternately expanding and contracting and, thus, producing a voltage on the wire which opposes any change in current flow. This opposition to change is called *self-inductance* and we call anything that possesses this quality an *inductor*. Straight-wire inductance might seem trivial, but as will be seen later in the chapter, the higher we go in frequency, the more important it becomes.

The inductance of a straight wire depends on both its length and its diameter, and is found by:

EXAMPLE 1-1

Given that the diameter of AWG 50 wire is 1.0 mil (0.001 inch), what is the diameter of AWG 14 wire?

Solution

$$\begin{aligned}
 \text{AWG 50} &= 1 \text{ mil} \\
 \text{AWG 44} &= 2 \times 1 \text{ mil} = 2 \text{ mils} \\
 \text{AWG 38} &= 2 \times 2 \text{ mils} = 4 \text{ mils} \\
 \text{AWG 32} &= 2 \times 4 \text{ mils} = 8 \text{ mils} \\
 \text{AWG 26} &= 2 \times 8 \text{ mils} = 16 \text{ mils} \\
 \text{AWG 20} &= 2 \times 16 \text{ mils} = 32 \text{ mils} \\
 \text{AWG 14} &= 2 \times 32 \text{ mils} = 64 \text{ mils (0.064 inch)}
 \end{aligned}$$

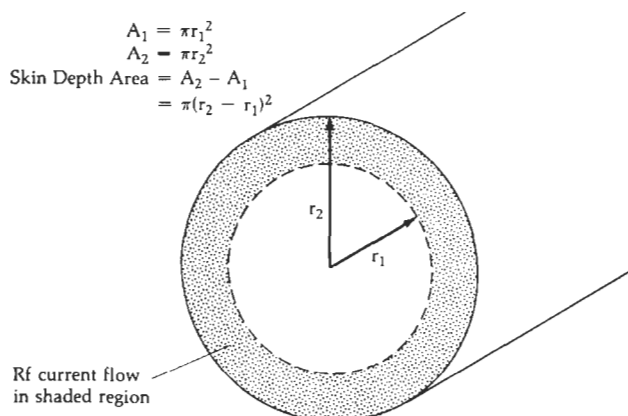


Fig. 1-1. Skin depth area of a conductor.

$$L = 0.002l \left[2.3 \log \left(\frac{4l}{d} - 0.75 \right) \right] \mu\text{H} \quad (\text{Eq. 1-1})$$

where,

- L = the inductance in μH ,
- l = the length of the wire in cm,
- d = the diameter of the wire in cm.

This is shown in calculations of Example 1-2.

EXAMPLE 1-2

Find the inductance of 5 centimeters of No. 22 copper wire.

Solution

From Table 1-1, the diameter of No. 22 copper wire is 25.3 mils. Since 1 mil equals 2.54×10^{-3} cm, this equals 0.0643 cm. Substituting into Equation 1-1 gives

$$L = (0.002)(5) \left[2.3 \log \left(\frac{4(5)}{0.0643} - 0.75 \right) \right] \\ = 57 \text{ nanohenries}$$

The concept of inductance is important because any and all conductors at radio frequencies (including hookup wire, capacitor leads, etc.) tend to exhibit the property of inductance. Inductors will be discussed in greater detail later in this chapter.

RESISTORS

Resistance is the property of a material that determines the rate at which electrical energy is converted into heat energy for a given electric current. By definition:

$$1 \text{ volt across } 1 \text{ ohm} = 1 \text{ coulomb per second} \\ = 1 \text{ ampere}$$

The thermal dissipation in this circumstance is 1 watt.

$$P = EI \\ = 1 \text{ volt} \times 1 \text{ ampere} \\ = 1 \text{ watt}$$

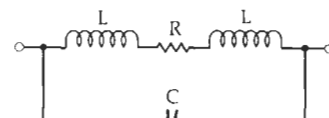


Fig. 1-2. Resistor equivalent circuit.

Resistors are used everywhere in circuits, as transistor bias networks, pads, and signal combiners. However, very rarely is there any thought given to how a resistor actually behaves once we depart from the world of direct current (dc). In some instances, such as in transistor biasing networks, the resistor will still perform its dc circuit function, but it may also disrupt the circuit's rf operating point.

Resistor Equivalent Circuit

The equivalent circuit of a resistor at radio frequencies is shown in Fig. 1-2. R is the resistor value itself, L is the lead inductance, and C is a combination of parasitic capacitances which varies from resistor to resistor depending on the resistor's structure. Carbon-composition resistors are notoriously poor high-frequency performers. A carbon-composition resistor consists of densely packed dielectric particulates or carbon granules. Between each pair of carbon granules is a very small parasitic capacitor. These parasitics, in aggregate, are not insignificant, however, and are the major component of the device's equivalent circuit.

Wirewound resistors have problems at radio frequencies too. As may be expected, these resistors tend to exhibit widely varying impedances over various frequencies. This is particularly true of the low resistance values in the frequency range of 10 MHz to 200 MHz. The inductor L, shown in the equivalent circuit of Fig. 1-2, is much larger for a wirewound resistor than for a carbon-composition resistor. Its value can be calculated using the single-layer air-core inductance approximation formula. This formula is discussed later in this chapter. Because wirewound resistors look like inductors, their impedances will first increase as the frequency increases. At some frequency (F_r), however, the inductance (L) will resonate with the shunt capaci-

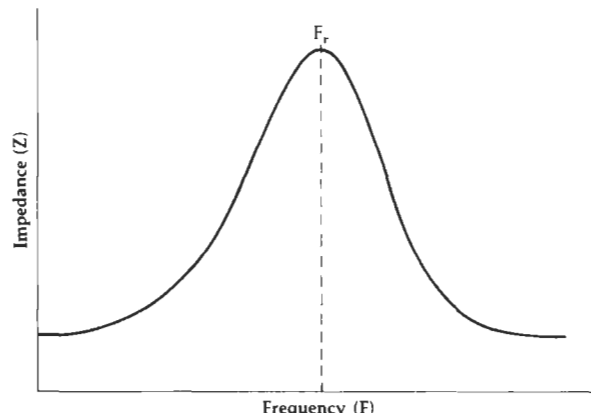


Fig. 1-3. Impedance characteristic of a wirewound resistor.

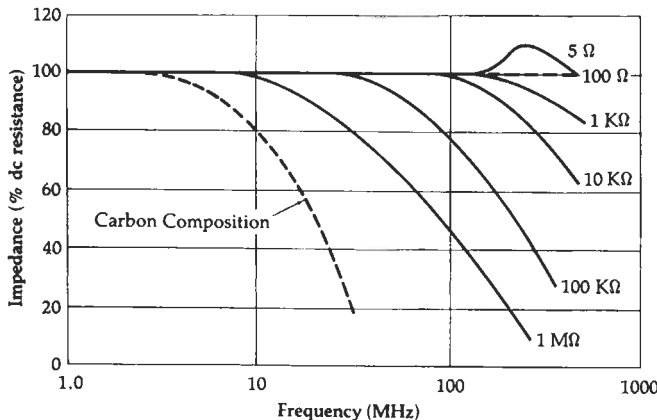


Fig. 1-4. Frequency characteristics of metal-film vs. carbon-composition resistors. (Adapted from *Handbook of Components for Electronics*, McGraw-Hill.)

tance (C), producing an impedance peak. Any further increase in frequency will cause the resistor's impedance to decrease as shown in Fig. 1-3.

A metal-film resistor seems to exhibit the best characteristics over frequency. Its equivalent circuit is the same as the carbon-composition and wirewound resistor, but the values of the individual parasitic elements in the equivalent circuit decrease.

The impedance of a metal-film resistor tends to decrease with frequency above about 10 MHz, as shown in Fig. 1-4. This is due to the shunt capacitance in the equivalent circuit. At very high frequencies, and with low-value resistors (under 50 ohms), lead inductance and skin effect may become noticeable. The lead in-

EXAMPLE 1-3

In Fig. 1-2, the lead lengths on the metal-film resistor are 1.27 cm (0.5 inch), and are made up of No. 14 wire. The total stray shunt capacitance (C) is 0.3 pF. If the resistor value is 10,000 ohms, what is its equivalent rf impedance at 200 MHz?

Solution

From Table 1-1, the diameter of No. 14 AWG wire is 64.1 mils (0.1628 cm). Therefore, using Equation 1-1:

$$L = 0.002(1.27) \left[2.3 \log \left(\frac{4(1.27)}{0.1628} - 0.75 \right) \right]$$

$$= 8.7 \text{ nanohenries}$$

This presents an equivalent reactance at 200 MHz of:

$$\begin{aligned} X_L &= \omega L \\ &= 2\pi(200 \times 10^6)(8.7 \times 10^{-9}) \\ &= 10.93 \text{ ohms} \end{aligned}$$

The capacitor (C) presents an equivalent reactance of:

$$\begin{aligned} X_C &= \frac{1}{\omega C} \\ &= \frac{1}{2\pi(200 \times 10^6)(0.3 \times 10^{-12})} \\ &= 2653 \text{ ohms} \end{aligned}$$

ductance produces a resonance peak, as shown for the 5-ohm resistance in Fig. 1-4, and skin effect decreases the slope of the curve as it falls off with frequency.

Many manufacturers will supply data on resistor behavior at radio frequencies but it can often be misleading. Once you understand the mechanisms involved in resistor behavior, however, it will not matter in what form the data is supplied. Example 1-3 illustrates that fact.

The recent trend in resistor technology has been to eliminate or greatly reduce the stray reactances associated with resistors. This has led to the development of thin-film chip resistors, such as those shown in Fig. 1-6. They are typically produced on alumina or beryllia substrates and offer very little parasitic reactance at frequencies from dc to 2 GHz.

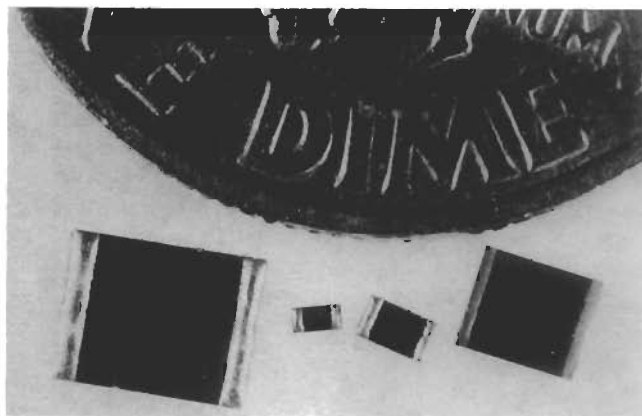


Fig. 1-6. Thin-film chip resistors. (Courtesy Piconics, Inc.)

The combined equivalent circuit for this resistor, at 200 MHz, is shown in Fig. 1-5. From this sketch, we can see that, in this case, the lead inductance is insignificant when compared with the 10K series resistance and it may be

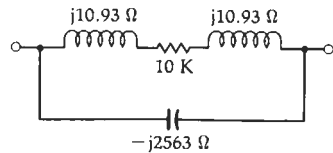


Fig. 1-5. Equivalent circuit values for Example 1-3.

neglected. The parasitic capacitance, on the other hand, cannot be neglected. What we now have, in effect, is a 2563-ohm reactance in parallel with a 10,000-ohm resistance. The magnitude of the combined impedance is:

$$\begin{aligned} Z &= \frac{RX_c}{\sqrt{R^2 + X_c^2}} \\ &= \frac{(10K)(2563)}{\sqrt{(10K)^2 + (2563)^2}} \\ &= 1890.5 \text{ ohms} \end{aligned}$$

Thus, our 10K resistor looks like 1890 ohms at 200 MHz.

CAPACITORS

Capacitors are used extensively in rf applications, such as bypassing, interstage coupling, and in resonant circuits and filters. It is important to remember, however, that not all capacitors lend themselves equally well to each of the above mentioned applications. The primary task of the rf circuit designer, with regard to capacitors, is to choose the best capacitor for his particular application. Cost effectiveness is usually a major factor in the selection process and, thus, many trade-offs occur. In this section, we'll take a look at the capacitor's equivalent circuit and we will examine a few of the various types of capacitors used at radio frequencies to see which are best suited for certain applications. But first, a little review.

Parallel-Plate Capacitor

A capacitor is any device which consists of two conducting surfaces separated by an insulating material or dielectric. The dielectric is usually ceramic, air, paper, mica, plastic, film, glass, or oil. The capacitance of a capacitor is that property which permits the storage of a charge when a potential difference exists between the conductors. Capacitance is measured in units of farads. A 1-farad capacitor's potential is raised by 1 volt when it receives a charge of 1 coulomb.

$$C = \frac{Q}{V}$$

where,

C = capacitance in farads,

Q = charge in coulombs,

V = voltage in volts.

However, the farad is much too impractical to work with, so smaller units were devised.

$$1 \text{ microfarad} = 1 \mu\text{F} = 1 \times 10^{-6} \text{ farad}$$

$$1 \text{ picofarad} = 1 \text{ pF} = 1 \times 10^{-12} \text{ farad}$$

As stated previously, a capacitor in its fundamental form consists of two metal plates separated by a dielectric material of some sort. If we know the area (A) of each metal plate, the distance (d) between the plate (in inches), and the permittivity (ϵ) of the dielectric material in farads/meter (f/m), the capacitance of a parallel-plate capacitor can be found by:

$$C = \frac{0.2249\epsilon A}{d\epsilon_0} \text{ picofarads} \quad (\text{Eq. 1-2})$$

where,

$$\epsilon_0 = \text{free-space permittivity} = 8.854 \times 10^{-12} \text{ f/m.}$$

In Equation 1-2, the area (A) must be large with respect to the distance (d). The ratio of ϵ to ϵ_0 is known as the dielectric constant (k) of the material. The dielectric constant is a number which provides a comparison of the given dielectric with air (see Fig. 1-7). The ratio of ϵ/ϵ_0 for air is, of course, 1. If the dielectric constant of a material is greater than 1, its use in a capacitor as a dielectric will permit a greater amount

Dielectric	K
Air	1
Polystyrene	2.5
Paper	4
Mica	5
Ceramic (low K)	10
Ceramic (high K)	100-10,000

Fig. 1-7. Dielectric constants of some common materials.

of capacitance for the same dielectric thickness as air. Thus, if a material's dielectric constant is 3, it will produce a capacitor having three times the capacitance of one that has air as its dielectric. For a given value of capacitance, then, higher dielectric-constant materials will produce physically smaller capacitors. But, because the dielectric plays such a major role in determining the capacitance of a capacitor, it follows that the influence of a dielectric on capacitor operation, over frequency and temperature, is often important.

Real-World Capacitors

The usage of a capacitor is primarily dependent upon the characteristics of its dielectric. The dielectric's characteristics also determine the voltage levels and the temperature extremes at which the device may be used. Thus, any losses or imperfections in the dielectric have an enormous effect on circuit operation.

The equivalent circuit of a capacitor is shown in Fig. 1-8, where C equals the capacitance, R_s is the heat-dissipation loss expressed either as a power factor (PF) or as a dissipation factor (DF), R_p is the insulation resistance, and L is the inductance of the leads and plates. Some definitions are needed now.

Power Factor—In a perfect capacitor, the alternating current will lead the applied voltage by 90° . This phase angle (ϕ) will be smaller in a real capacitor due to the total series resistance ($R_s + R_p$) that is shown in the equivalent circuit. Thus,

$$\text{PF} = \cos \phi$$

The power factor is a function of temperature, frequency, and the dielectric material.

Insulation Resistance—This is a measure of the amount of dc current that flows through the dielectric of a capacitor with a voltage applied. No material is a perfect insulator; thus, some leakage current must flow. This current path is represented by R_p in the equivalent circuit and, typically, it has a value of 100,000 megohms or more.

Effective Series Resistance—Abbreviated ESR, this resistance is the combined equivalent of R_s and R_p , and is the ac resistance of a capacitor.

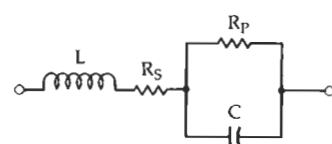


Fig. 1-8. Capacitor equivalent circuit.

$$ESR = \frac{PF}{\omega C} (1 \times 10^6)$$

where,

$$\omega = 2\pi f$$

Dissipation Factor—The DF is the ratio of ac resistance to the reactance of a capacitor and is given by the formula:

$$DF = \frac{ESR}{X_c} \times 100\%$$

Q—The Q of a circuit is the reciprocal of DF and is defined as the quality factor of a capacitor.

$$Q = \frac{1}{DF} = \frac{X_c}{ESR}$$

Thus, the larger the Q, the better the capacitor.

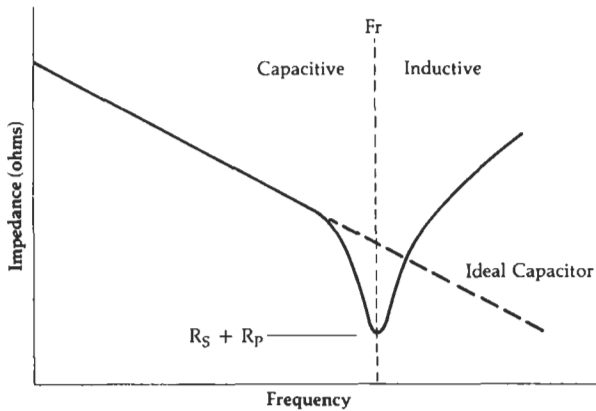


Fig. 1-9. Impedance characteristic vs. frequency.

The effect of these imperfections in the capacitor can be seen in the graph of Fig. 1-9. Here, the impedance characteristic of an ideal capacitor is plotted against that of a real-world capacitor. As shown, as the frequency of operation increases, the lead inductance becomes important. Finally, at F_r , the inductance becomes series resonant with the capacitor. Then, above F_r , the capacitor acts like an inductor. In general, larger-value capacitors tend to exhibit more internal inductance than smaller-value capacitors. Therefore, depending upon its internal structure, a 0.1- μ F capacitor may not be as good as a 330-pF capacitor in a bypass application at 250 MHz. In other words, the classic formula for capacitive reactance, $X_c = \frac{1}{\omega C}$, might seem to indicate that larger-value capacitors have less reactance than smaller-value capacitors at a given frequency. At rf frequencies, however, the opposite may be true. At certain higher frequencies, a 0.1- μ F capacitor might present a higher impedance to the signal than would a 330-pF capacitor. This is something that must be considered when designing circuits at frequencies above 100 MHz. Ideally, each component that is to be used in any vhf,

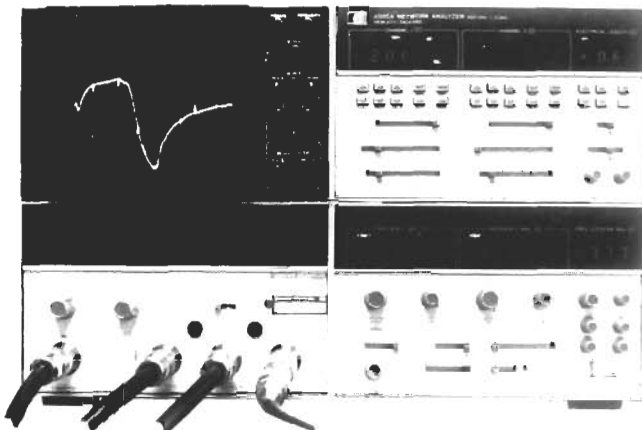


Fig. 1-10. Hewlett-Packard 8505A Network Analyzer.

or higher frequency, design should be examined on a network analyzer similar to the one shown in Fig. 1-10. This will allow the designer to know exactly what he is working with before it goes into the circuit.

Capacitor Types

There are many different dielectric materials used in the fabrication of capacitors, such as paper, plastic, ceramic, mica, polystyrene, polycarbonate, teflon, oil, glass, and air. Each material has its advantages and disadvantages. The rf designer is left with a myriad of capacitor types that he could use in any particular application and the ultimate decision to use a particular capacitor is often based on convenience rather than good sound judgement. In many applications, this approach simply cannot be tolerated. This is especially true in manufacturing environments where more than just one unit is to be built and where they must operate reliably over varying temperature extremes. It is often said in the engineering world that anyone can design something and make it work *once*, but it takes a good designer to develop a unit that can be produced in quantity and still operate as it should in different temperature environments.

Ceramic Capacitors—Ceramic dielectric capacitors vary widely in both dielectric constant ($K = 5$ to 10,000) and temperature characteristics. A good rule of thumb to use is: "The higher the K, the worse is its temperature characteristic." This is shown quite clearly in Fig. 1-11.

As illustrated, low-K ceramic capacitors tend to have linear temperature characteristics. These capacitors are generally manufactured using both magnesium titanate, which has a positive temperature coefficient (TC), and calcium titanate which has a negative TC. By combining the two materials in varying proportions, a range of controlled temperature coefficients can be generated. These capacitors are sometimes called temperature compensating capacitors, or NPO (negative positive zero) ceramics. They can have TCs that range anywhere from +150 to -4700 ppm/ $^{\circ}$ C (parts-per-

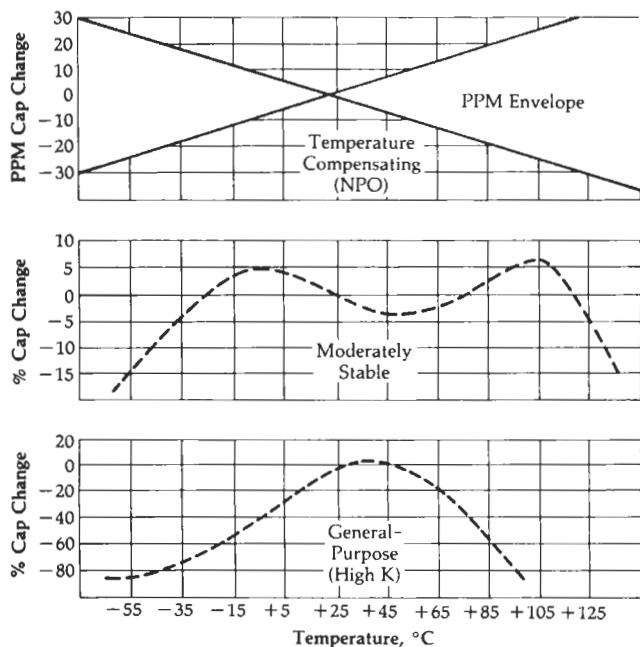


Fig. 1-11. Temperature characteristics for ceramic dielectric capacitors.

million-per-degree-Celsius) with tolerances as small as $\pm 15 \text{ ppm}/^\circ\text{C}$. Because of their excellent temperature stability, NPO ceramics are well suited for oscillator, resonant circuit, or filter applications.

Moderately stable ceramic capacitors (Fig. 1-11) typically vary $\pm 15\%$ of their rated capacitance over their temperature range. This variation is typically nonlinear, however, and care should be taken in their use in resonant circuits or filters where stability is important. These ceramics are generally used in switching circuits. Their main advantage is that they are generally smaller than the NPO ceramic capacitors and, of course, cost less.

High-K ceramic capacitors are typically termed general-purpose capacitors. Their temperature characteristics are very poor and their capacitance may vary as much as 80% over various temperature ranges (Fig. 1-11). They are commonly used only in bypass applications at radio frequencies.

There are ceramic capacitors available on the market which are specifically intended for rf applications. These capacitors are typically high-Q (low ESR) devices with flat ribbon leads or with no leads at all. The lead material is usually solid silver or silver plated and, thus, contains very low resistive losses. At vhf frequencies and above, these capacitors exhibit very low lead inductance due to the flat ribbon leads. These devices are, of course, more expensive and require special printed-circuit board areas for mounting. The capacitors that have no leads are called chip capacitors. These capacitors are typically used above 500 MHz where lead inductance cannot be tolerated. Chip capacitors and flat ribbon capacitors are shown in Fig. 1-12.

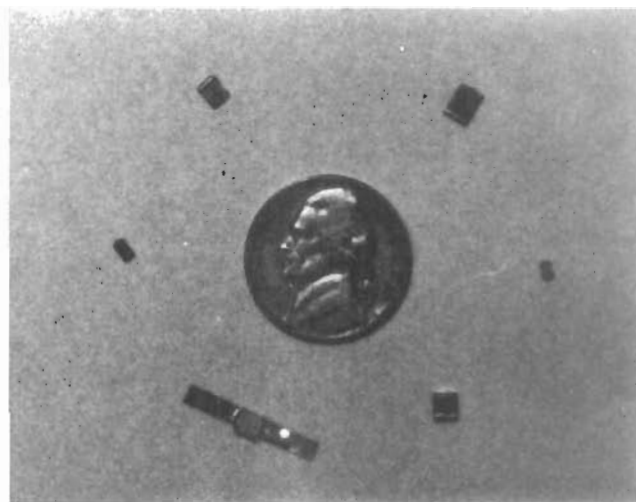


Fig. 1-12. Chip and ribbon capacitors.

Mica Capacitors—Mica capacitors typically have a dielectric constant of about 6, which indicates that for a particular capacitance value, mica capacitors are typically large. Their low K, however, also produces an extremely good temperature characteristic. Thus, mica capacitors are used extensively in resonant circuits and in filters where pc board area is of no concern.

Silvered mica capacitors are even more stable. Ordinary mica capacitors have plates of foil pressed against the mica dielectric. In silvered micas, the silver plates are applied by a process called *vacuum evaporation* which is a much more exacting process. This produces an even better stability with very tight and reproducible tolerances of typically $+20 \text{ ppm}/^\circ\text{C}$ over a range -60°C to $+89^\circ\text{C}$.

The problem with micas, however, is that they are becoming increasingly less cost effective than ceramic types. Therefore, if you have an application in which a mica capacitor would seem to work well, chances are you can find a less expensive NPO ceramic capacitor that will work just as well.

Metalized-Film Capacitors—“Metalized-film” is a

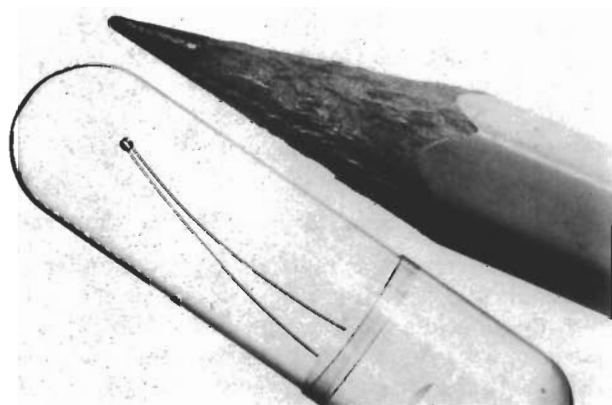


Fig. 1-13. A simple microwave air-core inductor.
(Courtesy Piconics, Inc.)

broad category of capacitor encompassing most of the other capacitors listed previously and which we have not yet discussed. This includes teflon, polystyrene, polycarbonate, and paper dielectrics.

Metalized-film capacitors are used in a number of applications, including filtering, bypassing, and coupling. Most of the polycarbonate, polystyrene, and teflon styles are available in very tight ($\pm 2\%$) capacitance tolerances over their entire temperature range. Polystyrene, however, typically cannot be used over $+85^{\circ}\text{C}$ as it is very temperature sensitive above this point. Most of the capacitors in this category are typically larger than the equivalent-value ceramic types and are used in applications where space is not a constraint.

INDUCTORS

An inductor is nothing more than a wire wound or coiled in such a manner as to increase the magnetic flux linkage between the turns of the coil (see Fig. 1-13). This increased flux linkage increases the wire's self-inductance (or just plain inductance) beyond that which it would otherwise have been. Inductors are used extensively in rf design in resonant circuits, filters, phase shift and delay networks, and as rf chokes used to prevent, or at least reduce, the flow of rf energy along a certain path.

Real-World Inductors

As we have discovered in previous sections of this chapter, there is no "perfect" component, and inductors are certainly no exception. As a matter of fact, of the components we have discussed, the inductor is probably the component most prone to very drastic changes over frequency.

Fig. 1-14 shows what an inductor really looks like

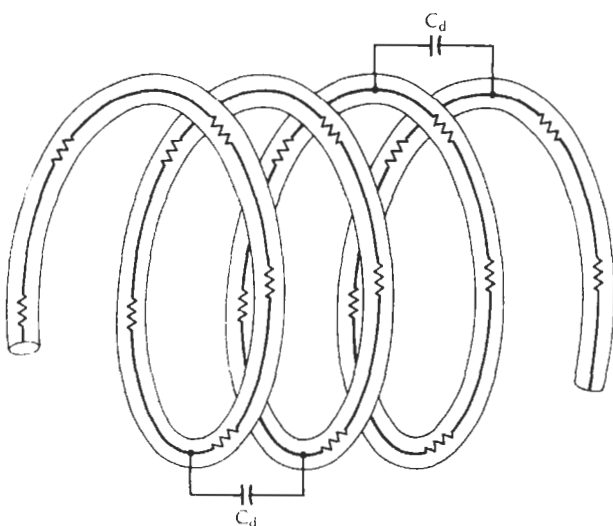


Fig. 1-14. Distributed capacitance and series resistance in an inductor.

at rf frequencies. As previously discussed, whenever we bring two conductors into close proximity but separated by a dielectric, and place a voltage differential between the two, we form a capacitor. Thus, if any wire resistance at all exists, a voltage drop (even though very minute) will occur between the windings, and small capacitors will be formed. This effect is shown in Fig. 1-14 and is called distributed capacitance (C_d). Then, in Fig. 1-15, the capacitance (C_d) is an aggregate of the individual parasitic distributed capacitances of the coil shown in Fig. 1-14.

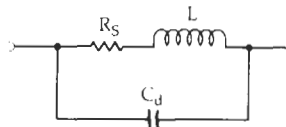


Fig. 1-15. Inductor equivalent circuit.

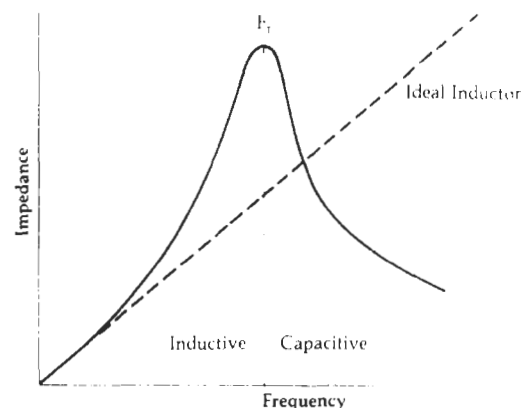


Fig. 1-16. Impedance characteristic vs. frequency for a practical and an ideal inductor.

The effect of C_d upon the reactance of an inductor is shown in Fig. 1-16. Initially, at lower frequencies, the inductor's reactance parallels that of an ideal inductor. Soon, however, its reactance departs from the ideal curve and increases at a much faster rate until it reaches a peak at the inductor's parallel resonant frequency (F_r). Above F_r , the inductor's reactance begins to decrease with frequency and, thus, the inductor begins to look like a capacitor. Theoretically, the resonance peak would occur at infinite reactance (see Example 1-4). However, due to the series resistance of the coil, some finite impedance is seen at resonance.

Recent advances in inductor technology have led to the development of microminiature fixed-chip inductors. One type is shown in Fig. 1-17. These inductors feature a ceramic substrate with gold-plated solderable wrap-around bottom connections. They come in values from $0.01 \mu\text{H}$ to 1.0 mH , with typical Qs that range from 40 to 60 at 200 MHz.

It was mentioned earlier that the series resistance of a coil is the mechanism that keeps the impedance of the coil finite at resonance. Another effect it has is

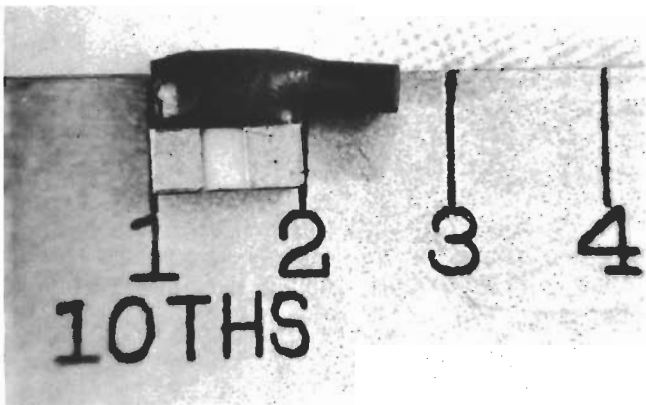


Fig. 1-17. Microminiature chip inductor.
(Courtesy Piconics, Inc.)

EXAMPLE 1-4

To show that the impedance of a lossless inductor at resonance is infinite, we can write the following:

$$Z = \frac{X_L X_C}{X_L + X_C} \quad (\text{Eq. 1-3})$$

where,

Z = the impedance of the parallel circuit,

X_L = the inductive reactance ($j\omega L$),

X_C = the capacitive reactance ($\frac{1}{j\omega C}$) .

Therefore,

$$Z = \frac{j\omega L \left(\frac{1}{j\omega C} \right)}{j\omega L + \frac{1}{j\omega C}} \quad (\text{Eq. 1-4})$$

Multiplying numerator and denominator by $j\omega C$, we get:

$$\begin{aligned} Z &= \frac{j\omega L}{(j\omega L)(j\omega C) + 1} \\ &= \frac{j\omega L}{j^2\omega^2 LC + 1} \end{aligned} \quad (\text{Eq. 1-5})$$

From algebra, $j^2 = -1$; then, rearranging:

$$Z = \frac{j\omega L}{1 - \omega^2 LC} \quad (\text{Eq. 1-6})$$

If the term $\omega^2 LC$, in Equation 1-6, should ever become equal to 1, then the denominator will be equal to zero and impedance Z will become infinite. The frequency at which $\omega^2 LC$ becomes equal to 1 is:

$$\begin{aligned} \omega^2 LC &= 1 \\ LC &= \frac{1}{\omega^2} \\ \sqrt{LC} &= \frac{1}{\omega} \\ 2\pi\sqrt{LC} &= \frac{1}{f} \\ \frac{1}{2\pi\sqrt{LC}} &= f \end{aligned} \quad (\text{Eq. 1-7})$$

which is the familiar equation for the resonant frequency of a tuned circuit.

to broaden the resonance peak of the impedance curve of the coil. This characteristic of resonant circuits is an important one and will be discussed in detail in Chapter 3.

The ratio of an inductor's reactance to its series resistance is often used as a measure of the quality of the inductor. The larger the ratio, the better is the inductor. This quality factor is referred to as the Q of the inductor.

$$Q = \frac{X}{R_s}$$

If the inductor were wound with a perfect conductor, its Q would be infinite and we would have a lossless inductor. Of course, there is no perfect conductor and, thus, an inductor always has some finite Q .

At low frequencies, the Q of an inductor is very good because the only resistance in the windings is the dc resistance of the wire—which is very small. But as the frequency increases, skin effect and winding capacitance begin to degrade the quality of the inductor. This is shown in the graph of Fig. 1-18. At low frequencies, Q will increase directly with frequency because its reactance is increasing and skin effect has not yet become noticeable. Soon, however, skin effect does become a factor. The Q still rises, but at a lesser rate, and we get a gradually decreasing slope in the curve. The flat portion of the curve in Fig. 1-18 occurs as the series resistance and the reactance are changing at the same rate. Above this point, the shunt capacitance and skin effect of the windings combine to decrease the Q of the inductor to zero at its resonant frequency.

Some methods of increasing the Q of an inductor and extending its useful frequency range are:

1. Use a larger diameter wire. This decreases the ac and dc resistance of the windings.
2. Spread the windings apart. Air has a lower dielectric constant than most insulators. Thus, an air gap between the windings decreases the interwinding capacitance.
3. Increase the permeability of the flux linkage path. This is most often done by winding the inductor around a magnetic-core material, such as iron or

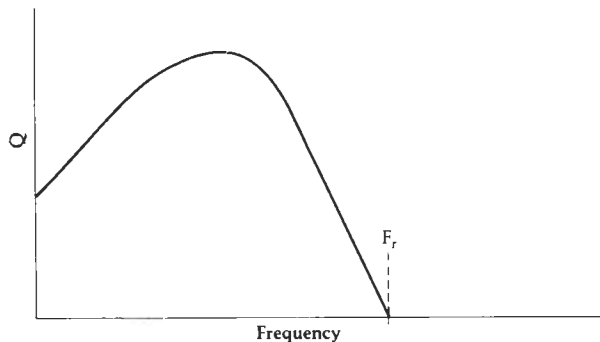


Fig. 1-18. The Q variation of an inductor vs. frequency.

ferrite. A coil made in this manner will also consist of fewer turns for a given inductance. This will be discussed in a later section of this chapter.

Single-Layer Air-Core Inductor Design

Every rf circuit designer needs to know how to design inductors. It may be tedious at times, but it's well worth the effort. The formula that is generally used to design single-layer air-core inductors is given in Equation 1-8 and diagrammed in Fig. 1-19.

$$L = \frac{0.394 r^2 N^2}{9r + 10l} \quad (\text{Eq. 1-8})$$

where,

r = the coil radius in cm,

l = the coil length in cm,

L = the inductance in microhenries.

However, coil length l must be greater than $0.67r$. This formula is accurate to within one percent. See Example 1-5.

Keep in mind that even though optimum Q is attained when the length of the coil (l) is equal to its diameter ($2r$), this is sometimes not practical and, in many cases, the length is much greater than the di-

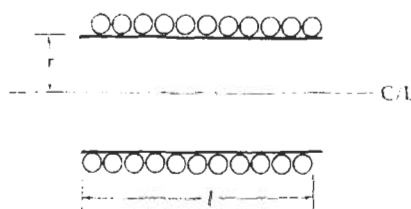


Fig. 1-19. Single-layer air-core inductor requirements.

EXAMPLE 1-5

Design a 100 nH (0.1 μ H) air-core inductor on a $\frac{1}{4}$ -inch (0.635 cm) coil form.

Solution

For optimum Q , the length of the coil should be equal to its diameter. Thus, $l = 0.635$ cm, $r = 0.317$ cm, and $L = 0.1 \mu$ H.

Using Equation 1-8 and solving for N gives:

$$N = \sqrt{\frac{29L}{0.394}}$$

where we have taken $l = 2r$, for optimum Q .

Substituting and solving:

$$N = \sqrt{\frac{29(0.1)}{(0.394)(0.317)}} \\ = 4.8 \text{ turns}$$

Thus, we need 4.8 turns of wire within a length of 0.635 cm. A look at Table 1-1 reveals that the largest diameter enamel-coated wire that will allow 4.8 turns in a length of 0.635 cm is No. 18 AWG wire which has a diameter of 42.4 mils (0.107 cm).

Table 1-1. AWG Wire Chart

Wire Size (AWG)	Dia in Mils ^a (Bare)	Dia in Mils (Coated)	Ohms/1000 ft.	Area Circular Mils
1	289.3		0.124	83690
2	257.6		0.156	66360
3	229.4		0.197	52620
4	204.3		0.249	41740
5	181.9		0.313	33090
6	162.0		0.395	26240
7	144.3		0.498	20820
8	128.5	131.6	0.628	16510
9	114.4	116.3	0.793	13090
10	101.9	104.2	0.999	10380
11	90.7	93.5	1.26	8230
12	80.8	83.3	1.59	6530
13	72.0	74.1	2.00	5180
14	64.1	66.7	2.52	4110
15	57.1	59.5	3.18	3260
16	50.8	52.9	4.02	2580
17	45.3	47.2	5.05	2050
18	40.3	42.4	6.39	1620
19	35.9	37.9	8.05	1290
20	32.0	34.0	10.1	1020
21	28.5	30.2	12.8	812
22	25.3	27.0	16.2	640
23	22.6	24.2	20.3	511
24	20.1	21.6	25.7	404
25	17.9	19.3	32.4	320
26	15.9	17.2	41.0	253
27	14.2	15.4	51.4	202
28	12.6	13.8	65.3	159
29	11.3	12.3	81.2	123
30	10.0	11.0	104.0	100
31	8.9	9.9	131	79.2
32	8.0	8.8	162	64.0
33	7.1	7.9	206	50.4
34	6.3	7.0	261	39.7
35	5.6	6.3	331	31.4
36	5.0	5.7	415	25.0
37	4.5	5.1	512	20.2
38	4.0	4.5	648	16.0
39	3.5	4.0	847	12.2
40	3.1	3.5	1080	9.61
41	2.8	3.1	1320	7.84
42	2.5	2.8	1660	6.25
43	2.2	2.5	2140	4.84
44	2.0	2.3	2590	4.00
45	1.76	1.9	3350	3.10
46	1.57	1.7	4210	2.46
47	1.40	1.6	5290	1.96
48	1.24	1.4	6750	1.54
49	1.11	1.3	8420	1.23
50	.99	1.1	10600	0.98

^a 1 mil = 2.54×10^{-3} cm

ameter. In Example 1-5, we calculated the need for 4.8 turns of wire in a length of 0.635 cm and decided that No. 18 AWG wire would fit. The only problem with this approach is that when the design is finished, we end up with a very tightly wound coil. This increases the distributed capacitance between the turns and, thus, lowers the useful frequency range of the inductor by lowering its resonant frequency. We could take either one of the following compromise solutions to this dilemma:

1. Use the next smallest AWG wire size to wind the inductor while keeping the length (l) the same. This approach will allow a small air gap between windings and, thus, decrease the interwinding capacitance. It also, however, increases the resistance of the windings by decreasing the diameter of the conductor and, thus, it lowers the Q.
2. Extend the length of the inductor (while retaining the use of No. 18 AWG wire) just enough to leave a small air gap between the windings. This method will produce the same effect as Method No. 1. It reduces the Q somewhat but it decreases the interwinding capacitance considerably.

Magnetic-Core Materials

In many rf applications, where large values of inductance are needed in small areas, air-core inductors cannot be used because of their size. One method of decreasing the size of a coil while maintaining a given inductance is to decrease the number of turns while at the same time increasing its magnetic flux density. The flux density can be increased by decreasing the "reluctance" or magnetic resistance path that links the windings of the inductor. We do this by adding a magnetic-core material, such as iron or ferrite, to the inductor. The permeability (μ) of this material is much greater than that of air and, thus, the magnetic flux isn't as "reluctant" to flow between the windings. The net result of adding a high permeability core to an inductor is the gaining of the capability to wind a given inductance with fewer turns than what would be required for an air-core inductor. Thus, several advantages can be realized.

1. Smaller size—due to the fewer number of turns needed for a given inductance.
2. Increased Q—fewer turns means less wire resistance.
3. Variability—obtained by moving the magnetic core in and out of the windings.

There are some major problems that are introduced by the use of magnetic cores, however, and care must be taken to ensure that the core that is chosen is the right one for the job. Some of the problems are:

1. Each core tends to introduce its own losses. Thus, adding a magnetic core to an air-core inductor could possibly *decrease* the Q of the inductor, depending on the material used and the frequency of operation.
2. The permeability of all magnetic cores changes with frequency and usually decreases to a very small value at the upper end of their operating range. It eventually approaches the permeability of air and becomes "invisible" to the circuit.
3. The higher the permeability of the core, the more sensitive it is to temperature variation. Thus, over wide temperature ranges, the inductance of the coil may vary appreciably.
4. The permeability of the magnetic core changes with applied signal level. If too large an excitation is applied, saturation of the core will result.

These problems can be overcome if care is taken, in the design process, to choose cores wisely. Manufacturers now supply excellent literature on available sizes and types of cores, complete with their important characteristics.

TOROIDS

A toroid, very simply, is a ring or doughnut-shaped magnetic material that is widely used to wind rf inductors and transformers. Toroids are usually made of iron or ferrite. They come in various shapes and sizes (Fig. 1-20) with widely varying characteristics. When used as cores for inductors, they can typically yield very high Qs. They are self-shielding, compact, and best of all, easy to use.

The Q of a toroidal inductor is typically high because the toroid can be made with an extremely high permeability. As was discussed in an earlier section, high permeability cores allow the designer to construct an inductor with a given inductance (for example, 35 μ H) with fewer turns than is possible with an air-core design. Fig. 1-21 indicates the potential savings obtained in number of turns of wire when coil design is changed from air-core to toroidal-core inductors. The air-core inductor, if wound for optimum

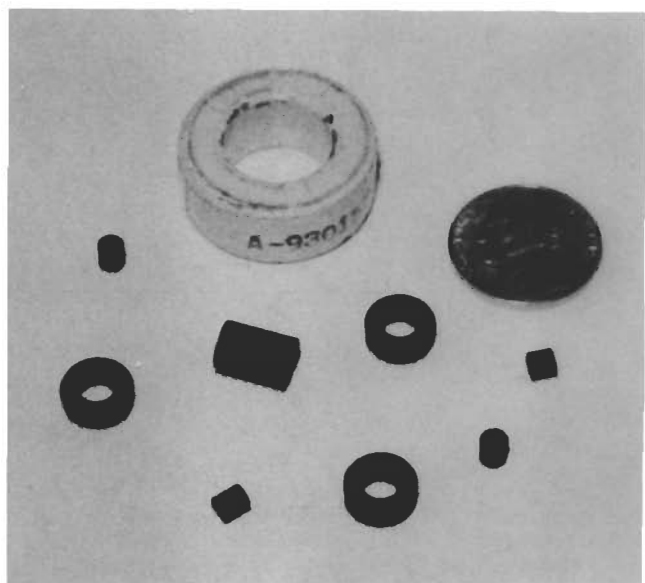
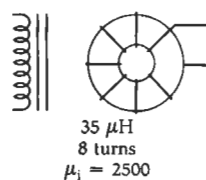
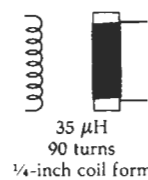


Fig. 1-20. Toroidal cores come in various shapes and sizes.



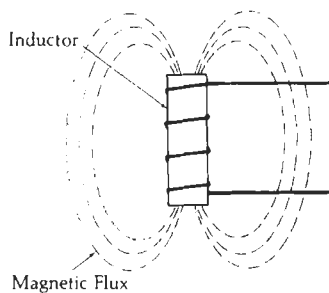
(A) Toroid inductor.



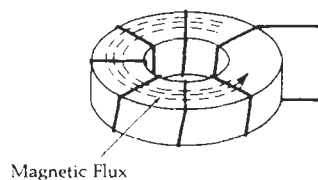
(B) Air-core inductor.

Fig. 1-21. Turns comparison between inductors for the same inductance.

Q , would take 90 turns of a very small wire (in order to fit all turns within a $\frac{1}{4}$ -inch length) to reach $35 \mu\text{H}$; however, the toroidal inductor would only need 8 turns to reach the design goal. Obviously, this is an extreme case but it serves a useful purpose and illustrates the point. The toroidal core does require fewer turns for a given inductance than does an air-core design. Thus, there is less ac resistance and the Q can be increased dramatically.



(A) Typical inductor.



(B) Toroidal inductor.

Fig. 1-22. Shielding effect of a toroidal inductor.

The self-shielding properties of a toroid become evident when Fig. 1-22 is examined. In a typical air-core inductor, the magnetic-flux lines linking the turns of the inductor take the shape shown in Fig. 1-22A. The sketch clearly indicates that the air surrounding the inductor is definitely part of the magnetic-flux path. Thus, this inductor tends to radiate the rf signals flowing within. A toroid, on the other hand (Fig. 1-22B), completely contains the magnetic flux within the material itself; thus, no radiation occurs. In actual practice, of course, some radiation will occur but it is minimized. This characteristic of toroids eliminates the need for bulky shields surrounding the inductor. The shields not only tend to reduce available space, but they also reduce the Q of the inductor that they are shielding.

Core Characteristics

Earlier, we discussed, in general terms, the relative advantages and disadvantages of using magnetic cores. The following discussion of typical toroidal-core characteristics will aid you in specifying the core that you need for your particular application.

Fig. 1-23 is a typical magnetization curve for a magnetic core. The curve simply indicates the magnetic-flux density (B) that occurs in the inductor with a specific magnetic-field intensity (H) applied. As the magnetic-field intensity is increased from zero (by in-

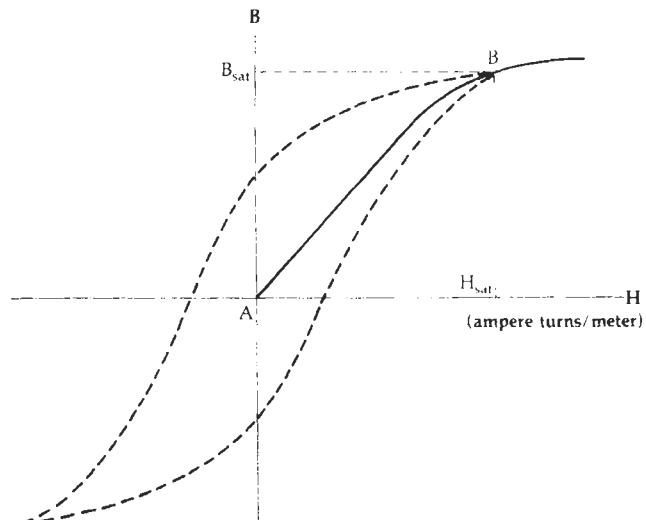


Fig. 1-23. Magnetization curve for a typical core.

creasing the applied signal voltage), the magnetic-flux density that links the turns of the inductor increases quite linearly. The ratio of the magnetic-flux density to the magnetic-field intensity is called the permeability of the material. This has already been mentioned on numerous occasions.

$$\mu = B/H \text{ (Webers/ampere-turn)} \quad (\text{Eq. 1-9})$$

Thus, the permeability of a material is simply a measure of how well it transforms an electrical excitation into a magnetic flux. The better it is at this transformation, the higher is its permeability.

As mentioned previously, initially the magnetization curve is linear. It is during this linear portion of the curve that permeability is usually specified and, thus, it is sometimes called initial permeability (μ_i) in various core literature. As the electrical excitation increases, however, a point is reached at which the magnetic-flux intensity does not continue to increase at the same rate as the excitation and the slope of the curve begins to decrease. Any further increase in excitation may cause saturation to occur. H_{sat} is the excitation point above which no further increase in magnetic-flux density occurs (B_{sat}). The incremental permeability above this point is the same as air. Typically, in rf circuit applications, we keep the excitation small enough to maintain linear operation.

B_{sat} varies substantially from core to core, depending upon the size and shape of the material. Thus, it is necessary to read and understand the manufacturer's literature that describes the particular core you are using. Once B_{sat} is known for the core, it is a very simple matter to determine whether or not its use in a particular circuit application will cause it to saturate. The in-circuit operational flux density (B_{op}) of the core is given by the formula:

$$B_{op} = \frac{E \times 10^8}{(4.44)fNA_e} \quad (\text{Eq. 1-10})$$

where,

- B_{op} = the magnetic-flux density in gauss,
- E = the maximum rms voltage across the inductor in volts,
- f = the frequency in hertz,
- N = the number of turns,
- A_e = the effective cross-sectional area of the core in cm^2 .

Thus, if the calculated B_{op} for a particular application is less than the published specification for B_{sat} , then the core will not saturate and its operation will be somewhat linear.

Another characteristic of magnetic cores that is very important to understand is that of internal loss. It has previously been mentioned that the careless addition of a magnetic core to an air-core inductor could possibly *reduce* the Q of the inductor. This concept might seem contrary to what we have studied so far, so let's examine it a bit more closely.

The equivalent circuit of an air-core inductor (Fig. 1-15) is reproduced in Fig. 1-24A for your convenience. The Q of this inductor is

$$Q = \frac{X_L}{R_s} \quad (\text{Eq. 1-11})$$

where,

- $X_L = \omega L$,
- R_s = the resistance of the windings.

If we add a magnetic core to the inductor, the equivalent circuit becomes like that shown in Fig. 1-24B. We have added resistance R_p to represent the losses which take place in the core itself. These losses are in the form of *hysteresis*. Hysteresis is the power lost in the core due to the realignment of the magnetic particles within the material with changes in excitation, and the eddy currents that flow in the core due to the voltages induced within. These two types of internal loss, which are inherent to some degree in every magnetic core and are thus unavoidable, combine to reduce the efficiency of the inductor and, thus, increase its loss. But what about the new Q for the magnetic-core inductor? This question isn't as easily answered. Remember, when a magnetic core is inserted into an existing inductor, the value of the inductance is increased. Therefore, at any given frequency, its reactance increases proportionally. The question that must be answered then, in order to de-

termine the new Q of the inductor, is: By what factors did the inductance and loss increase? Obviously, if by adding a toroidal core, the inductance were increased by a factor of two and its total loss was also increased by a factor of two, the Q would remain unchanged. If, however, the total coil loss were increased to four times its previous value while only doubling the inductance, the Q of the inductor would be reduced by a factor of two.

Now, as if all of this isn't confusing enough, we must also keep in mind that the additional loss introduced by the core is not constant, but varies (usually increases) with frequency. Therefore, the designer must have a complete set of manufacturer's data sheets for every core he is working with.

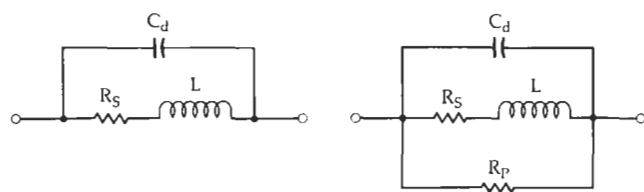
Toroid manufacturers typically publish data sheets which contain all the information needed to design inductors and transformers with a particular core. (Some typical specification and data sheets are given in Figs. 1-25 and 1-26.) In most cases, however, each manufacturer presents the information in a unique manner and care must be taken in order to extract the information that is needed without error, and in a form that can be used in the ensuing design process. This is not always as simple as it sounds. Later in this chapter, we will use the data presented in Figs. 1-25 and 1-26 to design a couple of toroidal inductors so that we may see some of those differences. Table 1-2 lists some of the commonly used terms along with their symbols and units.

Powdered Iron Vs. Ferrite

In general, there are no hard and fast rules governing the use of ferrite cores versus powdered-iron cores in rf circuit-design applications. In many instances, given the same permeability and type, either core could be used without much change in performance of the actual circuit. There are, however, special applications in which one core might out-perform another, and it is those applications which we will address here.

Powdered-iron cores, for instance, can typically handle more rf power without saturation or damage than the same size ferrite core. For example, ferrite, if driven with a large amount of rf power, tends to retain its magnetism permanently. This ruins the core by changing its permeability permanently. Powdered iron, on the other hand, if overdriven will eventually return to its initial permeability (μ_1). Thus, in any application where high rf power levels are involved, iron cores might seem to be the best choice.

In general, powdered-iron cores tend to yield higher-Q inductors, at higher frequencies, than an equivalent size ferrite core. This is due to the inherent core characteristics of powdered iron which produce much less internal loss than ferrite cores. This characteristic of powdered iron makes it very useful in narrow-band or tuned-circuit applications. Table 1-3 lists a few of the common powdered-iron core materials along with their typical applications.



(A) Air core.

(B) Magnetic core.

Fig. 1-24. Equivalent circuits for air-core and magnetic-core inductors.



BROAD BAND RATED FERRAMIC COMPONENTS

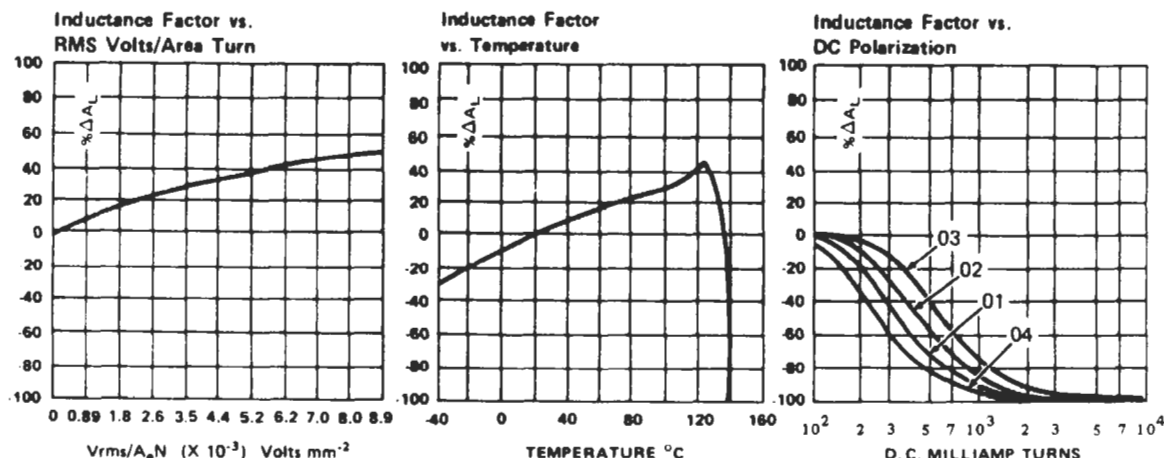
- Values measured at 100 KHz, T = 25°C.
- Temperature Coefficient (TC) = 0 to +0.75% /°C max., -40 to +70°C.
- Disaccommodation (D) = 3.0% max., 10-100 min., 25°C.
- Hysteresis Core Constant (η_i) measured at 20 KHz to 30 gauss (3 milli Tesla).
- For mm dimensions and core constants, see page 30.

7400 Series ToroidsNom. μ , 2500**MECHANICAL SPECIFICATIONS**

	PART NUMBER				TOL	UNITS	
	BBR-7401	BBR-7402	BBR-7403	BBR-7404			
d ₁	0.135	0.155	0.230	0.100	±0.005	in.	
d ₂	0.065	0.068	0.120	0.050	±0.005	in.	
h	0.055	0.051	0.080	0.050	±0.005	in.	

ELECTRICAL SPECIFICATIONS

	PART NUMBER				TOL	UNITS
	BBR-7401	BBR-7402	BBR-7403	BBR-7404		
A _L	510	365	495	440	±20%	nH/turn ²
X _p /N ²	0.320	0.229	0.310	0.276	±20%	ohm/turn ²
R _p /N ²	10.4	7.5	10.0	8.9	min.	ohm/turn ²
Q	54	54	54	54	min.	
V _{rms}	7.9	7.1	13.6	5.1	max.	mv
η_i	1,480	1,400	0,920	2,150	max.	VSA ⁻² H ^{-3/2}

TYPICAL CHARACTERISTIC CURVES – Part Numbers 7401, 7402, 7403 and 7404

Cont. on next page

Fig. 1-25. Data sheet for ferrite toroidal cores. (Courtesy Indiana General)

BROAD BAND-RATED FERRAMIC COMPONENTS

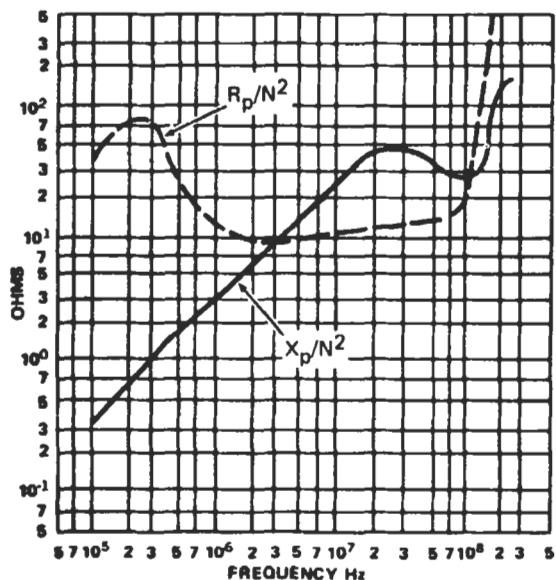


7401 • 7402 • 7403 • 7404 Toroids

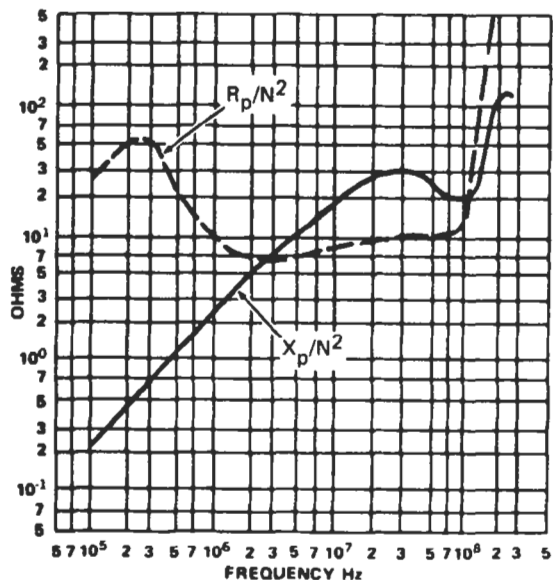
Nom. μ_i 2500

Shunt Reactance and Resistance per Turn Squared versus Frequency (sine wave)

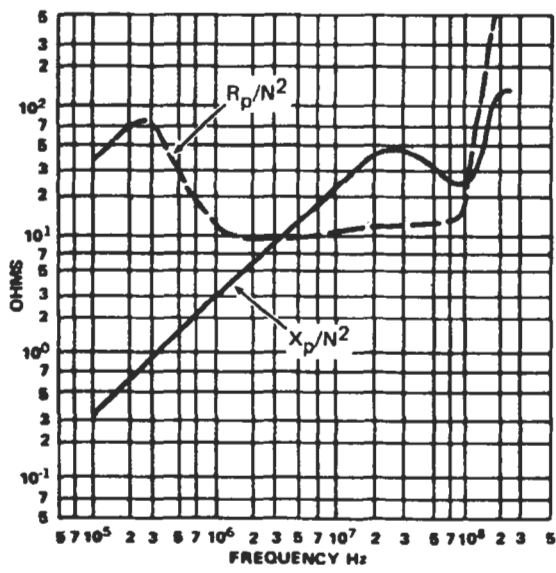
BBR-7401



BBR-7402



BBR-7403



BBR-7404

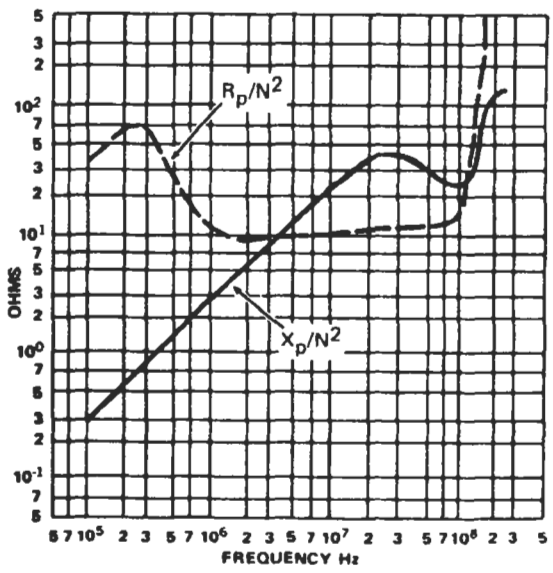


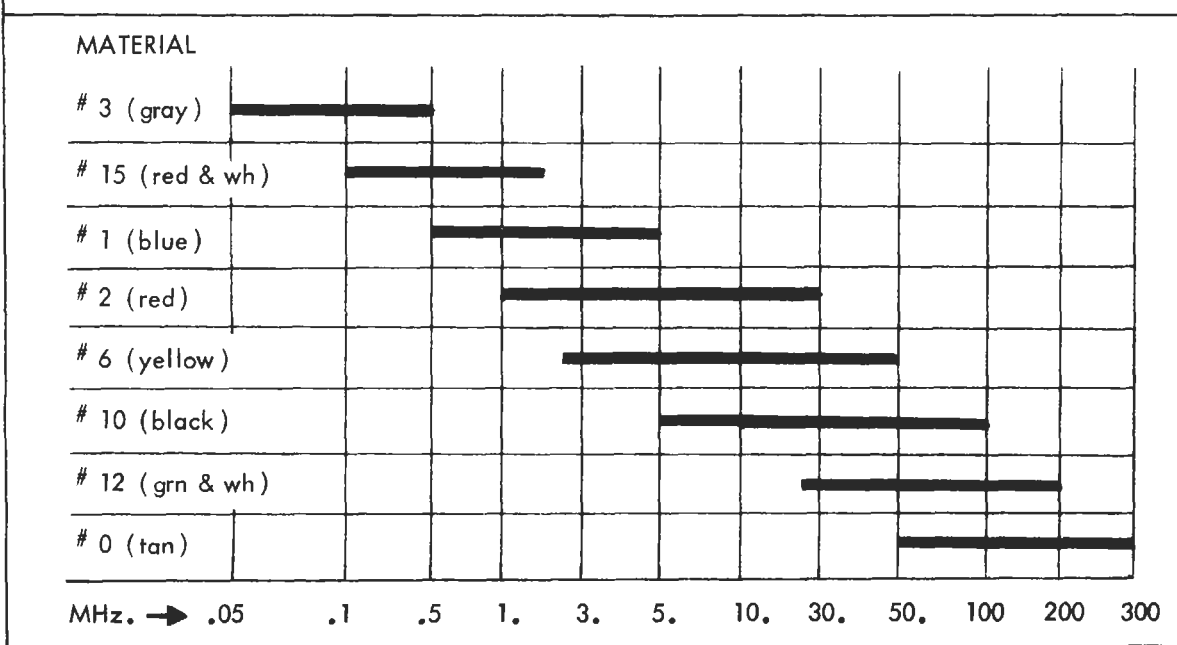
Fig. 1-25—cont. Data sheet for ferrite toroidal cores. (Courtesy Indiana General)

IRON-POWDER TOROIDAL CORES

Core size	PHYSICAL DIMENSIONS					Mean Length (cm)
	Outer Diam. (in)	Inner Diam. (in)	Height (in)	Cross Sect. Area (cm) ²		
T-225A --	2.250	1.400	1.000	2.742	14.56	
T-225 --	2.250	1.400	.550	1.508	14.56	
T-200 --	2.000	1.250	.550	1.330	12.97	
T-184 --	1.840	.960	.710	2.040	11.12	
T-157 --	1.570	.950	.570	1.140	10.05	
T-130 --	1.300	.780	.437	.930	8.29	
T-106 --	1.060	.560	.437	.706	6.47	
T- 94 --	.942	.560	.312	.385	6.00	
T- 80 --	.795	.495	.250	.242	5.15	
T- 68 --	.690	.370	.190	.196	4.24	
T- 50 --	.500	.303	.190	.121	3.20	
T- 44 --	.440	.229	.159	.107	2.67	
T- 37 --	.375	.204	.128	.070	2.32	
T- 30 --	.307	.150	.128	.065	1.83	
T- 25 --	.255	.120	.096	.042	1.50	
T- 20 --	.200	.088	.070	.034	1.15	
T- 16 --	.160	.078	.060	.016	0.75	
T- 12 --	.120	.062	.050	.010	0.74	

IRON - POWDER MATERIAL vs. FREQUENCY RANGE

Higher Q will be obtained in the upper portion of a materials frequency range when smaller cores are used. Likewise, in the lower portion of a materials frequency range, higher Q can be achieved when using the larger cores.



Cont. on next page

Fig. 1-26. Data sheet for powdered-iron toroidal cores. (Courtesy Amidon Associates)

IRON-POWDER TOROIDAL CORES

FOR RESONANT CIRCUITS

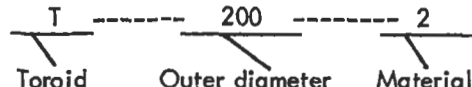
MATERIAL # 0 permeability 1 50 MHz to 300 MHz Tan

Core number	Outer diam. (in.)	Inner diam. (in.)	Height (in.)	A_L value uh / 100 t
T-130-0	.1300	.780	.437	15.0
T-106-0	.1060	.560	.437	19.2
T- 94-0	.942	.560	.312	10.6
T- 80-0	.795	.495	.250	8.5
T- 68-0	.690	.370	.190	7.5
T- 50-0	.500	.303	.190	6.4
T- 44-0	.440	.229	.159	6.5
T- 37-0	.375	.205	.128	4.9
T- 30-0	.307	.151	.128	6.0
T- 25-0	.255	.120	.096	4.5
T- 20-0	.200	.088	.067	3.5
T- 16-0	.160	.078	.060	3.0
T- 12-0	.125	.062	.050	3.0

MATERIAL # 12 permeability 3 20 MHz to 200 MHz Green & White

Core number	Outer diam. (in.)	Inner diam. (in.)	Height (in.)	A_L value uh / 100 t
T-80-12	.795	.495	.250	22
T-68-12	.690	.370	.190	21
T-50-12	.500	.300	.190	18
T-44-12	.440	.229	.159	18
T-37-12	.375	.205	.128	15
T-30-12	.307	.151	.128	16
T-25-12	.255	.120	.096	12
T-20-12	.200	.088	.067	10
T-16-12	.160	.078	.060	8
T-12-12	.125	.062	.050	7

Key to part numbers for :
IRON POWDER TOROIDAL CORES



Number of turns = 100

A_L values $\pm 5\%$

desired inductance (uh)

A_L value (uh per 100 turns)

Cont. on next page

Fig. 1-26—cont. Data sheet for powdered-iron toroidal cores. (Courtesy Amidon Associates)

IRON-POWDER TOROIDAL CORES

FOR RESONANT CIRCUITS

MATERIAL # 10	permeability 6	10 MHz to 100 MHz	Black	
Core number	Outer diam. (in.)	Inner diam. (in.)	Height (in.)	A _L value uh / 100 t
T-94-10	.942	.560	.312	58
T-80-10	.795	.495	.250	32
T-68-10	.690	.370	.190	32
T-50-10	.500	.303	.190	31
T-44-10	.440	.229	.159	33
T-37-10	.375	.205	.128	25
T-30-10	.307	.151	.128	25
T-25-10	.255	.120	.096	19
T-20-10	.200	.088	.067	16
T-16-10	.160	.078	.060	13
T-12-10	.125	.062	.050	12

Core Size	NUMBER OF TURNS vs. WIRE SIZE and CORE SIZE																
	Approximate number of turns of wire - single layer wound - single insulation																
	40	38	36	34	32	30	wire size	28	26	24	22	20	18	16	14	12	10
T-12	47	37	29	21	15	11	8	5	4	2	1	1	1	0	0	0	
T-16	63	49	38	29	21	16	11	8	5	3	3	1	1	1	0	0	
T-20	72	56	43	33	25	18	14	9	6	5	4	3	1	1	1	0	
T-25	101	79	62	48	37	28	21	15	11	7	5	4	3	1	1	1	
T-30	129	101	79	62	48	37	28	21	15	11	7	5	4	3	1	1	
T-37	177	140	110	87	67	53	41	31	23	17	12	9	7	5	3	1	
T-44	199	157	124	97	76	60	46	35	27	20	15	10	7	6	5	3	
T-50	265	210	166	131	103	81	63	49	37	28	21	16	11	8	6	5	
T-68	325	257	205	162	127	101	79	61	47	36	28	21	15	11	9	7	
T-80	438	347	276	219	172	137	108	84	66	51	39	30	23	17	12	8	
T-94	496	393	313	248	195	156	123	96	75	58	45	35	27	20	14	10	
T-106	496	393	313	248	195	156	123	96	75	58	45	35	27	20	14	10	
T-130	693	550	439	348	275	220	173	137	107	83	66	51	40	30	23	17	
T-157	846	672	536	426	336	270	213	168	132	104	82	64	50	38	29	22	
T-184	846	672	536	426	336	270	213	168	132	104	82	64	50	38	29	22	
T-200	1115	886	707	562	445	357	282	223	176	139	109	86	68	53	41	31	
T-225	1250	993	793	631	499	400	317	250	198	156	123	98	77	60	46	36	

Cont. on next page

Fig. 1-26—cont. Data sheet for powdered-iron toroidal cores. (Courtesy Amidon Associates)

Q-CURVES

IRON-POWDER TOROIDAL CORES

20 MHz to 200 MHz

180

20 MHz to 200 MHz

160

140

120

100

80

60

40

20

Mc.

40

60

100

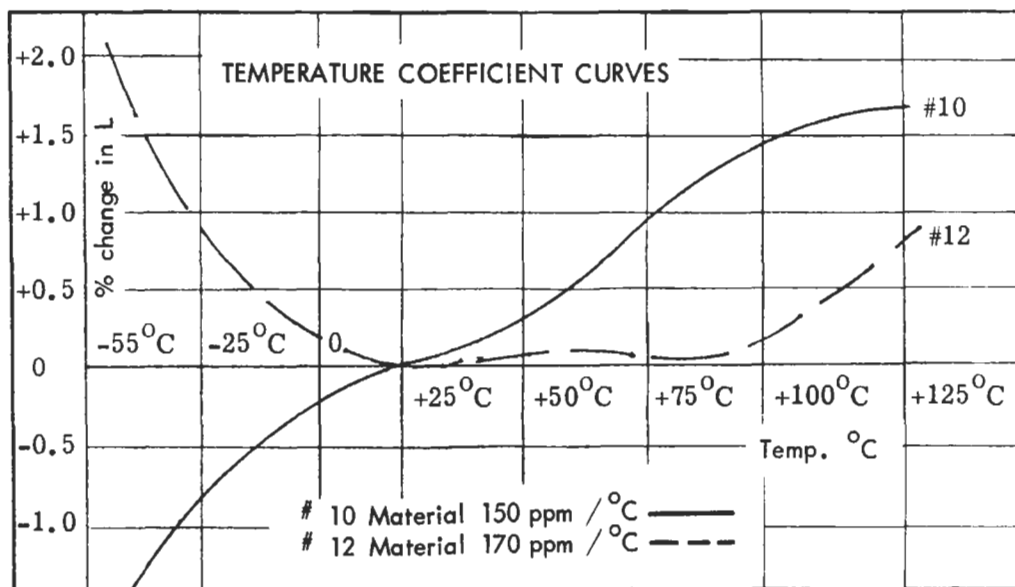
140

200

T-37-12 6t #20 L = .09 uh
 T-37-12 4t #22 L = .05 uh
 T-30-12 6t #22 L = .10 uh
 T-30-12 4t #22 L = .06 uh
 T-25-12 8t #24 L = .10 uh
 T-25-12 6t #22 L = .07 uh
 T-12-12 11t #30 L = .11 uh

IRON-POWDER TOROIDAL CORES

TEMPERATURE COEFFICIENT CURVES



AMIDON Associates • 12033 OTSEGO STREET • NORTH HOLLYWOOD, CALIF. 91607

Fig. 1-26—cont. Data sheet for powdered-iron toroidal cores. (Courtesy Amidon Associates)

Table 1-2. Toroidal Core Symbols and Definitions

Symbol	Description	Units
A_c	Available cross-sectional area. The area (perpendicular to the direction of the wire) for winding turns on a particular core.	cm ²
A_s	Effective area of core. The cross-sectional area that an equivalent gapless core would have.	cm ²
A_L	Inductive index. This relates the inductance to the number of turns for a particular core.	nH/turn ²
B_{sat}	Saturation flux density of the core.	gauss
B_{op}	Operating flux density of the core. This is with an applied voltage.	gauss
l_e	Effective length of the flux path.	cm
μ_i	Initial permeability. This is the effective permeability of the core at low excitation in the linear region.	numeric

Table 1-3. Powdered-Iron Materials

Material	Application/Classification
Carbonyl C	A medium-Q powdered-iron material at 150 kHz. A high-cost material for am tuning applications and low-frequency if transformers.
Carbonyl E	The most widely used of all powdered-iron materials. Offers high-Q and medium permeability in the 1 MHz to 30 MHz frequency range. A medium-cost material for use in if transformers, antenna coils, and general-purpose designs.
Carbonyl J	A high-Q powdered-iron material at 40 to 100 MHz, with a medium permeability. A high-cost material for fm and tv applications.
Carbonyl SF	Similar to carbonyl E, but with a better Q up through 50 MHz. Costs more than carbonyl E.
Carbonyl TH	A powdered-iron material with a higher Q than carbonyl E up to 30 MHz, but less than carbonyl SF. Higher cost than carbonyl E.
Carbonyl W	The highest cost powdered-iron material. Offers a high Q to 100 MHz, with medium permeability.
Carbonyl HP	Excellent stability and a good Q for lower frequency operation—to 50 kHz. A powdered-iron material.
Carbonyl GS6	For commercial broadcast frequencies. Offers good stability and a high Q.
IRN-8	A synthetic oxide hydrogen-reduced material with a good Q from 50 to 150 MHz. Medium priced for use in fm and tv applications.

At very low frequencies, or in broad-band circuits which span the spectrum from vlf up through vhf, ferrite seems to be the general choice. This is true because, for a given core size, ferrite cores have a much higher permeability. The higher permeability is needed at the low end of the frequency range where, for a given inductance, fewer windings would be needed with the ferrite core. This brings up another point. Since ferrite cores, in general, have a higher permeability than the same size powdered-iron core, a coil of a given inductance can usually be wound on a much smaller ferrite core and with fewer turns. Thus, we can save circuit board area.

TOROIDAL INDUCTOR DESIGN

For a toroidal inductor operating on the linear (nonsaturating) portion of its magnetization curve, its inductance is given by the following formula:

$$L = \frac{0.4\pi N^2 \mu_i A_c \times 10^{-2}}{l_e} \quad (\text{Eq. 1-12})$$

where,

L = the inductance in microhenries,

N = the number of turns,

μ_i = initial permeability,

A_c = the cross-sectional area of the core in cm²,

l_e = the effective length of the core in cm.

In order to make calculations easier, most manufacturers have combined μ_i , A_c , l_e , and other constants for a given core into a single quantity called the *inductance index*, A_L . The inductance index relates the inductance to the number of turns for a particular core. This simplification reduces Equation 1-12 to:

$$L = N^2 A_L \text{ nanohenries} \quad (\text{Eq. 1-13})$$

where,

L = the inductance in nanohenries,

N = the number of turns,

A_L = the inductance index in nanohenries/turn²

Thus, the number of turns to be wound on a given core for a specific inductance is given by:

$$N = \sqrt{\frac{L}{A_L}} \quad (\text{Eq. 1-14})$$

This is shown in Example 1-6.

The Q of the inductor cannot be *calculated* with the information given in Fig. 1-25. If we look at the X_p/N^2 , R_p/N^2 vs. Frequency curves given for the BBR-7403, however, we can make a calculated guess. At low frequencies (100 kHz), the Q of the coil would be approximately 54, where,

$$\begin{aligned} Q &= \frac{R_p/N^2}{X_p/N^2} \\ &= \frac{R_p}{X_p} \end{aligned} \quad (\text{Eq. 1-16})$$

As the frequency increases, resistance R_p decreases

EXAMPLE 1-6

Using the data given in Fig. 1-25, design a toroidal inductor with an inductance of 50 μH . What is the largest AWG wire that we could possibly use while still maintaining a single-layer winding? What is the inductor's Q at 100 MHz?

Solution

There are numerous possibilities in this particular design since no constraints were placed on us. Fig. 1-25 is a data sheet for the Indiana General 7400 Series of ferrite toroidal cores. This type of core would normally be used in broadband or low-Q transformer applications rather than in narrow-band tuned circuits. This exercise will reveal why.

The mechanical specifications for this series of cores indicate a fairly typical size for toroids used in small-signal rf circuit design. The largest core for this series is just under a quarter of an inch in diameter. Since no size constraints were placed on us in the problem statement, we will use the BBR-7403 which has an outside diameter of 0.0230 inch. This will allow us to use a larger diameter wire to wind the inductor.

The published value for A_L for the given core is 495 nH/turn^2 . Using Equation 1-14, the number of turns required for this core is:

$$\begin{aligned} N &= \sqrt{\frac{50,000 \text{ nH}}{495 \text{ nH/turn}^2}} \\ &= 10 \text{ turns} \end{aligned}$$

Note that the inductance of 50 μH was replaced with its equivalent of 50,000 nH. The next step is to determine the largest diameter wire that can be used to wind the transformer while still maintaining a single-layer winding. In some cases, the data supplied by the manufacturer will include this type of winding information. Thus, in those cases, the designer need only look in a table to determine the maximum wire size that can be used. In our case, this information was not given, so a simple calculation must be made. Fig. 1-27 illustrates the geometry of the problem. It is obvious from the diagram that the inner radius (r_1) of

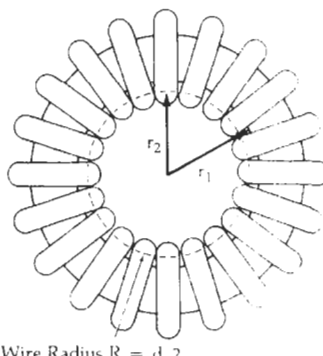


Fig. 1-27. Toroid coil winding geometry.

the toroid is the limiting factor in determining the maximum number of turns for a given wire diameter. The exact maximum diameter wire for a given number of turns can be found by:

$$d = \frac{2\pi r_1}{N + \pi} \quad (\text{Eq. 1-15})$$

where,

- d = the diameter of the wire in inches,
- r_1 = the inner radius of the core in inches,
- N = the number of turns.

For this example, we obtain the value of r_1 from Fig. 1-25 ($d_2 = 0.120$ inch).

$$\begin{aligned} d &= \frac{2\pi \frac{0.120}{2}}{10 + \pi} \\ &= 28.69 \times 10^{-3} \text{ inches} \\ &= 28.69 \text{ mils} \end{aligned}$$

As a practical rule of thumb, however, taking into account the insulation thickness variation among manufacturers, it is best to add a "fudge factor" and take 90% of the calculated value, or 25.82 mils. Thus, the largest diameter wire used would be the next size below 25.82 mils, which is AWG No. 22 wire.

EXAMPLE 1-7

Using the information provided in the data sheet of Fig. 1-26, design a high-Q ($Q > 80$), 300 nH, toroidal inductor for use at 100 MHz. Due to pc board space available, the toroid may not be any larger than 0.3 inch in diameter.

Solution

Fig. 1-26 is an excerpt from an Amidon Associates iron-powder toroidal-core data sheet. The recommended operating frequencies for various materials are shown in the Iron-Powder Material vs. Frequency Range graph. Either material No. 12 or material No. 10 seems to be well suited for operation at 100 MHz. Elsewhere on the data sheet, material No. 12 is listed as IRN-8. (IRN-8 is described in Table 1-3.) Material No. 10 is not described, so choose material No. 12.

Then, under a heading of Iron-Powder Toroidal Cores, the data sheet lists the physical dimensions of the toroids along with the value of A_L for each. Note, however, that this particular company chooses to specify A_L in $\mu\text{H}/100$ turns rather than $\mu\text{H}/100 \text{ turns}^2$. The conversion factor between their value of A_L and A_L in nH/turn^2 is to divide their value of A_L by 10. Thus, the T-80-12 core with an A_L of 22 $\mu\text{H}/100$ turns is equal to 2.2 nH/turn^2 .

Next, the data sheet lists a set of Q-curves for the cores listed in the preceding charts. Note that all of the curves shown indicate Qs that are greater than 80 at 100 MHz.

Choose the largest core available that will fit in the allotted pc board area. The core you should have chosen is the number T-25-12, with an outer diameter of 0.255 inch.

$$\begin{aligned} A_L &= 12 \mu\text{H}/100 \\ &\approx 1.2 \text{ nH/turn}^2 \end{aligned}$$

Therefore, using Equation 1-14, the number of turns required is

$$\begin{aligned} N &= \sqrt{\frac{L}{A_L}} \\ &= \sqrt{\frac{300}{1.2}} \\ &= 15.81 \\ &= 16 \text{ turns} \end{aligned}$$

Finally, the chart of Number of Turns vs. Wire Size and Core Size on the data sheet clearly indicates that, for a T-25 size core, the largest size wire we can use to wind this particular toroid is No. 28 AWG wire.

while reactance X_p increases. At about 3 MHz, X_p equals R_p and the Q becomes unity. The Q then falls below unity until about 100 MHz where resistance R_p begins to increase dramatically and causes the Q to again pass through unity. Thus, due to losses in the core itself, the Q of the coil at 100 MHz is probably very close to 1. Since the Q is so low, this coil would not be a very good choice for use in a narrow-band tuned circuit. See Example 1-7.

PRACTICAL WINDING HINTS

Fig. 1-28 depicts the correct method for winding a toroid. Using the technique of Fig. 1-28A, the interwinding capacitance is minimized, a good portion of the available winding area is utilized, and the resonant frequency of the inductor is increased, thus extending the useful frequency range of the device. Note that by using the methods shown in Figs. 1-28B and 1-28C, both lead capacitance and interwinding capacitance will affect the toroid.

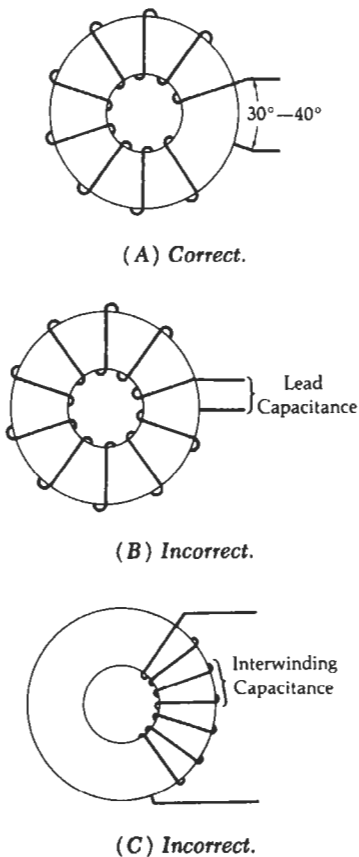
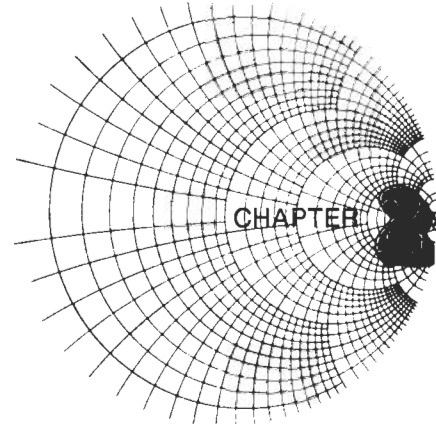


Fig. 1-28. Practical winding hints.



RESONANT CIRCUITS

In this chapter, we will explore the parallel resonant circuit and its characteristics at radio frequencies. We will examine the concept of loaded-Q and how it relates to source and load impedances. We will also see the effects of component losses and how they affect circuit operation. Finally, we will investigate some methods of coupling resonant circuits to increase their selectivity.

SOME DEFINITIONS

The resonant circuit is certainly nothing new in rf circuitry. It is used in practically every transmitter, receiver, or piece of test equipment in existence, to selectively pass a certain frequency or group of frequencies from a source to a load while attenuating all other frequencies outside of this passband. The perfect resonant-circuit *passband* would appear as shown in Fig. 2-1. Here we have a perfect rectangular-shaped passband with infinite attenuation above and below the frequency band of interest, while allowing the desired signal to pass undisturbed. The realization of this filter is, of course, impossible due to the physical characteristics of the components that make up a filter. As we learned in Chapter 1, there is no perfect component and, thus, there can be no perfect filter. If we understand the mechanics of resonant circuits, however, we can certainly tailor an imperfect circuit to suit our needs just perfectly.

Fig. 2-2 is a diagram of what a practical filter re-

sponse might resemble. Appropriate definitions are presented below:

1. **Bandwidth**—The bandwidth of any resonant circuit is most commonly defined as being the difference between the upper and lower frequency ($f_2 - f_1$) of the circuit at which its amplitude response is 3 dB below the passband response. It is often called the half-power bandwidth.
2. **Q** —The ratio of the center frequency of the resonant circuit to its bandwidth is defined as the circuit Q .

$$Q = \frac{f_c}{f_2 - f_1} \quad (\text{Eq. 2-1})$$

This Q should not be confused with component Q which was defined in Chapter 1. Component Q does have an effect on circuit Q , but the reverse is not true. Circuit Q is a measure of the selectivity of a resonant circuit. The higher its Q , the narrower its bandwidth, the higher is the selectivity of a resonant circuit.

3. **Shape Factor**—The shape factor of a resonant circuit is typically defined as being the ratio of the 60-dB bandwidth to the 3-dB bandwidth of the resonant circuit. Thus, if the 60-dB bandwidth ($f_4 - f_3$) were 3 MHz and the 3-dB bandwidth ($f_2 - f_1$) were 1.5 MHz, then the shape factor would be:

$$\begin{aligned} SF &= \frac{3 \text{ MHz}}{1.5 \text{ MHz}} \\ &= 2 \end{aligned}$$

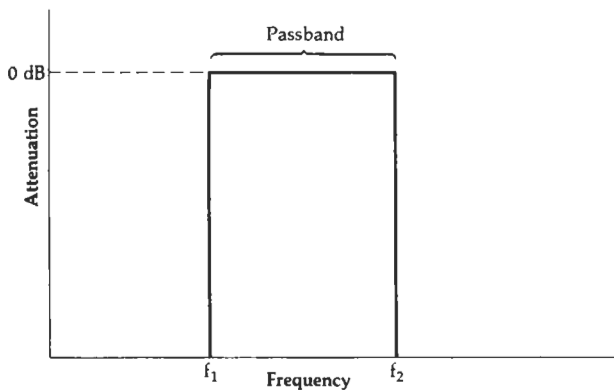


Fig. 2-1. The perfect filter response.

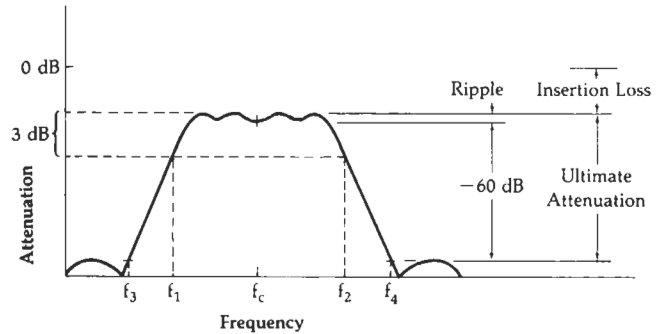


Fig. 2-2. A practical filter response.

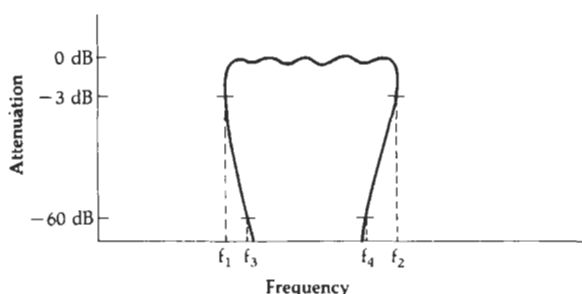


Fig. 2-3. An impossible shape factor.

Shape factor is simply a degree of measure of the steepness of the skirts. The smaller the number, the steeper are the response skirts. Notice that our perfect filter in Fig. 2-1 has a shape factor of 1, which is the ultimate. The passband for a filter with a shape factor smaller than 1 would have to look similar to the one shown in Fig. 2-3. Obviously, this is a physical impossibility.

4. **Ultimate Attenuation**—Ultimate attenuation, as the name implies, is the final *minimum* attenuation that the resonant circuit presents outside of the specified passband. A perfect resonant circuit would provide infinite attenuation outside of its passband. However, due to component imperfections, infinite attenuation is infinitely impossible to get. Keep in mind also, that if the circuit presents response peaks outside of the passband, as shown in Fig. 2-2, then this, of course, detracts from the ultimate attenuation specification of that resonant circuit.
5. **Insertion Loss**—Whenever a component or group of components is inserted between a generator and its load, some of the signal from the generator is absorbed in those components due to their inherent resistive losses. Thus, not as much of the transmitted signal is transferred to the load as when the load is connected directly to the generator. (I am assuming here that no impedance matching function is being performed.) The attenuation that results is called *insertion loss* and it is a very important characteristic of resonant circuits. It is usually expressed in decibels (dB).
6. **Ripple**—Ripple is a measure of the flatness of the passband of a resonant circuit and it is also expressed in decibels. Physically, it is measured in the response characteristics as the difference between the maximum attenuation *in the passband* and the minimum attenuation in the passband. In Chapter 3, we will actually design filters for a specific passband ripple.

RESONANCE (LOSSLESS COMPONENTS)

In Chapter 1, the concept of resonance was briefly mentioned when we studied the parasitics associated with individual component elements. We will now examine the subject of resonance in detail. We will

determine what causes resonance to occur and how we can use it to our best advantage.

The voltage division rule (illustrated in Fig. 2-4) states that whenever a shunt element of impedance Z_p is placed across the output of a generator with an internal resistance R_s , the maximum output voltage available from this circuit is

$$V_{out} = \frac{Z_p}{R_s + Z_p} (V_{in}) \quad (\text{Eq. 2-2})$$

Thus, V_{out} will always be less than V_{in} . If Z_p is a frequency-dependent impedance, such as a capacitive or inductive reactance, then V_{out} will also be frequency dependent and the ratio of V_{out} to V_{in} , which is the gain (or, in this case, loss) of the circuit, will also be frequency dependent. Let's take, for example, a 25-pF capacitor as the shunt element (Fig. 2-5A) and plot the function of V_{out}/V_{in} in dB versus frequency, where we have:

$$\frac{V_{out}}{V_{in}} = 20 \log_{10} \frac{X_C}{R_s + X_C} \quad (\text{Eq. 2-3})$$

where,

$\frac{V_{out}}{V_{in}}$ = the loss in dB,

R_s = the source resistance,

X_C = the reactance of the capacitor.

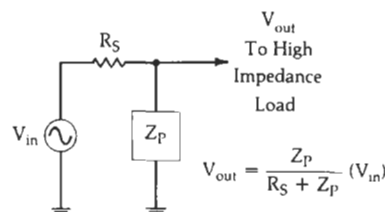
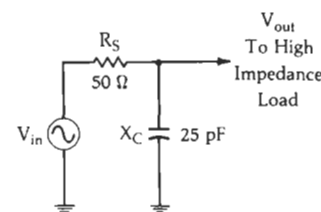
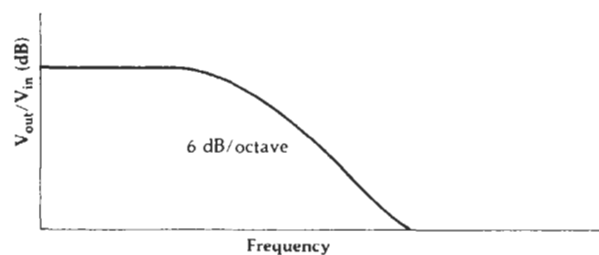


Fig. 2-4. Voltage division rule.



(A) Simple circuit.



(B) Response curve.

Fig. 2-5. Frequency response of a simple RC low-pass filter.

and, where,

$$X_C = \frac{1}{j\omega C}.$$

The plot of this equation is shown in the graph of Fig. 2-5B. Notice that the loss of this circuit increases as the frequency increases; thus, we have formed a simple *low-pass filter*. Notice, also, that the attenuation slope eventually settles down to the rate of 6 dB for every octave (doubling) increase in frequency. This is due to the single reactive element in the circuit. As we will see later, this attenuation slope will increase an additional 6 dB for each *significant* reactive element that we insert into the circuit.

If we now delete the capacitor from the circuit and insert a 0.05- μ H inductor in its place, we obtain the circuit of Fig. 2-6A and the plot of Fig. 2-6B, where we are plotting:

$$\frac{V_{out}}{V_{in}} = 20 \log_{10} \frac{X_L}{R_s + X_L} \quad (\text{Eq. 2-4})$$

where,

$\frac{V_{out}}{V_{in}}$ = the loss in dB,

R_s = the source resistance,

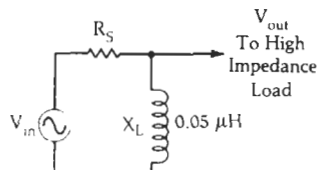
X_L = the reactance of the coil.

and, where,

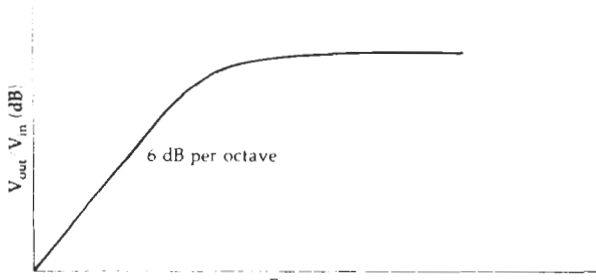
$$X_L = j\omega L.$$

Here, we have formed a simple *high-pass filter* with a final attenuation slope of 6 dB per octave.

Thus, through simple calculations involving the basic voltage division formula (Equation 2-2), we were able to plot the frequency response of two separate and opposite reactive components. But what happens if we place both the inductor and capacitor



(A) Simple circuit.



(B) Response curve.

Fig. 2-6. Simple high-pass filter.

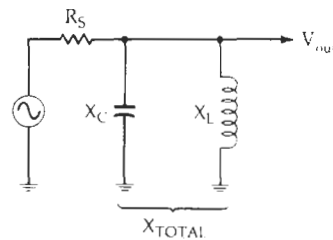


Fig. 2-7. Resonant circuit with two reactive components.

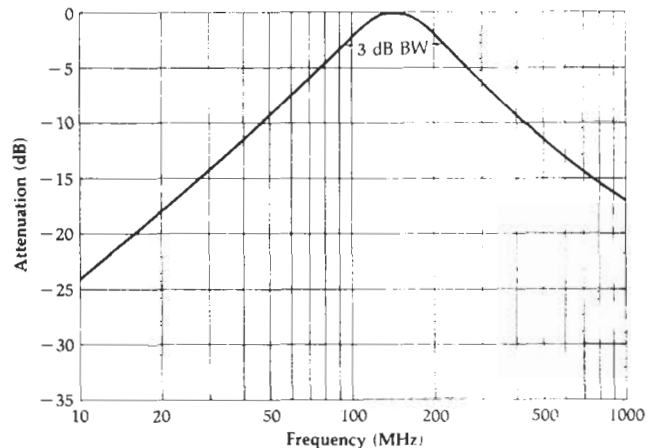


Fig. 2-8. Frequency response of an LC resonant circuit.

across the generator simultaneously? Actually, this case is no more difficult to analyze than the previous two circuits. In fact, at any frequency, we can simply apply the basic voltage division rule as before. The only difference here is that we now have two reactive components to deal with instead of one and these components are in parallel (Fig. 2-7). If we make the calculation for all frequencies of interest, we will obtain the plot shown in Fig. 2-8. The mathematics behind this calculation are as follows:

$$V_{out} = \frac{X_{total}}{R_s + X_{total}} (V_{in}) \quad (\text{Eq. 2-5})$$

where,

$$X_{total} = \frac{X_C X_L}{X_C + X_L}.$$

and, where,

$$X_C = \frac{1}{j\omega C},$$

$$X_L = j\omega L.$$

Therefore, we have:

$$\begin{aligned} X_{total} &= \frac{\frac{1}{j\omega C} (j\omega L)}{\frac{1}{j\omega C} + j\omega L} \\ &= \frac{\frac{L}{C}}{\frac{1}{j\omega C} + j\omega L} \end{aligned}$$

Multiply the numerator and the denominator by $j\omega C$. (Remember that $j^2 = -1$.)

$$\begin{aligned} X_{\text{total}} &= \frac{j\omega L}{1 + (j\omega L)(j\omega C)} \\ &= \frac{j\omega L}{1 - \omega^2 LC} \end{aligned}$$

Thus, substituting and transposing in Equation 2-5, we have:

$$\frac{V_{\text{out}}}{V_{\text{in}}} = \frac{\frac{j\omega L}{1 - \omega^2 LC}}{R_s + \frac{j\omega L}{1 - \omega^2 LC}}$$

Multiplying the numerator and the denominator through by $1 - \omega^2 LC$ yields:

$$\frac{V_{\text{out}}}{V_{\text{in}}} = \frac{j\omega L}{(R_s - \omega^2 R_s LC) + j\omega L}$$

Thus, the loss at any frequency may be calculated from the above equation or, if needed, in dB.

$$\frac{V_{\text{out}}}{V_{\text{in}}} = 20 \log_{10} \left| \frac{j\omega L}{R_s - \omega^2 R_s LC + j\omega L} \right|$$

where $\left| \cdot \right|$ represents the magnitude of the quantity within the brackets.

Notice, in Fig. 2-8, that as we near the resonant frequency of the tuned circuit, the slope of the resonance curve increases to 12 dB/octave. This is due to the fact that we now have two *significant* reactances present and each one is changing at the rate of 6 dB/octave and sloping in opposite directions. As we move away from resonance in either direction, however, the curve again settles to a 6-dB/octave slope because, again, only one reactance becomes significant. The other reactance presents a very high impedance to the circuit at these frequencies and the circuit behaves as if the reactance were no longer there.

LOADED Q

The *Q* of a resonant circuit was defined earlier to be equal to the ratio of the center frequency of the circuit to its 3-dB bandwidth (Equation 2-1). This "circuit *Q*," as it was called, is often given the label *loaded Q* because it describes the passband characteristics of the resonant circuit under actual in-circuit or *loaded* conditions. The loaded *Q* of a resonant circuit is dependent upon three main factors. (These are illustrated in Fig. 2-9.)

1. The source resistance (R_s).
2. The load resistance (R_L).
3. The component *Q* as defined in Chapter 1.

Effect of R_s and R_L on the Loaded Q

Let's discuss briefly the role that source and load impedances play in determining the loaded *Q* of a resonant circuit. This role is probably best illustrated

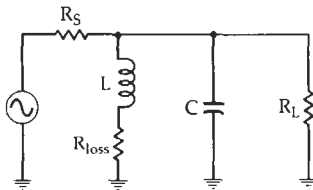


Fig. 2-9. Circuit for loaded-*Q* calculations.

through an example. In Fig. 2-8, we plotted a resonance curve for a circuit consisting of a 50-ohm source, a 0.05- μ H lossless inductor, and a 25-pF lossless capacitor. The loaded *Q* of this circuit, as defined by Equation 2-1 and determined from the graph, is approximately 1.1. Obviously, this is not a very narrow-band or high-*Q* design. But now, let's replace the 50-ohm source with a 1000-ohm source and again plot our results using the equation derived in Fig. 2-7 (Equation 2-5). This new plot is shown in Fig. 2-10. (The resonance curve for the 50-ohm source circuit is shown with dashed lines for comparison purposes.) Notice that the *Q*, or selectivity of the resonant circuit, has been increased dramatically to about 22. Thus, by raising the source impedance, we have increased the *Q* of our resonant circuit.

Neither of these plots addresses the effect of a load impedance on the resonance curve. If an external load of some sort were attached to the resonant circuit, as shown in Fig. 2-11A, the effect would be to broaden or "de-*Q*" the response curve to a degree that depends on the value of the load resistance. The equivalent circuit, for resonance calculations, is shown in Fig. 2-11B. The resonant circuit sees an equivalent resistance of R_s in parallel with R_L as its true load. This total external resistance is, by definition, smaller in value than either R_s or R_L , and the loaded *Q* must decrease. If we put this observation in equation form, it becomes (assuming lossless components):

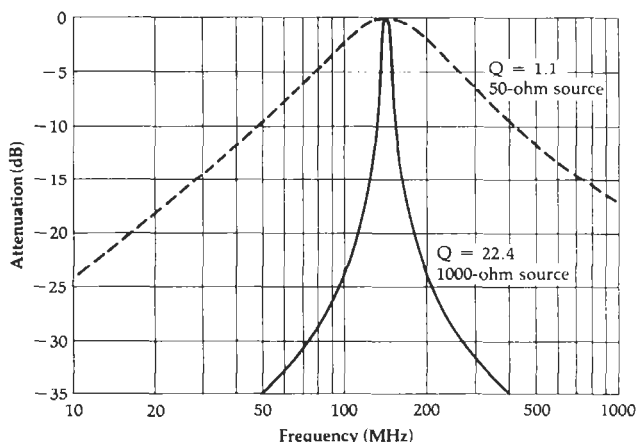
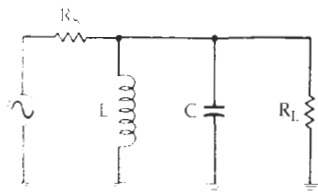
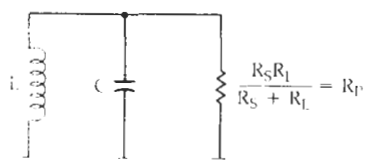


Fig. 2-10. The effect of R_s and R_L on loaded *Q*.



(A) Resonant circuit with an external load.



(B) Equivalent circuit for Q calculations.

Fig. 2-11. The equivalent parallel impedance across a resonant circuit.

$$Q = \frac{R_p}{X_p} \quad (\text{Eq. 2-6})$$

where,

R_p = the equivalent parallel resistance of R_s and R_L ,
 X_p = either the inductive or capacitive reactance.
 (They are equal at resonance.)

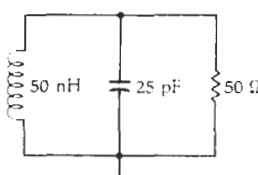
Equation 2-6 illustrates that a decrease in R_p will decrease the Q of the resonant circuit and an increase in R_p will increase the circuit Q , and it also illustrates another very important point. The same effect can be obtained by keeping R_p constant and varying X_p . Thus, for a given source and load impedance, the optimum Q of a resonant circuit is obtained when the inductor is a small value and the capacitor is a large value. Therefore, in either case, X_p is decreased. This effect is shown using the circuits in Fig. 2-12 and the characteristics curves in Fig. 2-13.

The circuit designer, therefore, has two approaches he can follow in designing a resonant circuit with a particular Q (Example 2-1).

1. He can select an optimum value of source and load impedance.
2. He can select component values of L and C which optimize Q .

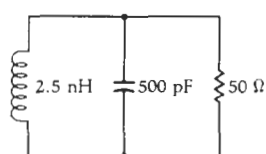
Often there is no real choice in the matter because, in many instances, the source and load are defined and we have no control over them. When this occurs, X_p

$$Q \approx 1.1 \quad f = 142.35 \text{ MHz}$$

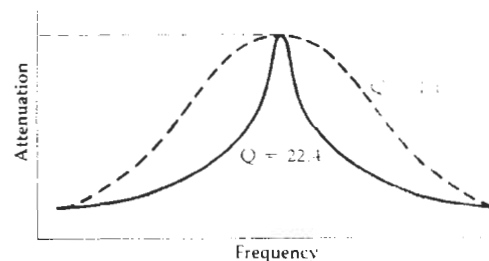


(A) Large inductor, small capacitor

$$Q \approx 22.4, f = 142.35 \text{ MHz}$$



(B) Small inductor, large capacitor

Fig. 2-12. Effect of Q vs. X_p at 142.35 MHz.Fig. 2-13. Plot of loaded- Q curves for circuits in Fig. 2-12.

is automatically defined for a given Q and we usually end up with component values that are impractical at best. Later in this chapter, we will study some methods of eliminating this problem.

EXAMPLE 2-1

Design a resonant circuit to operate between a source resistance of 150 ohms and a load resistance of 1000 ohms. The loaded Q must be equal to 20 at the resonant frequency of 50 MHz. Assume lossless components and no impedance matching.

Solution

The effective parallel resistance across the resonant circuit is 150 ohms in parallel with 1000 ohms, or

$$R_p = 130 \text{ ohms}$$

Thus, using Equation 2-6:

$$\begin{aligned} X_p &= \frac{R_p}{Q} \\ &= \frac{130}{20} \\ &= 6.5 \text{ ohms} \end{aligned}$$

and,

$$X_p = \omega L = \frac{1}{\omega C}$$

Therefore, $L = 20.7 \text{ nH}$, and $C = 489.7 \text{ pF}$.

The Effect of Component Q on Loaded Q

Thus far in this chapter, we have assumed that the components used in the resonant circuits are lossless and, thus, produce no degradation in loaded Q . In reality, however, such is not the case and the individual component Q 's must be taken into account. In a lossless resonant circuit, the impedance seen across the circuit's terminals at resonance is infinite. In a practical circuit, however, due to component losses, there exists some finite equivalent parallel resistance. This is illustrated in Fig. 2-14. The resistance (R_p) and its associated shunt reactance (X_p) can be found from the following transformation equations:

$$R_p = (Q^2 + 1)R_s \quad (\text{Eq. 2-7})$$

where,

R_p = the equivalent parallel resistance,
 R_s = the series resistance of the component.

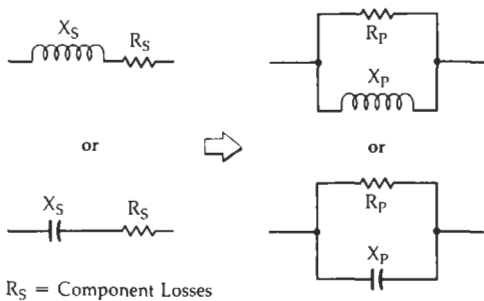


Fig. 2-14. A series-to-parallel transformation.

$Q = Q_s$ which equals Q_p which equals the Q of the component.

and,

$$X_p = \frac{R_p}{Q_p} \quad (\text{Eq. 2-8})$$

If the Q of the component is greater than 10, then,

$$R_p \approx Q^2 R_s \quad (\text{Eq. 2-9})$$

and,

$$X_p \approx X_s \quad (\text{Eq. 2-10})$$

These transformations are valid at only one frequency because they involve the component reactance which is frequency dependent (Example 2-2).

Example 2-2 vividly illustrates the potential drastic effects that can occur if poor-quality (low Q) components are used in highly selective resonant circuit designs. The net result of this action is that we effectively place a low-value shunt resistor directly across the circuit. As was shown earlier, any low-value resistance that shunts a resonant circuit drastically reduces its loaded Q and, thus, increases its bandwidth.

In most cases, we only need to involve the Q of the inductor in loaded- Q calculations. The Q of most capacitors is quite high over their useful frequency range, and the equivalent shunt resistance they present to the circuit is also quite high and can usually be neglected. Care must be taken, however, to ensure that this is indeed the case.

INSERTION LOSS

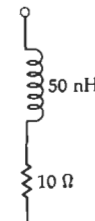
Insertion loss (defined earlier in this chapter) is another direct effect of component Q . If inductors and capacitors were perfect and contained no internal resistive losses, then insertion loss for LC resonant circuits and filters would not exist. This is, of course, not the case and, as it turns out, insertion loss is a very critical parameter in the specification of any resonant circuit.

Fig. 2-16 illustrates the effect of inserting a resonant circuit between a source and its load. In Fig. 2-16A, the source is connected directly to the load. Using the voltage division rule, we find that:

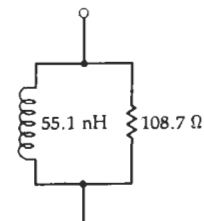
$$V_1 = 0.5 V_{in}$$

EXAMPLE 2-2

Given a 50-nanohenry coil as shown in Fig. 2-15A, compute its Q at 100 MHz. Then, transform the series circuit of Fig. 2-15A into the equivalent parallel inductance and resistance circuit of Fig. 2-15B.



(A) Series circuit.



(B) Equivalent parallel circuit.

Fig. 2-15. Example of a series-to-parallel transformation.

Solution

The Q of this coil at 100 MHz is, from Chapter 1,

$$\begin{aligned} Q &= \frac{X_s}{R_s} \\ &= \frac{2\pi(100 \times 10^6)(50 \times 10^{-9})}{10} \\ &= 3.14 \end{aligned}$$

Then, since the Q is less than 10, use Equation 2-7 to find R_p .

$$\begin{aligned} R_p &= (Q^2 + 1)R_s \\ &= [(3.14)^2 + 1]10 \\ &= 108.7 \text{ ohms} \end{aligned}$$

Next, we find X_p using Equation 2-8:

$$\begin{aligned} X_p &= \frac{R_p}{Q_p} \\ &= \frac{108.7}{3.14} \\ &= 34.62 \end{aligned}$$

Thus, the parallel inductance becomes:

$$\begin{aligned} L_p &= \frac{X_p}{\omega} \\ &= \frac{34.62}{2\pi(100 \times 10^6)} \\ &= 55.1 \text{ nH} \end{aligned}$$

These values are shown in the equivalent circuit of Fig. 2-15B.

Fig. 2-16B shows that a resonant circuit has been placed between the source and the load. Then, Fig. 2-16C illustrates the equivalent circuit at resonance. Notice that the use of an inductor with a Q of 10 at the resonant frequency creates an effective shunt resistance of 4500 ohms at resonance. This resistance, combined with R_L , produces an 0.9-dB voltage loss at V_1 when compared to the equivalent point in the circuit of Fig. 2-16A.

An insertion loss of 0.9 dB doesn't sound like much, but it can add up very quickly if we cascade several

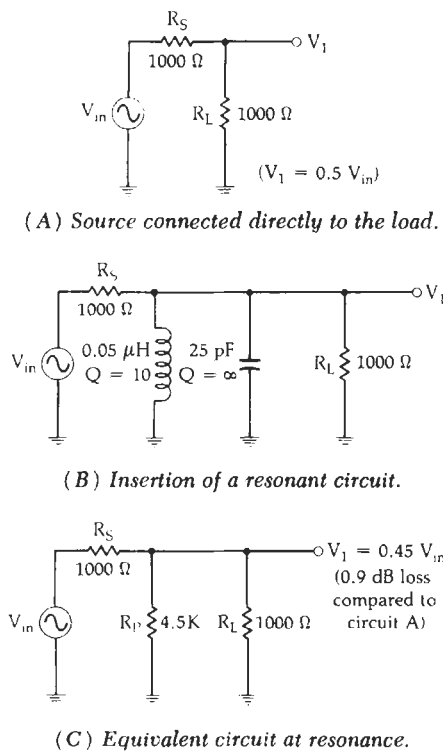


Fig. 2-16. The effect of component Q on insertion loss.

resonant circuits. We will see some very good examples of this later in Chapter 3. For now, examine the problem given in Example 2-3.

IMPEDANCE TRANSFORMATION

As we have seen in earlier sections of this chapter, low values of source and load impedance tend to load a given resonant circuit down and, thus, tend to decrease its loaded Q and increase its bandwidth. This makes it very difficult to design a simple LC high-Q resonant circuit for use between two very low values of source and load resistance. In fact, even if we were able to come up with a design on paper, it most likely would be impossible to build due to the extremely small (or negative) inductor values that would be required.

One method of getting around this potential design problem is to make use of one of the impedance transforming circuits shown in Fig. 2-18. These handy circuits fool the resonant circuit into seeing a source or load resistance that is much larger than what is actually present. For example, an impedance transformer could present an impedance (R'_s) of 500 ohms to the resonant circuit, when in reality there is an impedance (R_s) of 50 ohms. Consequently, by utilizing these transformers, both the Q of the resonant tank and its selectivity can be increased. In many cases, these methods can make a previously unworkable problem workable again, complete with realistic values for the coils and capacitors involved.

The design equations for each of the transformers

are presented in the following equations and are useful for designs that need loaded Q's that are greater than 10 (Example 2-4). For the tapped-C transformer (Fig. 2-18A), we use the formula:

$$R'_s = R_s \left(1 + \frac{C_1}{C_2} \right)^2 \quad (\text{Eq. 2-13})$$

The equivalent capacitance (C_T) that will resonate with the inductor is equal to C_1 in series with C_2 , or:

$$C_T = \frac{C_1 C_2}{C_1 + C_2} \quad (\text{Eq. 2-14})$$

For the tapped-L network of Fig. 2-18B, we use the following formula:

$$R'_s = R_s \left(\frac{n}{n_1} \right)^2 \quad (\text{Eq. 2-15})$$

As an exercise, you might want to rework Example 2-4 without the aid of an impedance transformer. You will find that the inductor value which results is much more difficult to obtain and control physically because it is so small.

COUPLING OF RESONANT CIRCUITS

In many applications where steep passband skirts and small shape factors are needed, a single resonant circuit might not be sufficient. In situations such as this, individual resonant circuits are often coupled together to produce more attenuation at certain frequencies than would normally be available with a single resonator. The coupling mechanism that is used is generally chosen specifically for each application as each type of coupling has its own peculiar characteristics that must be dealt with. The most common forms of coupling are: capacitive, inductive, transformer (mutual), and active (transistor).

Capacitive Coupling

Capacitive coupling is probably the most frequently used method of linking two or more resonant circuits. This is true mainly due to the simplicity of the arrangement but another reason is that it is relatively inexpensive. Fig. 2-19 indicates the circuit arrangement for a two-resonator capacitively coupled filter.

The value of the capacitor that is used to couple each resonator cannot be just chosen at random, as Fig. 2-20 indicates. If capacitor C_{12} of Fig. 2-19 is too large, too much coupling occurs and the frequency response broadens drastically with two response peaks in the filter's passband. If capacitor C_{12} is too small, not enough signal energy is passed from one resonant circuit to the other and the insertion loss can increase to an unacceptable level. The compromise solution to these two extremes is the point of *critical coupling*, where we obtain a reasonable bandwidth and the lowest possible insertion loss and, consequently, a maximum transfer of signal power. There are instances in

EXAMPLE 2-3

Design a simple parallel resonant circuit to provide a 3-dB bandwidth of 10 MHz at a center frequency of 100 MHz. The source and load impedances are each 1000 ohms. Assume the capacitor to be lossless. The Q of the inductor (that is available to us) is 85. What is the insertion loss of the network?

Solution

From Equation 2-1, the required loaded Q of the resonant circuit is:

$$\begin{aligned} Q &= \frac{f_c}{f_2 - f_1} \\ &= \frac{100 \text{ MHz}}{10 \text{ MHz}} \\ &= 10 \end{aligned}$$

To find the inductor and capacitor values needed to complete the design, it is necessary that we know the equivalent shunt resistance and reactance of the components at resonance. Thus, from Equation 2-8:

$$X_p = \frac{R_p}{Q_p}$$

where,

X_p = the reactance of the inductor and capacitor at resonance,

R_p = the equivalent shunt resistance of the inductor,

Q_p = the Q of the inductor.

Thus,

$$R_p = (85)X_p \quad (\text{Eq. 2-11})$$

The loaded Q of the resonant circuit is equal to:

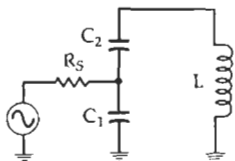
$$Q = \frac{R_{\text{total}}}{X_p}$$

$$10 = \frac{R_{\text{total}}}{X_p}$$

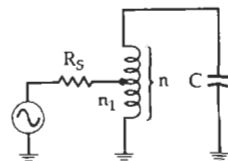
where,

R_{total} = the shunt resistance, which equals $R_p \parallel R_s \parallel R_L$. Therefore, we have:

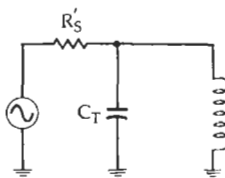
$$10 = \frac{R_p(500)}{R_p + 500} \quad (\text{Eq. 2-12})$$



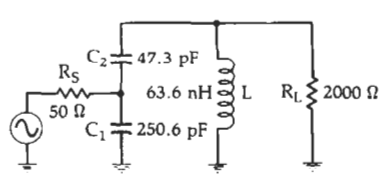
(A) Tapped-C circuit.



(B) Tapped-L circuit.



(C) Equivalent circuit.



(D) Final circuit.

Fig. 2-18. Two methods used to perform an impedance transformation.

which overcoupling or undercoupling might serve a useful purpose in a design, such as in tailoring a specific frequency response that a critically coupled filter

We now have two equations and two unknowns (X_p , R_p). If we substitute Equation 2-11 into Equation 2-12 and solve for X_p , we get:

$$X_p = 44.1 \text{ ohms}$$

Plugging this value back into Equation 2-11 gives:

$$R_p = 3.75 \text{ k}\Omega$$

Thus, our component values must be

$$L = \frac{X_p}{\omega} = 70 \text{ nH}$$

$$C = \frac{1}{\omega X_p} = 36 \text{ pF}$$

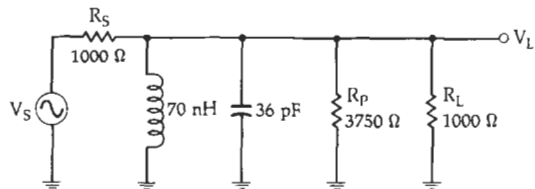


Fig. 2-17. Resonant circuit design for Example 2-3.

The final circuit is shown in Fig. 2-17.

The insertion-loss calculation, at center frequency, is now very straightforward and can be found by applying the voltage division rule as follows. Resistance R_p in parallel with resistance R_L is equal to 789.5 ohms. The voltage at V_L is, therefore,

$$\begin{aligned} V_L &= \frac{789.5}{789.5 + 1000} (V_s) \\ &= .44 \text{ V}_s \end{aligned}$$

The voltage at V_L , without the resonant circuit in place, is equal to 0.5 V_s due to the 1000-ohm load. Thus, we have:

$$\begin{aligned} \text{Insertion Loss} &= 20 \log_{10} \frac{0.44 \text{ V}_s}{0.5 \text{ V}_s} \\ &= 1.1 \text{ dB} \end{aligned}$$

cannot provide. But these applications are generally left to the multiple resonator filter. The multiple resonator filter is covered in Chapter 3. In this section, we will only concern ourselves with critical coupling as it pertains to resonant circuit design.

The loaded Q of a critically coupled two-resonator circuit is approximately equal to 0.707 times the loaded Q of one of its resonators. Therefore, the 3-dB bandwidth of a two-resonator circuit is actually wider than that of one of its resonators. This might seem contrary to what we have studied so far, but remember, the

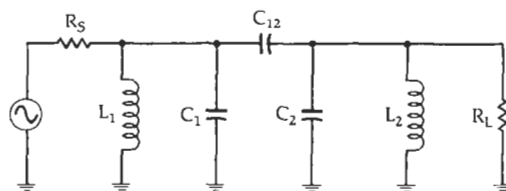


Fig. 2-19. Capacitive coupling.

EXAMPLE 2-4

Design a resonant circuit with a loaded Q of 20 at a center frequency of 100 MHz that will operate between a source resistance of 50 ohms and a load resistance of 2000 ohms. Use the tapped-C approach and assume that inductor Q is 100 at 100 MHz.

Solution

We will use the tapped-C transformer to step the source resistance up to 2000 ohms to match the load resistance for optimum power transfer. (Impedance matching will be covered in detail in Chapter 4.) Thus,

$$R_s' = 2000 \text{ ohms}$$

and from Equation 2-13, we have:

$$\frac{C_1}{C_2} = \sqrt{\frac{R_s'}{R_s}} - 1 \\ = 5.3$$

or,

$$C_1 = 5.3C_2 \quad (\text{Eq. 2-16})$$

Proceeding as we did in Example 2-3, we know that for the inductor:

$$Q_p = \frac{R_p}{X_p} = 100$$

Therefore,

$$R_p = 100 X_p \quad (\text{Eq. 2-17})$$

We also know that the loaded Q of the resonant circuit is equal to:

$$Q = \frac{R_{\text{total}}}{X_p}$$

where,

$$R_{\text{total}} = \text{the total equivalent shunt resistance,} \\ = R_s' \parallel R_p \parallel R_L \\ = 1000 \parallel R_p$$

and, where we have taken R_s' and R_L to each be 2000 ohms, in parallel. Hence, the loaded Q is

$$Q = \frac{1000R_p}{(1000 + R_p)X_p} \quad (\text{Eq. 2-18})$$

Substituting Equation 2-17 (and the value of the desired loaded Q) into Equation 2-18, and solving for X_p , yields:

$$X_p = 40 \text{ ohms}$$

And, substituting this result back into Equation 2-17 gives

$$R_p = 4000 \text{ ohms}$$

and,

$$L = \frac{X_p}{\omega} \\ = 63.6 \text{ nH} \\ C_T = \frac{1}{X_p \omega} \\ = 39.78 \text{ pF}$$

We now know what the total capacitance must be to resonate with the inductor. We also know from Equation 2-16 that C_1 is 5.3 times larger than C_2 . Thus, if we substitute Equation 2-16 into Equation 2-14, and solve the equations simultaneously, we get:

$$C_2 = 47.3 \text{ pF}$$

$$C_1 = 250.6 \text{ pF}$$

The final circuit is shown in Fig. 2-18D.

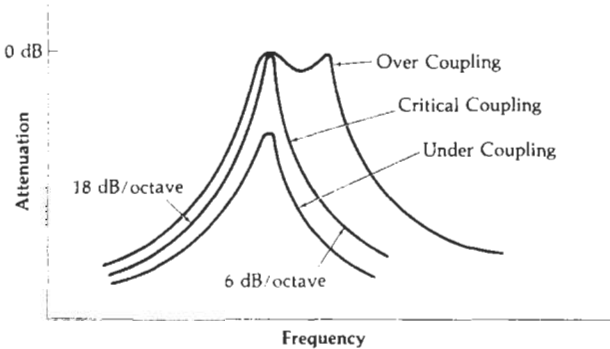


Fig. 2-20. The effects of various values of capacitive coupling on passband response.

main purpose of the two-resonator passively coupled filter is not to provide a narrower 3-dB bandwidth, but to increase the steepness of the stopband skirts and, thus, to reach an ultimate attenuation much faster than a single resonator could. This characteristic is shown in Fig. 2-21. Notice that the shape factor has decreased for the two-resonator design. Perhaps one way to get an intuitive feel for how this occurs is to consider that each resonator is itself a load for the other resonator, and each decreases the loaded Q of the other. But as we move away from the passband and into the stopband, the response tends to fall much

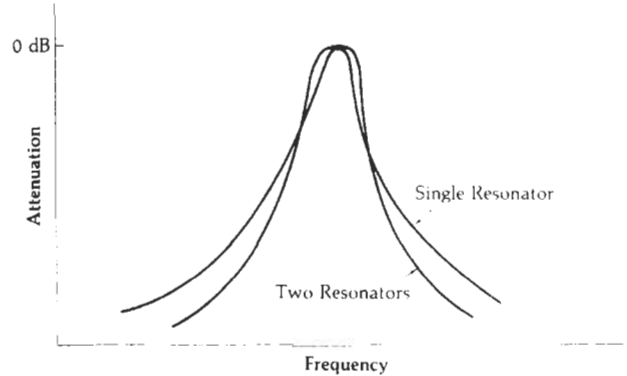


Fig. 2-21. Selectivity of single- and two-resonator designs.

more quickly due to the *combined* response of each resonator.

The value of the capacitor used to couple two identical resonant circuits is given by

$$C_{12} = \frac{C}{Q} \quad (\text{Eq. 2-19})$$

where,

C_{12} = the coupling capacitance.

C = the resonant circuit capacitance,

Q = the loaded Q of a single resonator.

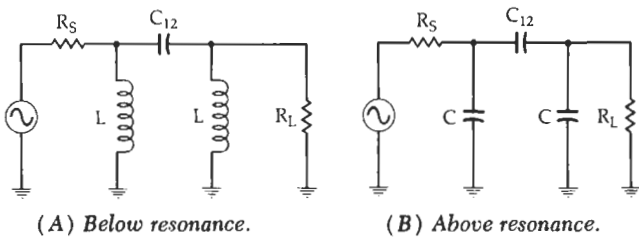


Fig. 2-22. Equivalent circuit of capacitively coupled resonant circuits.

One other important characteristic of a capacitively coupled resonant circuit can be seen if we take another look at Fig. 2-20. Notice that even for the critically coupled case, the response curve is not symmetric around the center frequency but is skewed somewhat. The lower frequency portion of the response plummets down at the rate of 18 dB per octave while the upper slope decreases at only 6 dB per octave. This can be explained if we take a look at the equivalent circuit both above and below resonance. Below resonance, we have the circuit of Fig. 2-22A. The reactance of the two resonant-circuit capacitors (Fig. 2-19) has increased, and the reactance of the two inductors has decreased to the point that only the inductor is seen as a shunt element and the capacitors can be ignored. This leaves three reactive components and each contributes 6 dB per octave to the response.

On the high side of resonance, the equivalent circuit approaches the configuration of Fig. 2-22B. Here the inductive reactance has increased above the capacitive reactance to the point where the inductive reactance can be ignored as a shunt element. We now have an arrangement of three capacitors that effectively looks like a single shunt capacitor and yields a slope of 6 dB per octave.

Inductive Coupling

Two types of inductively coupled resonant circuits are shown in Fig. 2-23. One type (Fig. 2-23A) uses

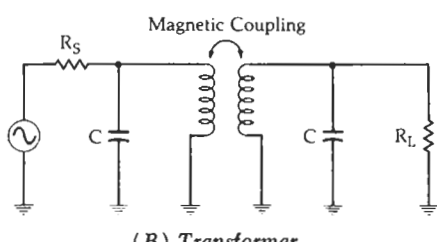
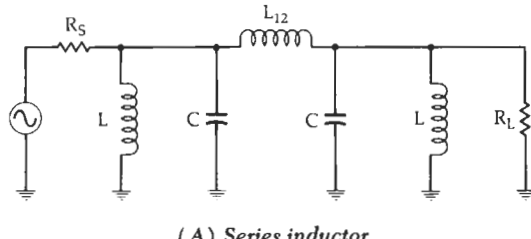


Fig. 2-23. Inductive coupling.

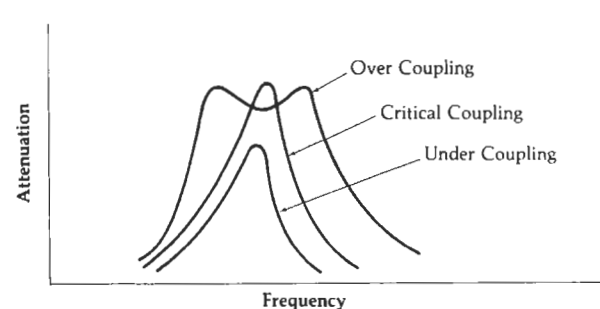
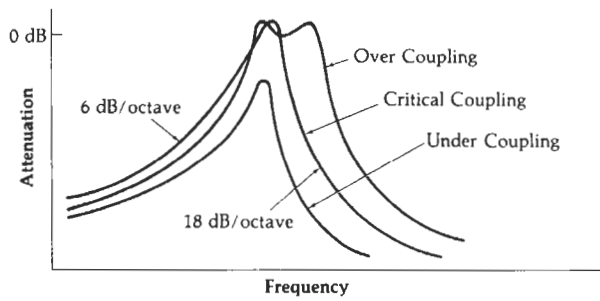


Fig. 2-24. The effects of various values of inductive coupling on passband response.

a series inductor or coil to transfer energy from the first resonator to the next, and the other type (Fig. 2-23B) uses transformer coupling for the same purpose. In either case, the frequency response curves will resemble those of Fig. 2-24 depending on the amount of coupling. If we compare Fig. 2-24A with Fig. 2-20, we see that the two are actually mirror images of each other. The response of the inductively coupled resonator is skewed toward the higher end of the frequency spectrum, while the capacitively coupled response is skewed toward the low frequency side. An examination of the equivalent circuit reveals why. Fig. 2-25A indicates that below resonance, the capaci-

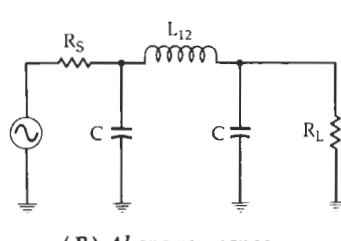
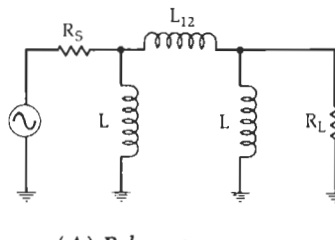


Fig. 2-25. Equivalent circuit of inductively coupled resonant circuits.

tors drop out of the equivalent circuit very quickly because their reactance becomes much greater than the shunt inductive reactance. This leaves an arrangement of three inductors which can be thought of as a single tapped inductor and which produces a 6-dB per octave rolloff. Above resonance, the shunt inductors can be ignored for the same reasons, and you have the circuit of Fig. 2-25B. We now have three effective elements in the equivalent circuit with each contributing 6 dB per octave to the response for a combined slope of 18 dB per octave.

The mirror-image characteristic of inductively and capacitively coupled resonant circuits is a very useful concept. This is especially true in applications that require symmetrical response curves. For example, suppose that a capacitively coupled design exhibited too much skew for your application. One very simple way to correct the problem would be to add a "top-L" coupled section to the existing network. The top-L coupling would attempt to skew the response in the opposite direction and would, therefore, tend to counteract any skew caused by the capacitive coupling. The net result is a more symmetric response shape.

The value of the inductor used to couple two identical resonant circuits can be found by

$$L_{12} = QL \quad (\text{Eq. 2-20})$$

where,

L_{12} = the inductance of the coupling inductor,
 Q = the loaded Q of a single resonator,
 L = the resonant circuit inductance.

A little manipulation of Equations 2-19 and 2-20 will reveal a very interesting point. The reactance of C_{12} calculated with Equation 2-19 will equal the reactance of L_{12} calculated with Equation 2-20 for the same operating Q and resonant frequency. The designer now has the option of changing any "top-C" coupled resonator to a top-L design simply by replacing the coupling capacitor with an inductor of equal reactance at the resonant frequency. When this is done, the degree of coupling, Q , and resonant frequency of the design will remain unchanged while the slope of the stopband skirts will flip-flop from one side to the other. For obvious reasons, top-L coupled designs work best in applications where the primary objective is a certain ultimate attenuation that must be met above the passband. Likewise, top-C designs are best for meeting ultimate attenuation specifications below the passband.

Transformer coupling does not lend itself well to an exact design procedure because there are so many factors which influence the degree of coupling. The geometry of the coils, the spacing between them, the core materials used, and the shielding, all have a pronounced effect on the degree of coupling attained in any design.

Probably the best way to design your own transformer is to use the old trial-and-error method. But do

it in an orderly fashion and be consistent. It's a very sad day when one forgets how he got from point A to point B, especially if point B is an improvement in the design. Remember:

1. Decreasing the spacing between the primary and secondary increases the coupling.
2. Increasing the permeability of the magnetic path increases the coupling.
3. Shielding a transformer decreases its loaded Q and has the effect of increasing the coupling.

Begin the design by setting the loaded Q of each resonator to about twice what will be needed in the actual design. Then, slowly decrease the spacing between the primary and secondary until the response broadens to the loaded Q that is actually needed. If that response can't be met, try changing the geometry of the windings or the permeability of the magnetic path. Then, vary the spacing again. Use this as an iterative process to zero-in on the response that is needed. Granted, this is not an exact process, but it works and, if documented, can be reproduced.

There are literally thousands of commercially available transformers on the market that just might suit your needs perfectly. So before the trial-and-error method is put into practice, try a little research—it just might save a lot of time and money.

Active Coupling

It is possible to achieve very narrow 3-dB bandwidths in cascaded resonant circuits through the use of active coupling. Active coupling, for this purpose, is defined as being either a transistor or vacuum tube which, at least theoretically, allows signal flow in only one direction (Fig. 2-26). If each of the tuned circuits is the same and if each has the same loaded Q , the total loaded Q of the cascaded circuit is approximately equal to

$$Q_{\text{total}} = \frac{Q}{\sqrt{2^{1/n} - 1}} \quad (\text{Eq. 2-21})$$

where,

Q_{total} = the total Q of the cascaded circuit,
 Q = the Q of each individual resonant circuit.
 n = the number of resonant circuits.

The first step in any design procedure must be to

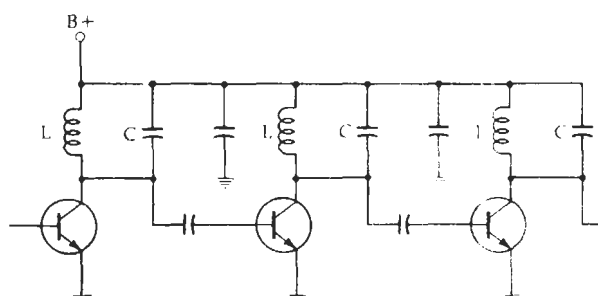


Fig. 2-26. Active coupling.

relate the required Q_{total} of the network back to the individual loaded Q of each resonator. This is done by rearranging Equation 2-21 to solve for Q . As an example, with $n = 4$ resonators, and given that Q_{total} of the cascaded circuit must be 50, Equation 2-21 tells us that the Q of the individual resonator need only be about 22—a fairly simple and realizable design task.

Active coupling is obviously more expensive than passive coupling due to the added cost of each active device. But, in some applications, there is no real

EXAMPLE 2-5

Design a top-L coupled two-resonator tuned circuit to meet the following requirements:

1. Center frequency = 75 MHz
2. 3-dB bandwidth = 3.75 MHz
3. Source resistance = 100 ohms
4. Load resistance = 1000 ohms

Assume that inductors are available that have an unloaded Q of 85 at the frequency of interest. Finally, use a tapped-C transformer to present an effective source resistance (R_s') of 1000 ohms to the filter.

Solution

The solution to this design problem is not a very difficult one, but it does involve quite a few separate and distinct calculations which might tend to make you lose sight of our goal. For this reason, we will walk through the solution in a very orderly fashion with a complete explanation of each calculation.

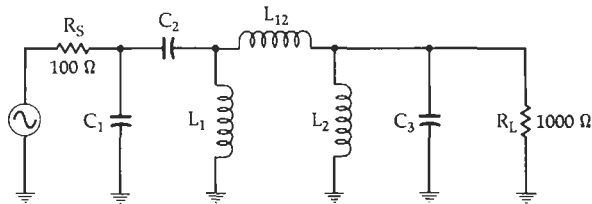


Fig. 2-27. Circuit for Example 2-5.

The circuit we are designing is shown in Fig. 2-27. Let's begin with a few definitions.

- Q_{total} = the loaded Q of the entire circuit
- Q_p = the Q of the inductor
- Q_R = the loaded Q of each resonator

From our discussion on coupling and its effects on bandwidth, we know that

$$Q_R = \frac{Q_{\text{total}}}{0.707}$$

and,

$$\begin{aligned} Q_{\text{total}} &= \frac{f_c}{B} \\ &= \frac{75 \text{ MHz}}{3.75 \text{ MHz}} \\ &= 20 \end{aligned}$$

so,

$$\begin{aligned} Q_R &= \frac{20}{0.707} \\ &= 28.3 \end{aligned}$$

trade-off involved because passive coupling just might not yield the required loaded Q . Example 2-5 illustrates some of the factors you must deal with.

This chapter was meant to provide an insight into how resonant circuits actually perform their function as well as to provide you with the capability for designing one to operate at a certain value of loaded Q . In Chapter 3, we will carry our study one step further to include low-pass, high-pass, and bandpass filters of various shapes and sizes.

Thus, to provide a total loaded Q of 20, it is necessary that the loaded Q of each resonator be 28.3. For the inductor,

$$\begin{aligned} Q_p &= \frac{R_p}{X_p} \\ &= 85 \end{aligned}$$

or,

$$R_p = 85 X_p \quad (\text{Eq. 2-22})$$

The loaded Q of each resonant circuit is

$$Q_R = \frac{R_{\text{total}}}{X_p} \quad (\text{Eq. 2-23})$$

where,

- R_{total} = the total equivalent shunt resistance for each resonator and
- $= R_s' \parallel R_p$
- $= R_L \parallel R_p$

since both circuits are identical. Remember, we have already taken into account the loading effect that each resonant circuit has on the other through the factor 0.707, which was used at the beginning of the example. Now, we have:

$$R_{\text{total}} = \frac{R_s' R_p}{R_s' + R_p}$$

Substituting into Equation 2-23:

$$Q_R = \frac{R_s' R_p}{(R_s' + R_p) X_p}$$

and,

$$\begin{aligned} X_p &= \frac{R_s' R_p}{(R_s' + R_p) Q_R} \\ &= \frac{1000 R_p}{(1000 + R_p) 28.3} \end{aligned} \quad (\text{Eq. 2-24})$$

We can now substitute Equation 2-22 into Equation 2-24 and solve for X_p .

$$\begin{aligned} X_p &= \frac{(1000)(85 X_p)}{(1000 + 85 X_p) 28.3} \\ &= 23.57 \text{ ohms} \end{aligned}$$

and,

$$\begin{aligned} R_p &= 85 X_p \\ &= 2003 \text{ ohms} \end{aligned}$$

To find the component values

$$\begin{aligned} L_1 &= L_2 = \frac{X_p}{\omega} \\ &= 50 \text{ nH} \end{aligned}$$

Continued on next page

EXAMPLE 2-5—cont

and,

$$\begin{aligned}C_a &= \frac{1}{\omega X_p} \\&= 90 \text{ pF}\end{aligned}$$

Now all that remains is to design the tapped-C transformer and the coupling inductor. From Equation 2-12:

$$R_s' = R_s \left(1 + \frac{C_1}{C_2} \right)^2$$

or,

$$\begin{aligned}\frac{C_1}{C_2} &= \sqrt{\frac{R_s'}{R_s}} - 1 \\&= 2.16\end{aligned}$$

and,

$$C_1 = 2.16C_2 \quad (\text{Eq. 2-25})$$

We know that the total capacitance that must be used to resonate with the inductor is 90 pF and

$$C_{\text{total}} = \frac{C_1 C_2}{C_1 + C_2} \quad (\text{Eq. 2-26})$$

Substituting Equation 2-25 into Equation 2-26 and taking C_{total} to be 90 pF yields:

$$90 \text{ pF} = \frac{2.16C_2^2}{3.16C_2}$$

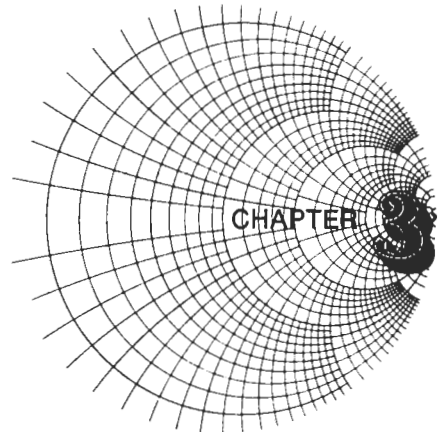
and,

$$\begin{aligned}C_2 &= 132 \text{ pF} \\C_1 &= 285 \text{ pF}\end{aligned}$$

To solve for the coupling inductance from Equation 2-20:

$$\begin{aligned}L_{12} &= Q_B L \\&= (28.3)(50 \text{ nH}) \\&= 1.415 \mu\text{H}\end{aligned}$$

The design is now complete. Notice that the tapped-C transformer is actually serving a dual purpose. It provides a dc block between the source and load in addition to its transformation properties.



FILTER DESIGN

Filters occur so frequently in the instrumentation and communications industries that no book covering the field of rf circuit design could be complete without at least one chapter devoted to the subject. Indeed, entire books have been written on the art of filter design alone, so this single chapter cannot possibly cover all aspects of all types of filters. But it will familiarize you with the characteristics of four of the most commonly used filters and will enable you to design very quickly and easily a filter that will meet, or exceed, most of the common filter requirements that you will encounter.

We will cover Butterworth, Chebyshev, and Bessel filters in all of their common configurations: *low-pass*, *high-pass*, *bandpass*, and *bandstop*. We will learn how to take advantage of the attenuation characteristics unique to each type of filter. Finally, we will learn how to design some very powerful filters in as little as 5 minutes by merely looking through a catalog to choose a design to suit your needs.

BACKGROUND

In Chapter 2, the concept of resonance was explored and we determined the effects that component value changes had on resonant circuit operation. You should now be somewhat familiar with the methods that are used in analyzing passive resonant circuits to find quantities, such as loaded Q , insertion loss, and bandwidth. You should also be capable of designing one- or two-resonator circuits for any loaded Q desired (or, at least, determine why you cannot). Quite a few of the filter applications that you will encounter, however, cannot be satisfied with the simple bandpass arrangement given in Chapter 2. There are occasions when, instead of passing a certain band of frequencies while rejecting frequencies above and below (bandpass), we would like to attenuate a small band of frequencies while passing all others. This type of filter is called, appropriately enough, a *bandstop filter*. Still other requirements call for a low-pass or high-pass response. The characteristic curves for these responses are shown in Fig. 3-1. The low-pass filter will allow all signals below a certain cutoff frequency to pass while attenuating all others. A high-pass filter's response is the mirror-image of the low-pass response

and attenuates all signals below a certain cutoff frequency while allowing those above cutoff to pass. These types of response simply cannot be handled very well with the two-resonator bandpass designs of Chapter 2.

In this chapter, we will use the low-pass filter as our workhorse, as all other responses will be derived from it. So let's take a quick look at a simple low-pass filter and examine its characteristics. Fig. 3-2 is an example of a very simple *two-pole*, or *second-order* low-pass filter. The order of a filter is determined by the slope of the attenuation curve it presents in the stopband. A second-order filter is one whose rolloff is a function of the frequency squared, or 12 dB per octave. A third-order filter causes a rolloff that is proportional to frequency cubed, or 18 dB per octave. Thus, the order of a filter can be equated with the number of significant reactive elements that it presents to the source as the signal deviates from the passband.

The circuit of Fig. 3-2 can be analyzed in much the same manner as was done in Chapter 2. For instance, an examination of the effects of loaded Q on the response would yield the family of curves shown in Fig. 3-3. Surprisingly, even this circuit configuration can cause a peak in the response. This is due to the fact that at some frequency, the inductor and capacitor will become resonant and, thus, peak the response if the loaded Q is high enough. The resonant frequency can be determined from

$$F_r = \frac{1}{2\pi\sqrt{LC}} \quad (\text{Eq. 3-1})$$

For low values of loaded Q , however, no response peak will be noticed.

The loaded Q of this filter is dependent upon the individual Q 's of the series leg and the shunt leg where, assuming perfect components,

$$Q_1 = \frac{X_L}{R_s} \quad (\text{Eq. 3-2})$$

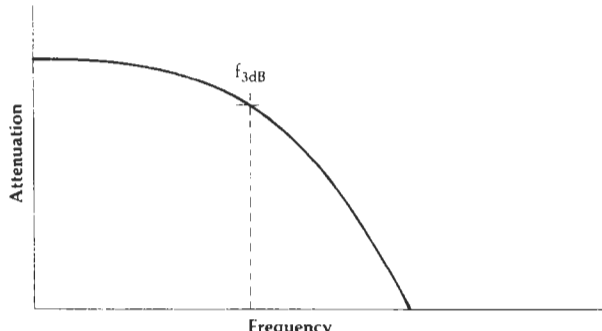
and,

$$Q_2 = \frac{R_L}{X_c} \quad (\text{Eq. 3-3})$$

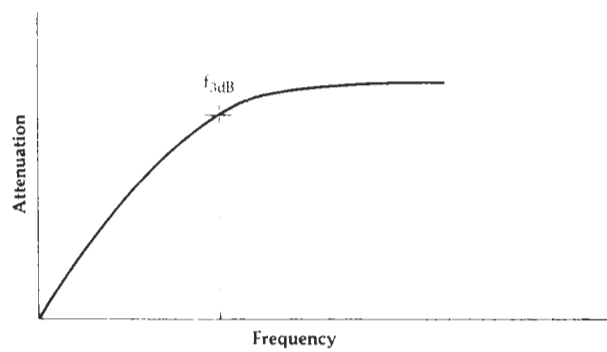
and the total Q is:

$$Q_{\text{total}} = \frac{Q_1 Q_2}{Q_1 + Q_2} \quad (\text{Eq. 3-4})$$

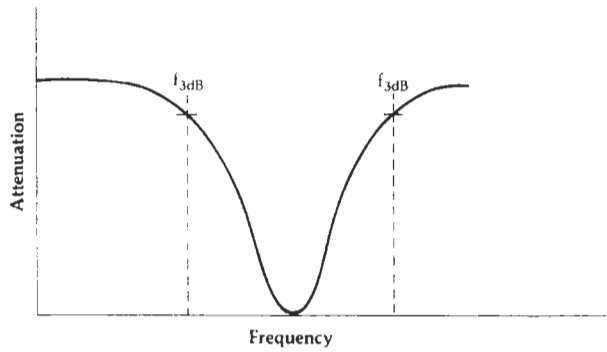
If the total Q of the circuit is greater than about 0.5, then for optimum transfer of power from the source to the load, Q_1 should equal Q_2 . In this case, at the



(A) Low-pass.



(B) High-pass.



(C) Bandstop.

Fig. 3-1. Typical filter response curves.

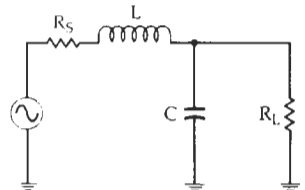


Fig. 3-2. A simple low-pass filter.

peak frequency, the response will approach 0-dB insertion loss. If the total Q of the network is less than about 0.5, there will be no peak in the response and, for optimum transfer of power, R_s should equal R_L . The peaking of the filter's response is commonly called ripple (defined in Chapter 2) and can vary consider-

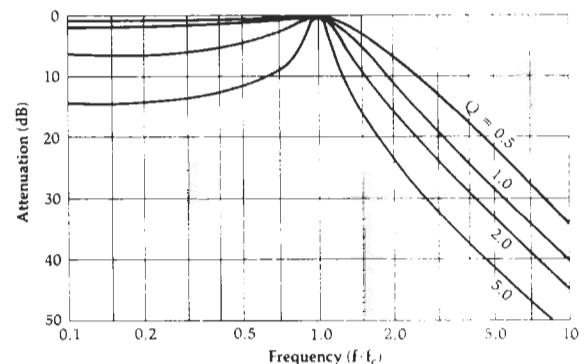


Fig. 3-3. Typical two-pole filter response curves.

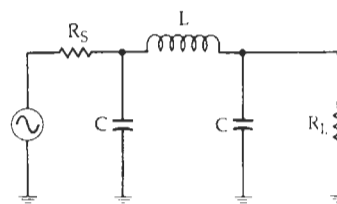


Fig. 3-4. Three-element low-pass filter.

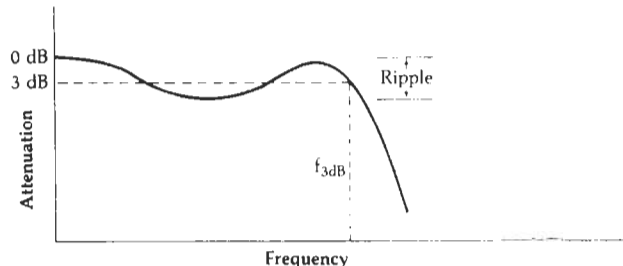


Fig. 3-5. Typical response of a three-element low-pass filter.

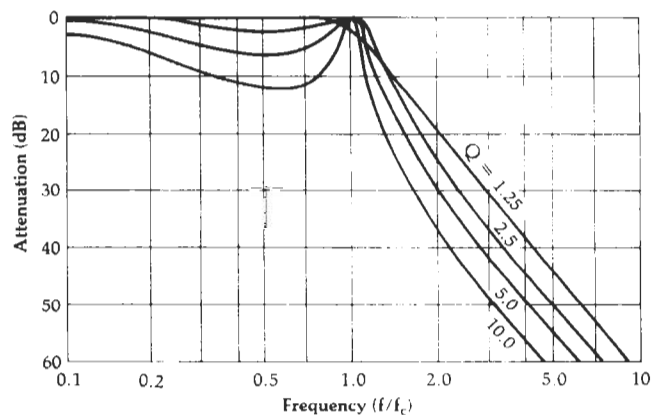


Fig. 3-6. Curves showing frequency response vs. loaded Q for three-element low-pass filters.

ably from one filter design to the next depending on the application. As shown, the two-element filter exhibits only one response peak at the edge of the passband.

It can be shown that the number of peaks within the passband is directly related to the number of elements in the filter by:

$$\text{Number of Peaks} = N - 1$$

where,

N = the number of elements.

Thus, the three-element low-pass filter of Fig. 3-4 should exhibit two response peaks as shown in Fig. 3-5. This is true only if the loaded Q is greater than one. Typical response curves for various values of loaded Q for the circuit given in Fig. 3-4 are shown in Fig. 3-6. For all odd-order networks, the response at dc and at the upper edge of the passband approaches 0 dB with dips in the response between the two frequencies. All even-order networks will produce an insertion loss at dc equal to the amount of passband ripple in dB. Keep in mind, however, that either of these two networks, if designed for low values of loaded Q , can be made to exhibit little or no passband ripple. But, as you can see from Figs. 3-3 and 3-6, the elimination of passband ripple can be made only at the expense of bandwidth. The smaller the ripple that is allowed, the wider the bandwidth becomes and, therefore, selectivity suffers. Optimum flatness in the passband occurs when the loaded Q of the three-element circuit is equal to one (1). Any value of loaded Q that is less than one will cause the response to roll off noticeably even at very low frequencies, within the defined passband. Thus, not only is the selectivity poorer but the passband insertion loss is too. In an application where there is not much signal to begin with, an even further decrease in signal strength could be disastrous.

Now that we have taken a quick look at two representative low-pass filters and their associated responses, let's discuss filters in general:

1. High- Q filters tend to exhibit a far greater initial slope toward the stopband than their low- Q counterparts with the same number of elements. Thus, at any frequency in the stopband, the attenuation will be greater for a high- Q filter than for one with a lower Q . The penalty for this improvement is the increase in passband ripple that must occur as a result.
2. Low- Q filters tend to have the flattest passband response but their initial attenuation slope at the band edge is small. Thus, the penalty for the reduced passband ripple is a decrease in the *initial* stopband attenuation.
3. As with the resonant circuits discussed in Chapter 2, the source and load resistors loading a filter will have a profound effect on the Q of the filter and, therefore, on the passband ripple and shape factor

of the filter. If a filter is inserted between two resistance values for which it was not designed, the performance will suffer to an extent, depending upon the degree of error in the terminating impedance values.

4. The *final* attenuation slope of the response is dependent upon *the order of the network*. The order of the network is equal to the number of reactive elements *in the low-pass filter*. Thus, a second-order network (2 elements) falls off at a final attenuation slope of 12 dB per octave, a third-order network (3 elements) at the rate of 18 dB per octave, and so on, with the addition of 6 dB per octave per element.

MODERN FILTER DESIGN

Modern filter design has evolved through the years from a subject known only to specialists in the field (because of the advanced mathematics involved) to a practical well-organized catalog of ready-to-use circuits available to anyone with a knowledge of eighth grade level math. In fact, an average individual with absolutely no prior practical filter design experience should be able to sit down, read this chapter, and within 30 minutes be able to design a practical high-pass, low-pass, bandpass, or bandstop filter to his specifications. It sounds simple and it is—once a few basic rules are memorized.

The approach we will take in all of the designs in this chapter will be to make use of the myriad of normalized *low-pass prototypes* that are now available to the designer. The actual design procedure is, therefore, nothing more than determining your requirements and, then, finding a filter in a catalog which satisfies these requirements. Each normalized element value is then scaled to the frequency and impedance you desire and, then, transformed to the type of response (bandpass, high-pass, bandstop) that you wish. With practice, the procedure becomes very simple and soon you will be defining and designing filters.

The concept of normalization may at first seem foreign to the person who is a newcomer to the field of filter design, and the idea of transforming a low-pass filter into one that will give one of the other three types of responses might seem absurd. The best advice I can give (to anyone not familiar with these practices and who might feel a bit skeptical at this point) is to press on. The only way to truly realize the beauty and simplicity of this approach is to try a few actual designs. Once you try a few, you will be hooked, and any other approach to filter design will suddenly seem tedious and unnecessarily complicated.

NORMALIZATION AND THE LOW-PASS PROTOTYPE

In order to offer a catalog of useful filter circuits to the electronic filter designer, it became necessary to

standardize the presentation of the material. Obviously, in practice, it would be extremely difficult to compare the performance and evaluate the usefulness of two filter networks if they were operating under two totally different sets of circumstances. Similarly, the presentation of any comparative design information for filters, if not standardized, would be totally useless. This concept of standardization or *normalization*, then, is merely a tool used by filter experts to present all filter design and performance information in a manner useful to circuit designers. Normalization assures the designer of the capability of comparing the performance of any two filter types when given the same operating conditions.

All of the catalogued filters in this chapter are low-pass filters normalized for a cutoff frequency of one radian per second (0.159 Hz) and for source and load resistors of one ohm. A characteristic response of such a filter is shown in Fig. 3-7. The circuit used to generate this response is called the *low-pass prototype*.

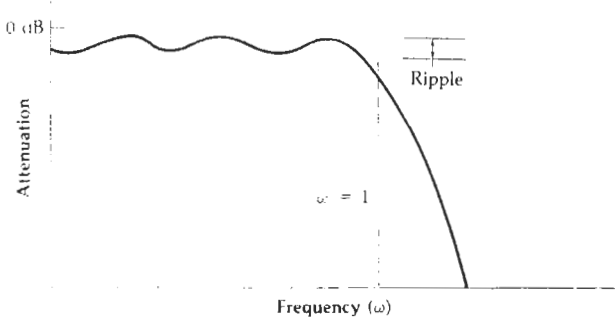


Fig. 3-7. Normalized low-pass response.

Obviously, the design of a filter with such a low cutoff frequency would require component values much larger than those we are accustomed to working with; capacitor values would be in farads rather than microfarads and picofarads, and the inductor values would be in henries rather than in microhenries and nanohenries. But once we choose a suitable low-pass prototype from the catalog, we can change the impedance level and cutoff frequency of the filter to any value we wish through a simple process called *scaling*. The net result of this process is a practical filter design with realizable component values.

FILTER TYPES

Many of the filters used today bear the names of the men who developed them. In this section, we will take a look at three such filters and examine their attenuation characteristics. Their relative merits will be discussed and their low-pass prototypes presented. The three filter types discussed will include the Butterworth, Chebyshev, and Bessel responses.

The Butterworth Response

The Butterworth filter is a medium-Q filter that is used in designs which require the amplitude response

of the filter to be as flat as possible. The Butterworth response is the flattest passband response available and contains no ripple. The typical response of such a filter might look like that of Fig. 3-8.

Since the Butterworth response is only a medium-Q filter, its initial attenuation steepness is not as good as some filters but it is better than others. This characteristic often causes the Butterworth response to be called a middle-of-the-road design.

The attenuation of a Butterworth filter is given by

$$A_{dB} = 10 \log \left[1 + \left(\frac{\omega}{\omega_c} \right)^{2n} \right] \quad (\text{Eq. 3-5})$$

where,

ω = the frequency at which the attenuation is desired,

ω_c = the cutoff frequency (ω_{3dB}) of the filter,

n = the number of elements in the filter.

If Equation 3-5 is evaluated at various frequencies for various numbers of elements, a family of curves is generated which will give a very good graphical representation of the attenuation provided by any order of filter at any frequency. This information is illustrated in Fig. 3-9. Thus, from Fig. 3-9, a 5-element (fifth order) Butterworth filter will provide an attenuation of approximately 30 dB at a frequency equal to

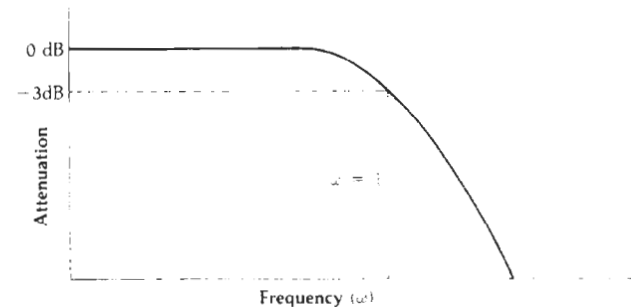


Fig. 3-8. The Butterworth response.

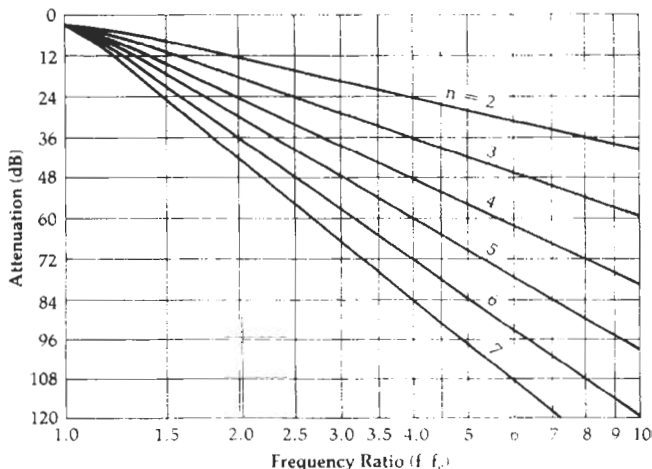


Fig. 3-9. Attenuation characteristics for Butterworth filters.

twice the cutoff frequency of the filter. Notice here that the frequency axis is normalized to ω/ω_c and the graph begins at the cutoff (-3 dB) point. This graph is extremely useful as it provides you with a method of determining, at a glance, the order of a filter needed to meet a given attenuation specification. A brief example should illustrate this point (Example 3-1).

EXAMPLE 3-1

How many elements are required to design a Butterworth filter with a cutoff frequency of 50 MHz, if the filter must provide at least 50 dB of attenuation at 150 MHz?

Solution

The first step in the solution is to find the ratio of $\omega/\omega_c = f/f_c$.

$$\begin{aligned} \frac{f}{f_c} &= \frac{150 \text{ MHz}}{50 \text{ MHz}} \\ &= 3 \end{aligned}$$

Thus, at 3 times the cutoff frequency, the response must be down by at least 50 dB. Referring to Fig. 3-9, it is seen very quickly that a minimum of 6 elements is required to meet this design goal. At an f/f_c of 3, a 6-element design would provide approximately 57 dB of attenuation, while a 5-element design would provide only about 47 dB, which is not quite good enough.

The element values for a normalized Butterworth low-pass filter operating between equal 1-ohm terminations (source and load) can be found by

$$A_k = 2 \sin \frac{(2k-1)\pi}{2n}, k = 1, 2, \dots, n \quad (\text{Eq. 3-6})$$

where,

n is the number of elements,

A_k is the k -th reactance in the ladder and may be either an inductor or capacitor.

The term $(2k-1)\pi/2n$ is in radians. We can use Equation 3-6 to generate our first entry into the catalog of low-pass prototypes shown in Table 3-1. The placement of each component of the filter is shown immediately above and below the table.

The rules for interpreting Butterworth tables are simple. The schematic shown above the table is used whenever the ratio R_S/R_L is calculated as the design criteria. The table is read from the top down. Alternately, when R_L/R_S is calculated, the schematic below the table is used. Then, the element designators in the table are read from the bottom up. Thus, a four-element low-pass prototype could appear as shown in Fig. 3-10. Note here that the element values not given in Table 3-1 are simply left out of the prototype ladder network. The 1-ohm load resistor is then placed directly across the output of the filter.

Remember that the cutoff frequency of each filter is 1 radian per second, or 0.159 Hz. Each capacitor value given is in farads, and each inductor value is in hen-

ties. The network will later be scaled to the impedance and frequency that is desired through a simple multiplication and division process. The component values will then appear much more realistic.

Occasionally, we have the need to design a filter that will operate between two unequal terminations as shown in Fig. 3-11. In this case, the circuit is normal-

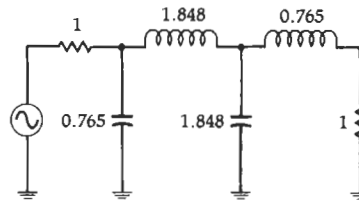


Fig. 3-10. A four-element Butterworth low-pass prototype circuit.

Table 3-1. Butterworth Equal Termination Low-Pass Prototype Element Values ($R_S = R_L$)

n	C_1	L_2	C_3	L_4	C_5	L_6	C_7
2	1.414	1.414					
3	1.000	2.000	1.000				
4	0.765	1.848	1.848	0.765			
5	0.618	1.618	2.000	1.618	0.618		
6	0.518	1.414	1.932	1.932	1.414	0.518	
7	0.445	1.247	1.802	2.000	1.802	1.247	0.445

n	L_1	C_2	L_3	C_4	L_5	C_6	L_7

Fig. 3-11. Unequal terminations.

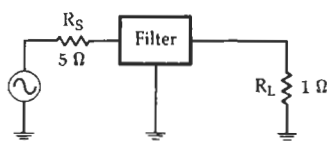


Fig. 3-12. Normalized unequal terminations.

ized for a load resistance of 1 ohm, while taking what we get for the source resistance. Dividing both the load and source resistor by 10 will yield a load resistance of 1 ohm and a source resistance of 5 ohms as shown in Fig. 3-12. We can use the normalized terminating resistors to help us find a low-pass prototype circuit.

Table 3-2 is a list of Butterworth low-pass prototype values for various ratios of source to load impedance (R_s/R_L). The schematic shown above the table is used when R_s/R_L is calculated, and the element values are read down from the top of the table.

Table 3-2A. Butterworth Low-Pass Prototype Element Values

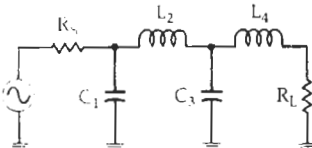
					
<i>n</i>	R_s/R_L	C_1	L_2	C_3	L_4
2	1.111	1.035	1.835		
	1.250	0.849	2.121		
	1.429	0.697	2.439		
	1.667	0.566	2.828		
	2.000	0.448	3.346		
	2.500	0.342	4.095		
	3.333	0.245	5.313		
	5.000	0.156	7.707		
	10.000	0.074	14.814		
	∞	1.414	0.707		
	3	0.900	0.808	1.633	1.599
4	0.800	0.844	1.384	1.926	
	0.700	0.915	1.165	2.277	
	0.600	1.023	0.965	2.702	
	0.500	1.181	0.779	3.261	
	0.400	1.425	0.604	4.064	
	0.300	1.838	0.440	5.363	
	0.200	2.669	0.284	7.910	
	0.100	5.167	0.138	15.455	
	∞	1.500	1.333	0.500	
	5	0.900	0.808	1.633	1.599
	0.800	0.844	1.384	1.926	
6	0.700	0.915	1.165	2.277	
	0.600	1.023	0.965	2.702	
	0.500	1.181	0.779	3.261	
	0.400	1.425	0.604	4.064	
	0.300	1.838	0.440	5.363	
	0.200	2.669	0.284	7.910	
	0.100	5.167	0.138	15.455	
	∞	1.500	1.333	0.500	
	7	0.900	0.808	1.633	1.599
	0.800	0.844	1.384	1.926	
8	0.700	0.915	1.165	2.277	
	0.600	1.023	0.965	2.702	
	0.500	1.181	0.779	3.261	
	0.400	1.425	0.604	4.064	
	0.300	1.838	0.440	5.363	
	0.200	2.669	0.284	7.910	
	0.100	5.167	0.138	15.455	
	∞	1.500	1.333	0.500	
	9	0.900	0.808	1.633	1.599
	0.800	0.844	1.384	1.926	
10	0.700	0.915	1.165	2.277	
	0.600	1.023	0.965	2.702	
	0.500	1.181	0.779	3.261	
	0.400	1.425	0.604	4.064	
	0.300	1.838	0.440	5.363	
	0.200	2.669	0.284	7.910	
	0.100	5.167	0.138	15.455	
	∞	1.500	1.333	0.500	
	11	0.900	0.808	1.633	1.599
	0.800	0.844	1.384	1.926	
12	0.700	0.915	1.165	2.277	
	0.600	1.023	0.965	2.702	
	0.500	1.181	0.779	3.261	
	0.400	1.425	0.604	4.064	
	0.300	1.838	0.440	5.363	
	0.200	2.669	0.284	7.910	
	0.100	5.167	0.138	15.455	
	∞	1.500	1.333	0.500	
	13	0.900	0.808	1.633	1.599
	0.800	0.844	1.384	1.926	
14	0.700	0.915	1.165	2.277	
	0.600	1.023	0.965	2.702	
	0.500	1.181	0.779	3.261	
	0.400	1.425	0.604	4.064	
	0.300	1.838	0.440	5.363	
	0.200	2.669	0.284	7.910	
	0.100	5.167	0.138	15.455	
	∞	1.500	1.333	0.500	
	15	0.900	0.808	1.633	1.599
	0.800	0.844	1.384	1.926	
16	0.700	0.915	1.165	2.277	
	0.600	1.023	0.965	2.702	
	0.500	1.181	0.779	3.261	
	0.400	1.425	0.604	4.064	
	0.300	1.838	0.440	5.363	
	0.200	2.669	0.284	7.910	
	0.100	5.167	0.138	15.455	
	∞	1.500	1.333	0.500	
	17	0.900	0.808	1.633	1.599
	0.800	0.844	1.384	1.926	
18	0.700	0.915	1.165	2.277	
	0.600	1.023	0.965	2.702	
	0.500	1.181	0.779	3.261	
	0.400	1.425	0.604	4.064	
	0.300	1.838	0.440	5.363	
	0.200	2.669	0.284	7.910	
	0.100	5.167	0.138	15.455	
	∞	1.500	1.333	0.500	
	19	0.900	0.808	1.633	1.599
	0.800	0.844	1.384	1.926	
20	0.700	0.915	1.165	2.277	
	0.600	1.023	0.965	2.702	
	0.500	1.181	0.779	3.261	
	0.400	1.425	0.604	4.064	
	0.300	1.838	0.440	5.363	
	0.200	2.669	0.284	7.910	
	0.100	5.167	0.138	15.455	
	∞	1.500	1.333	0.500	
	21	0.900	0.808	1.633	1.599
	0.800	0.844	1.384	1.926	
22	0.700	0.915	1.165	2.277	
	0.600	1.023	0.965	2.702	
	0.500	1.181	0.779	3.261	
	0.400	1.425	0.604	4.064	
	0.300	1.838	0.440	5.363	
	0.200	2.669	0.284	7.910	
	0.100	5.167	0.138	15.455	
	∞	1.500	1.333	0.500	
	23	0.900	0.808	1.633	1.599
	0.800	0.844	1.384	1.926	
24	0.700	0.915	1.165	2.277	
	0.600	1.023	0.965	2.702	
	0.500	1.181	0.779	3.261	
	0.400	1.425	0.604	4.064	
	0.300	1.838	0.440	5.363	
	0.200	2.669	0.284	7.910	
	0.100	5.167	0.138	15.455	
	∞	1.500	1.333	0.500	
	25	0.900	0.808	1.633	1.599
	0.800	0.844	1.384	1.926	
26	0.700	0.915	1.165	2.277	
	0.600	1.023	0.965	2.702	
	0.500	1.181	0.779	3.261	
	0.400	1.425	0.604	4.064	
	0.300	1.838	0.440	5.363	
	0.200	2.669	0.284	7.910	
	0.100	5.167	0.138	15.455	
	∞	1.500	1.333	0.500	
	27	0.900	0.808	1.633	1.599
	0.800	0.844	1.384	1.926	
28	0.700	0.915	1.165	2.277	
	0.600	1.023	0.965	2.702	
	0.500	1.181	0.779	3.261	
	0.400	1.425	0.604	4.064	
	0.300	1.838	0.440	5.363	
	0.200	2.669	0.284	7.910	
	0.100	5.167	0.138	15.455	
	∞	1.500	1.333	0.500	
	29	0.900	0.808	1.633	1.599
	0.800	0.844	1.384	1.926	
30	0.700	0.915	1.165	2.277	
	0.600	1.023	0.965	2.702	
	0.500	1.181	0.779	3.261	
	0.400	1.425	0.604	4.064	
	0.300	1.838	0.440	5.363	
	0.200	2.669	0.284	7.910	
	0.100	5.167	0.138	15.455	
	∞	1.500	1.333	0.500	
	31	0.900	0.808	1.633	1.599
	0.800	0.844	1.384	1.926	
32	0.700	0.915	1.165	2.277	
	0.600	1.023	0.965	2.702	
	0.500	1.181	0.779	3.261	
	0.400	1.425	0.604	4.064	
	0.300	1.838	0.440	5.363	
	0.200	2.669	0.284	7.910	
	0.100	5.167	0.138	15.455	
	∞	1.500	1.333	0.500	
	33	0.900	0.808	1.633	1.599
	0.800	0.844	1.384	1.926	
34	0.700	0.915	1.165	2.277	
	0.600	1.023	0.965	2.702	
	0.500	1.181	0.779	3.261	
	0.400	1.425	0.604	4.064	
	0.300	1.838	0.440	5.363	
	0.200	2.669	0.284	7.910	
	0.100	5.167	0.138	15.455	
	∞	1.500	1.333	0.500	
	35	0.900	0.808	1.633	1.599
	0.800	0.844	1.384	1.926</	

Table 3-2B. Butterworth Low-Pass Prototype Element Values

Series Resonant Circuit									
Parallel Resonant Circuit									
n	R_S/R_L	C_1	L_2	C_3	L_4	C_5	L_6	C_7	
		0.442	1.027	1.910	1.756	1.389			
5	0.900	0.470	0.866	2.061	1.544	1.738			
	0.800	0.517	0.731	2.285	1.333	2.108			
	0.700	0.586	0.609	2.600	1.126	2.552			
	0.600	0.686	0.496	3.051	0.924	3.133			
	0.500	0.838	0.388	3.736	0.727	3.965			
	0.400	1.094	0.285	4.884	0.537	5.307			
	0.200	1.608	0.186	7.185	0.352	7.935			
	0.100	3.512	0.091	14.095	0.173	15.710			
	∞	1.545	1.694	1.382	0.894	0.309			
6	1.111	0.289	1.040	1.322	2.054	1.744	1.335		
	1.250	0.245	1.116	1.126	2.239	1.550	1.688		
	1.429	0.207	1.236	0.957	2.499	1.346	2.062		
	1.667	0.173	1.407	0.801	2.858	1.143	2.509		
	2.000	0.141	1.653	0.654	3.369	0.942	3.094		
	2.500	0.111	2.028	0.514	4.141	0.745	3.931		
	3.333	0.082	2.656	0.379	5.433	0.552	5.280		
	5.000	0.054	3.917	0.248	8.020	0.363	7.922		
	10.000	0.026	7.705	0.122	15.786	0.179	15.738		
	∞	1.553	1.759	1.553	1.202	0.758	0.259		
7	0.900	0.299	0.711	1.404	1.489	2.125	1.727	1.296	
	0.800	0.322	0.606	1.517	1.278	2.334	1.546	1.652	
	0.700	0.357	0.515	1.688	1.091	2.618	1.350	2.028	
	0.600	0.408	0.432	1.928	0.917	3.005	1.150	2.477	
	0.500	0.480	0.354	2.273	0.751	3.553	0.951	3.064	
	0.400	0.590	0.278	2.795	0.592	4.380	0.754	3.904	
	0.300	0.775	0.206	3.671	0.437	5.761	0.560	5.258	
	0.200	1.145	0.135	5.427	0.287	8.526	0.369	7.908	
	0.100	2.257	0.067	10.700	0.142	16.822	0.182	15.748	
	∞	1.558	1.799	1.659	1.397	1.055	0.656	0.223	
Parallel Resonant Circuit									
n	R_L/R_S	L_1	C_2	L_3	C_4	L_5	C_6	L_7	
		0.442	1.027	1.910	1.756	1.389			
5	0.900	0.470	0.866	2.061	1.544	1.738			
	0.800	0.517	0.731	2.285	1.333	2.108			
	0.700	0.586	0.609	2.600	1.126	2.552			
	0.600	0.686	0.496	3.051	0.924	3.133			
	0.500	0.838	0.388	3.736	0.727	3.965			
	0.400	1.094	0.285	4.884	0.537	5.307			
	0.200	1.608	0.186	7.185	0.352	7.935			
	0.100	3.512	0.091	14.095	0.173	15.710			
	∞	1.545	1.694	1.382	0.894	0.309			
6	1.111	0.289	1.040	1.322	2.054	1.744	1.335		
	1.250	0.245	1.116	1.126	2.239	1.550	1.688		
	1.429	0.207	1.236	0.957	2.499	1.346	2.062		
	1.667	0.173	1.407	0.801	2.858	1.143	2.509		
	2.000	0.141	1.653	0.654	3.369	0.942	3.094		
	2.500	0.111	2.028	0.514	4.141	0.745	3.931		
	3.333	0.082	2.656	0.379	5.433	0.552	5.280		
	5.000	0.054	3.917	0.248	8.020	0.363	7.922		
	10.000	0.026	7.705	0.122	15.786	0.179	15.738		
	∞	1.553	1.759	1.553	1.202	0.758	0.259		
7	0.900	0.299	0.711	1.404	1.489	2.125	1.727	1.296	
	0.800	0.322	0.606	1.517	1.278	2.334	1.546	1.652	
	0.700	0.357	0.515	1.688	1.091	2.618	1.350	2.028	
	0.600	0.408	0.432	1.928	0.917	3.005	1.150	2.477	
	0.500	0.480	0.354	2.273	0.751	3.553	0.951	3.064	
	0.400	0.590	0.278	2.795	0.592	4.380	0.754	3.904	
	0.300	0.775	0.206	3.671	0.437	5.761	0.560	5.258	
	0.200	1.145	0.135	5.427	0.287	8.526	0.369	7.908	
	0.100	2.257	0.067	10.700	0.142	16.822	0.182	15.748	
	∞	1.558	1.799	1.659	1.397	1.055	0.656	0.223	

The attenuation of a Chebyshev filter can be found by making a few simple but tiresome calculations, and can be expressed as:

$$A_{dB} = 10 \log \left[1 + \epsilon^2 C_n^2 \left(\frac{\omega}{\omega_c} \right)^2 \right] \quad (\text{Eq. 3-7})$$

where,

$C_n^2 \left(\frac{\omega}{\omega_c} \right)'$ is the Chebyshev polynomial to the order n evaluated at $\left(\frac{\omega}{\omega_c} \right)'$.

The Chebyshev polynomials for the first seven orders

are given in Table 3-3. The parameter ϵ is given by:

$$\epsilon = \sqrt{10^{R_{AB}/10} - 1} \quad (\text{Eq. 3-8})$$

where,

R_{dB} is the passband ripple in decibels.

Note that $\left(\frac{\omega}{\omega_c}\right)'$ is not the same as $\left(\frac{\omega}{\omega_c}\right)$. The quantity $\left(\frac{\omega}{\omega_c}\right)'$ can be found by defining another parameter:

$$B = \frac{1}{n} \cosh^{-1}\left(\frac{1}{\epsilon}\right) \quad (\text{Eq. 3-9})$$

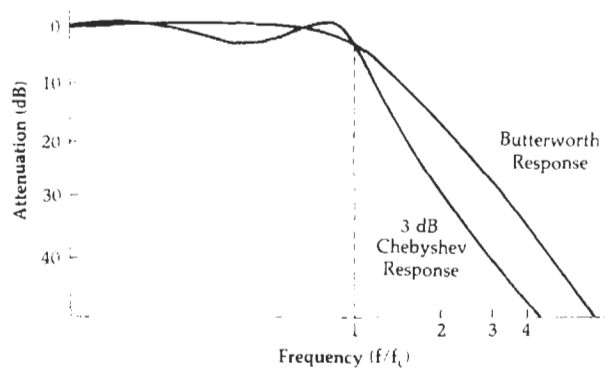


Fig. 3-14. Comparison of three-element Chebyshev and Butterworth responses.

Table 3-3. Chebyshev Polynomials to the Order n

<i>n</i>	<i>Chebyshev Polynomial</i>
1	$\frac{\omega}{\omega_c}$
2	$2\left(\frac{\omega}{\omega_c}\right)^2 - 1$
3	$4\left(\frac{\omega}{\omega_c}\right)^3 - 3\left(\frac{\omega}{\omega_c}\right)$
4	$8\left(\frac{\omega}{\omega_c}\right)^4 - 8\left(\frac{\omega}{\omega_c}\right)^2 + 1$
5	$16\left(\frac{\omega}{\omega_c}\right)^5 - 20\left(\frac{\omega}{\omega_c}\right)^3 + 5\left(\frac{\omega}{\omega_c}\right)$
6	$32\left(\frac{\omega}{\omega_c}\right)^6 - 48\left(\frac{\omega}{\omega_c}\right)^4 + 18\left(\frac{\omega}{\omega_c}\right)^2 - 1$
7	$64\left(\frac{\omega}{\omega_c}\right)^7 - 112\left(\frac{\omega}{\omega_c}\right)^5 + 56\left(\frac{\omega}{\omega_c}\right)^3 - 7\left(\frac{\omega}{\omega_c}\right)$

where,

n = the order of the filter,

ϵ = the parameter defined in Equation 3-8,

\cosh^{-1} = the inverse hyperbolic cosine of the quantity in parentheses.

Finally, we have:

$$\left(\frac{\omega}{\omega_c}\right)' = \left(\frac{\omega}{\omega_c}\right) \cosh B \quad (\text{Eq. 3-10})$$

where,

$\left(\frac{\omega}{\omega_c}\right)$ = the ratio of the frequency of interest to the cutoff frequency,

\cosh = the hyperbolic cosine.

If your calculator does not have hyperbolic and inverse hyperbolic functions, they can be manually determined from the following relations:

$$\cosh x = 0.5(e^x + e^{-x})$$

and

$$\cosh^{-1} x = \ln(x \pm \sqrt{x^2 - 1})$$

The preceding equations yield families of attenuation curves, each classified according to the amount of

ripple allowed in the passband. Several of these families of curves are shown in Figs. 3-15 through 3-18, and include 0.01-dB, 0.1-dB, 0.5-dB, and 1.0-dB ripple. Each curve begins at $\omega/\omega_c = 1$, which is the normalized cutoff, or 3-dB frequency. The passband ripple is, therefore, not shown.

If other families of attenuation curves are needed with different values of passband ripple, the preceding Chebyshev equations can be used to derive them. The problem in Example 3-3 illustrates this.

Obviously, performing the calculations of Example 3-3 for various values of ω/ω_c , ripple, and filter order is a very time-consuming chore unless a programmable calculator or computer is available to do most of the work for you.

The low-pass prototype element values corresponding to the Chebyshev responses of Figs. 3-15 through 3-18 are given in Tables 3-4 through 3-7. Note that the Chebyshev prototype values could not be separated into two distinct sets of tables covering the equal and

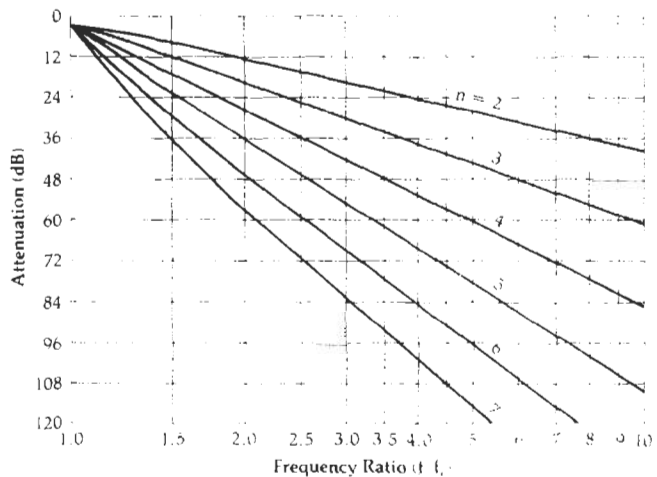


Fig. 3-15. Attenuation characteristics for a Chebyshev filter with 0.01-dB ripple.

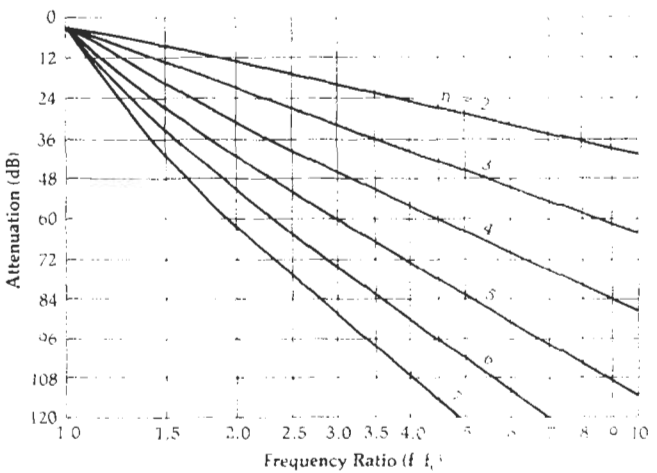


Fig. 3-16. Attenuation characteristics for a Chebyshev filter with 0.1-dB ripple.

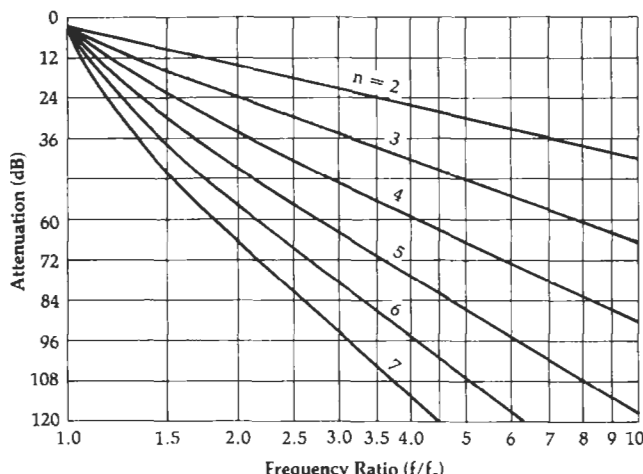


Fig. 3-17. Attenuation characteristics for a Chebyshev filter with 0.5-dB ripple.

unequal termination cases, as was done for the Butterworth prototypes. This is because the even order ($n = 2, 4, 6, \dots$) Chebyshev filters cannot have equal terminations. The source and load must always be different for proper operation as shown in the tables.

EXAMPLE 3-3

Find the attenuation of a 4-element, 2.5-dB ripple, low-pass Chebyshev filter at $\omega/\omega_c = 2.5$.

Solution

First evaluate the parameter:

$$\epsilon = \sqrt{10^{2.5}/10 - 1} \\ = 0.882$$

Next, find B.

$$B = \frac{1}{4} \left[\cosh^{-1} \left(\frac{1}{0.882} \right) \right] \\ = 0.1279$$

Then, $(\omega/\omega_c)'$ is:

$$(\omega/\omega_c)' = 2.5 \cosh .1279 \\ = 2.5204$$

Finally, we evaluate the fourth order ($n = 4$) Chebyshev polynomial at $(\omega/\omega_c)' = 2.52$,

$$C_n \left(\frac{\omega}{\omega_c} \right) = 8 \left(\frac{\omega}{\omega_c} \right)^4 - 8 \left(\frac{\omega}{\omega_c} \right)^2 + 1 \\ = 8(2.5204)^4 - 8(2.5204)^2 + 1 \\ = 273.05$$

We can now evaluate the final equation.

$$A_{dB} = 10 \log_{10} \left[1 + \epsilon^2 C_n^2 \left(\frac{\omega}{\omega_c} \right)^2 \right] \\ = 10 \log_{10} [1 + (0.882)^2 (273.05)^2] \\ = 47.63 \text{ dB}$$

Thus, at an ω/ω_c of 2.5, you can expect 47.63 dB of attenuation for this filter.

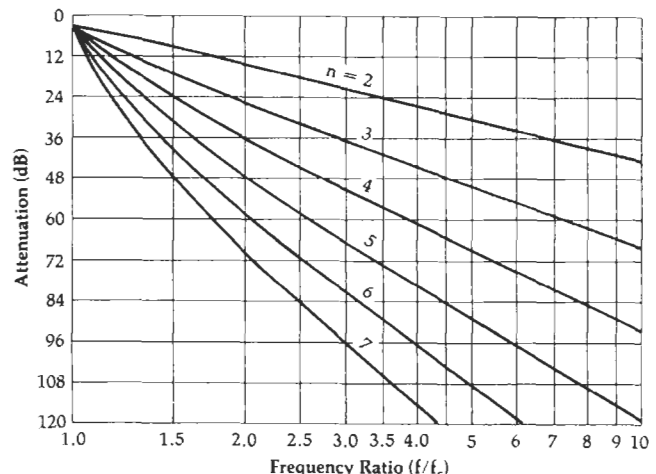


Fig. 3-18. Attenuation characteristics for a Chebyshev filter with 1-dB ripple.

The rules used for interpreting the Butterworth tables apply here also. The schematic shown above the table is used, and the element designators are read down from the top, when the ratio R_s/R_L is calculated as a design criteria. Alternately, with R_L/R_s calculations, use the schematic given below the table and read the element designators upwards from the bottom of the table. Example 3-4 is a practice problem for use in understanding the procedure.

EXAMPLE 3-4

Find the low-pass prototype values for an $n = 5$, 0.1-dB ripple, Chebyshev filter if the source resistance you are designing for is 50 ohms and the load resistance is 250 ohms.

Solution

Normalization of the source and load resistors yields an $R_s/R_L = 0.2$. A look at Table 3-5, for a 0.1-dB ripple filter with an $n = 5$ and an $R_s/R_L = 0.2$, yields the circuit values shown in Fig. 3-19.

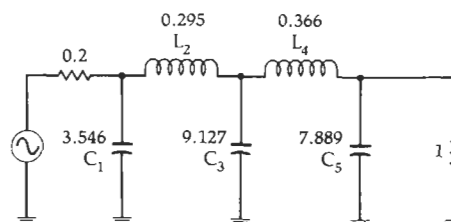
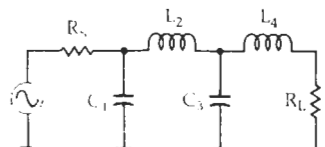
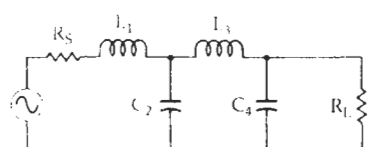


Fig. 3-19. Low-pass prototype circuit for Example 3-4.

It should be mentioned here that equations could have been presented in this section for deriving the element values for the Chebyshev low-pass prototypes. The equations are extremely long and tedious, however, and there would be little to be gained from their presentation.

Table 3-4A. Chebyshev Low-Pass Element Values for 0.01-dB Ripple

					
<i>n</i>	R_S/R_L	C_1	L_2	C_3	L_4
2	1.101	1.347	1.483		
	1.111	1.247	1.595		
	1.250	0.943	1.997		
	1.429	0.759	2.344		
	1.667	0.609	2.750		
	2.000	0.479	3.277		
	2.500	0.363	4.033		
	3.333	0.259	5.255		
	5.000	0.164	7.650		
	10.000	0.078	14.749		
3	∞	1.412	0.742		
	1.000	1.181	1.821	1.181	
	0.900	1.092	1.660	1.480	
	0.800	1.097	1.443	1.806	
	0.700	1.160	1.228	2.165	
	0.600	1.274	1.024	2.598	
	0.500	1.452	0.829	3.164	
	0.400	1.734	0.645	3.974	
	0.300	2.216	0.470	5.280	
	0.200	3.193	0.305	7.834	
4	0.100	6.141	0.148	15.390	
	∞	1.501	1.433	0.591	
	1.100	0.950	1.938	1.761	1.046
	1.111	0.854	1.946	1.744	1.165
	1.250	0.618	2.075	1.542	1.617
	1.429	0.495	2.279	1.334	2.008
	1.667	0.398	2.571	1.128	2.461
	2.000	0.316	2.994	0.926	3.045
	2.500	0.242	3.641	0.729	3.875
	3.333	0.174	4.727	0.538	5.209
5	5.000	0.112	6.910	0.352	7.813
	10.000	0.054	13.469	0.173	15.510
	∞	1.529	1.691	1.312	0.523
<i>n</i>	R_L/R_S	L_1	C_2	L_3	C_4
					

The Bessel Filter

The initial stopband attenuation of the Bessel filter is very poor and can be approximated by:

$$A_{dB} = 3\left(\frac{\omega}{\omega_c}\right)^2 \quad (\text{Eq. 3-11})$$

This expression, however, is not very accurate above an ω/ω_c that is equal to about 2. For values of ω/ω_c greater than 2, a straight-line approximation of 6 dB

per octave per element can be made. This yields the family of curves shown in Fig. 3-20.

But why would anyone deliberately design a filter with very poor initial stopband attenuation characteristics? The Bessel filter was originally optimized to obtain a *maximally flat group delay* or *linear phase* characteristic in the filter's passband. Thus, selectivity or stopband attenuation is not a primary concern when dealing with the Bessel filter. In high- and medium-Q filters, such as the Chebyshev and Butterworth filters, the phase response is extremely nonlinear over the filter's passband. This phase nonlinearity results in distortion of wideband signals due to the widely varying time delays associated with the different spectral components of the signal. Bessel filters, on the other hand, with their maximally flat (constant) group delay are able to pass wideband signals with a minimum of distortion, while still providing some selectivity.

The low-pass prototype element values for the Bessel filter are given in Table 3-8. Table 3-8 tabulates the prototype element values for various ratios of source to load resistance.

FREQUENCY AND IMPEDANCE SCALING

Once you specify the filter, choose the appropriate attenuation response, and write down the low-pass prototype values, the next step is to transform the prototype circuit into a usable filter. Remember, the cutoff frequency of the prototype circuit is 0.159 Hz ($\omega = 1$ rad/sec), and it operates between a source and load resistance that are normalized so that $R_L = 1$ ohm.

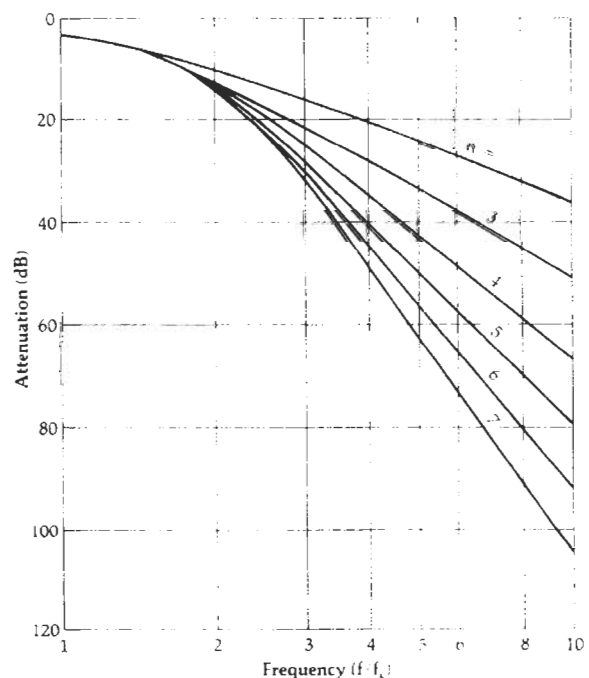


Fig. 3-20. Attenuation characteristics of Bessel filters.

Table 3-4B. Chebyshev Low-Pass Element Values for 0.01-dB Ripple

<i>n</i>	R_S/R_L	C_1	L_2	C_3	L_4	C_5	L_6	C_7
5	1.000	0.977	1.685	2.037	1.685	0.977		
	0.900	0.880	1.456	2.174	1.641	1.274		
	0.800	0.877	1.235	2.379	1.499	1.607		
	0.700	0.926	1.040	2.658	1.323	1.977		
	0.600	1.019	0.863	3.041	1.135	2.424		
	0.500	1.166	0.699	3.584	0.942	3.009		
	0.400	1.398	0.544	4.403	0.749	3.845		
	0.300	1.797	0.398	5.772	0.557	5.193		
	0.200	2.604	0.259	8.514	0.368	7.826		
	0.100	5.041	0.127	16.741	0.182	15.613		
	∞	1.547	1.795	1.645	1.237	0.488		
6	1.101	0.851	1.796	1.841	2.027	1.631	0.937	
	1.111	0.760	1.782	1.775	2.094	1.638	1.053	
	1.250	0.545	1.864	1.489	2.403	1.507	1.504	
	1.429	0.436	2.038	1.266	2.735	1.332	1.899	
	1.667	0.351	2.298	1.061	3.167	1.145	2.357	
	2.000	0.279	2.678	0.867	3.768	0.954	2.948	
	2.500	0.214	3.261	0.682	4.667	0.761	3.790	
	3.333	0.155	4.245	0.503	6.163	0.568	5.143	
	5.000	0.100	6.223	0.330	9.151	0.376	7.785	
	10.000	0.048	12.171	0.162	18.105	0.187	15.595	
	∞	1.551	1.847	1.790	1.598	1.190	0.469	
7	1.000	0.913	1.595	2.002	1.870	2.002	1.595	0.913
	0.900	0.816	1.362	2.089	1.722	2.202	1.581	1.206
	0.800	0.811	1.150	2.262	1.525	2.465	1.464	1.538
	0.700	0.857	0.967	2.516	1.323	2.802	1.307	1.910
	0.600	0.943	0.803	2.872	1.124	3.250	1.131	2.359
	0.500	1.080	0.650	3.382	0.928	3.875	0.947	2.948
	0.400	1.297	0.507	4.156	0.735	4.812	0.758	3.790
	0.300	1.669	0.372	5.454	0.546	6.370	0.568	5.148
	0.200	2.242	0.242	8.057	0.360	9.484	0.378	7.802
	0.100	4.701	0.119	15.872	0.173	18.818	0.188	15.652
	∞	1.559	1.867	1.866	1.765	1.563	1.161	0.456
<i>n</i>	R_L/R_S	L_1	C_2	L_3	C_4	L_5	C_6	L_7

The transformation is affected through the following formulas:

$$C = \frac{C_n}{2\pi f_c R} \quad (\text{Eq. 3-12})$$

and

$$L = \frac{RL_n}{2\pi f_c} \quad (\text{Eq. 3-13})$$

where,

C = the final capacitor value,

L = the final inductor value,
 C_n = a low-pass prototype element value,
 L_n = a low-pass prototype element value,
 R = the final load resistor value,
 f_c = the final cutoff frequency.

The normalized low-pass prototype source resistor must also be transformed to its final value by multiplying it by the final value of the load resistor (Example 3-5). Thus, the ratio of the two always remains the same.

Table 3-5A. Chebyshev Low-Pass Prototype Element Values for 0.1-dB Ripple

<i>n</i>	R_S/R_L	C_1	L_2	C_3	L_4
2	1.355	1.209	1.638		
	1.429	0.977	1.982		
	1.667	0.733	2.489		
	2.000	0.560	3.054		
	2.500	0.417	3.827		
	3.333	0.293	5.050		
	5.000	0.184	7.426		
	10.000	0.087	14.433		
	∞	1.391	0.819		
3	1.000	1.433	1.594	1.433	
	0.900	1.426	1.494	1.622	
	0.800	1.451	1.356	1.871	
	0.700	1.521	1.193	2.190	
	0.600	1.648	1.017	2.603	
	0.500	1.853	0.838	3.159	
	0.400	2.186	0.660	3.968	
	0.300	2.763	0.486	5.279	
	0.200	3.942	0.317	7.850	
	0.100	7.512	0.155	15.466	
	∞	1.513	1.510	0.716	
4	1.355	0.992	2.148	1.585	1.341
	1.429	0.779	2.348	1.429	1.700
	1.667	0.576	2.730	1.185	2.243
	2.000	0.440	3.227	0.967	2.856
	2.500	0.329	3.961	0.760	3.698
	3.333	0.233	5.178	0.560	5.030
	5.000	0.148	7.607	0.367	7.614
	10.000	0.070	14.887	0.180	15.230
	∞	1.511	1.768	1.455	0.673
<i>n</i>	R_L/R_S	L_1	C_2	L_3	C_4

R_S	L_1	C_2	L_3	C_4	R_L

The process for designing a low-pass filter is a very simple one which involves the following procedure:

1. Define the response you need by specifying the required attenuation characteristics at selected frequencies.
2. Normalize the frequencies of interest by dividing them by the cutoff frequency of the filter. This step forces your data to be in the same form as that of the attenuation curves of this chapter, where the 3-dB point on the curve is:

$$\frac{f}{f_c} = 1$$

EXAMPLE 3-5

Scale the low-pass prototype values of Fig. 3-19 (Example 3-4) to a cutoff frequency of 50 MHz and a load resistance of 250 ohms.

Solution

Use Equations 3-12 and 3-13 to scale each component as follows:

$$C_1 = \frac{3.546}{2\pi(50 \times 10^6)(250)} = 45 \text{ pF}$$

$$C_3 = \frac{9.127}{2\pi(50 \times 10^6)(250)} = 116 \text{ pF}$$

$$C_5 = \frac{7.889}{2\pi(50 \times 10^6)(250)} = 100 \text{ pF}$$

$$L_2 = \frac{(250)(0.295)}{2\pi(50 \times 10^6)} = 235 \text{ nH}$$

$$L_4 = \frac{(250)(0.366)}{2\pi(50 \times 10^6)} = 291 \text{ nH}$$

The source resistance is scaled by multiplying its normalized value by the final value of the load resistor.

$$R_{S(\text{final})} = 0.2(250) = 50 \text{ ohms}$$

The final circuit appears in Fig. 3-21.

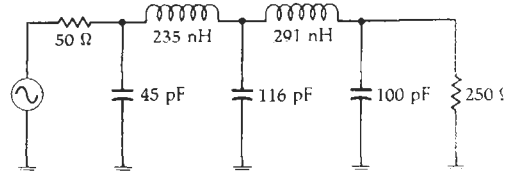


Fig. 3-21. Low-pass filter circuit for Example 3-5.

3. Determine the maximum amount of ripple that you can allow in the passband. Remember, the greater the amount of ripple allowed, the more selective the filter is. Higher values of ripple may allow you to eliminate a few components.
4. Match the normalized attenuation characteristics (Steps 1 and 2) with the attenuation curves provided in this chapter. Allow yourself a small "fudge-factor" for good measure. This step reveals the minimum number of circuit elements that you can get away with—given a certain filter type.
5. Find the low-pass prototype values in the tables.
6. Scale all elements to the frequency and impedance of the final design.

Example 3-6 diagrams the process of designing a low-pass filter using the preceding steps.

Table 3-5B. Chebyshev Low-Pass Prototype Element Values for 0.1-dB Ripple

<i>n</i>	R_s/R_L	C_1	L_2	C_3	L_4	C_5	L_6	C_7
5	1.000	1.301	1.556	2.241	1.556	1.301		
	0.900	1.285	1.433	2.380	1.488	1.488		
	0.800	1.300	1.282	2.582	1.382	1.738		
	0.700	1.358	1.117	2.868	1.244	2.062		
	0.600	1.470	0.947	3.269	1.085	2.484		
	0.500	1.654	0.778	3.845	0.913	3.055		
	0.400	1.954	0.612	4.720	0.733	3.886		
	0.300	2.477	0.451	6.196	0.550	5.237		
	0.200	3.546	0.295	9.127	0.366	7.889		
	0.100	6.787	0.115	17.957	0.182	15.745		
	∞	1.561	1.807	1.766	1.417	0.651		
6	1.355	0.942	2.080	1.659	2.247	1.534	1.277	
	1.429	0.735	2.249	1.454	2.544	1.405	1.629	
	1.667	0.542	2.600	1.183	3.064	1.185	2.174	
	2.000	0.414	3.068	0.958	3.712	0.979	2.794	
	2.500	0.310	3.765	0.749	4.651	0.778	3.645	
	3.333	0.220	4.927	0.551	6.195	0.580	4.996	
	5.000	0.139	7.250	0.361	9.261	0.384	7.618	
	10.000	0.067	14.220	0.178	18.427	0.190	15.350	
	∞	1.534	1.884	1.831	1.749	1.394	0.638	
7	1.000	1.262	1.520	2.239	1.680	2.239	1.520	1.262
	0.900	1.242	1.395	2.361	1.578	2.397	1.459	1.447
	0.800	1.255	1.245	2.548	1.443	2.624	1.362	1.697
	0.700	1.310	1.083	2.819	1.283	2.942	1.233	2.021
	0.600	1.417	0.917	3.205	1.209	3.384	1.081	2.444
	0.500	1.595	0.753	3.764	0.928	4.015	0.914	3.018
	0.400	1.885	0.593	4.618	0.742	4.970	0.738	3.855
	0.300	2.392	0.437	6.054	0.556	6.569	0.557	5.217
	0.200	3.428	0.286	8.937	0.369	9.770	0.372	7.890
	0.100	6.570	0.141	17.603	0.184	19.376	0.186	15.813
	∞	1.575	1.858	1.921	1.827	1.734	1.379	0.631
<i>n</i>	R_L/R_s	L_1	C_2	L_3	C_4	L_5	C_6	L_7

HIGH-PASS FILTER DESIGN

Once you have learned the mechanics of low-pass filter design, high-pass design becomes a snap. You can use all of the attenuation response curves presented, thus far, for the low-pass filters by simply inverting the f/f_c axis. For instance, a 5-element, 0.1-dB-ripple Chebyshev *low-pass filter* will produce an attenuation of about 60 dB at an f/f_c of 3 (Fig. 3-16). If you were working instead with a *high-pass filter* of the same size and type, you could still use Fig. 3-16 to tell you

that at an f/f_c of 1/3 (or, $f_c/f = 3$) a 5-element, 0.1-dB-ripple Chebyshev *high-pass filter* will also produce an attenuation of 60 dB. This is obviously more convenient than having to refer to more than one set of curves.

After finding the response which satisfies all of the requirements, the next step is to simply refer to the tables of low-pass prototype values and copy down the prototype values that are called for. High-pass values for the elements are then obtained directly from the low-pass prototype values as follows (refer to Fig. 3-24):

Table 3-6B. Chebyshev Low-Pass Prototype Element Values for 0.5-dB Ripple

n	R_S/R_L	C_1	L_2	C_3	L_4	C_5	L_6	C_7
5	1.000	1.807	1.303	2.691	1.303	1.807		
	0.900	1.854	1.222	2.849	1.238	1.970		
	0.800	1.926	1.126	3.060	1.157	2.185		
	0.700	2.035	1.015	3.353	1.058	2.470		
	0.600	2.200	0.890	3.765	0.942	2.861		
	0.500	2.457	0.754	4.367	0.810	3.414		
	0.400	2.870	0.609	5.296	0.664	4.245		
	0.300	3.588	0.459	6.871	0.508	5.625		
	0.200	5.064	0.306	10.054	0.343	8.367		
	0.100	9.556	0.153	19.647	0.173	16.574		
6	∞	1.630	1.740	1.922	1.514	0.903		
	1.984	0.905	2.577	1.368	2.713	1.299	1.796	
	2.000	0.830	2.704	1.291	2.872	1.237	1.956	
	2.500	0.506	3.722	0.890	4.109	0.881	3.103	
	3.333	0.337	5.055	0.632	5.699	0.635	4.481	
	5.000	0.206	7.615	0.406	8.732	0.412	7.031	
7	10.000	0.096	15.186	0.197	17.681	0.202	14.433	
	1.000	1.790	1.296	2.718	1.385	2.718	1.296	1.790
	0.900	1.835	1.215	2.869	1.308	2.883	1.234	1.953
	0.800	1.905	1.118	3.076	1.215	3.107	1.155	2.168
	0.700	2.011	1.007	3.364	1.105	3.416	1.058	2.455
	0.600	2.174	0.882	3.772	0.979	3.852	0.944	2.848
	0.500	2.428	0.747	4.370	0.838	2.289	0.814	3.405
	0.400	2.835	0.604	5.295	0.685	5.470	0.669	4.243
	0.300	3.546	0.455	6.867	0.522	7.134	0.513	5.635
	0.200	5.007	0.303	10.049	0.352	10.496	0.348	8.404
8	0.100	9.456	0.151	19.649	0.178	20.631	0.176	16.665
	∞	1.646	1.777	2.031	1.789	1.924	1.503	0.895
n	R_L/R_S	L_1	C_2	L_3	C_4	L_5	C_6	L_7

band) skirts remains the same. Example 3-7 illustrates the design of high-pass filters.

A closer look at the filter designed in Example 3-7 reveals that it is symmetric. Indeed, all filters given for the equal termination class are symmetric. The equal termination class of filter thus yields a circuit that is easier to design (fewer calculations) and, in most cases, cheaper to build for a high-volume product, due to the number of equal valued components.

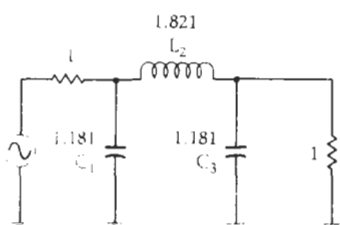
THE DUAL NETWORK

Thus far, we have been referring to the group of low-pass prototype element value tables presented and, then, we choose the schematic that is located

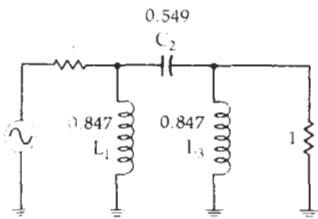
either above or below the tables for the form of the filter that we are designing, depending on the value of R_L/R_S . Either form of the filter will produce exactly the same attenuation, phase, and group-delay characteristics, and each form is called the *dual* of the other.

Any filter network in a ladder arrangement, such as the ones presented in this chapter, can be changed into its dual form by application of the following rules:

1. Change all inductors to capacitors, and vice-versa, without changing element values. Thus, 3 henries becomes 3 farads.
2. Change all resistances into conductances, and vice-versa, with the value unchanged. Thus, 3 ohms becomes 3 mhos, or $1/3$ ohm.



(A) Low-pass prototype circuit.



(B) Equivalent high-pass prototype circuit.

Fig. 3-24. Low-pass to high-pass filter transformation.

3. Change all shunt branches to series branches, and vice-versa.
4. Change all elements in series with each other into elements that are in parallel with each other.
5. Change all voltage sources into current sources, and vice-versa.

Fig. 3-26 shows a ladder network and its dual representation.

Dual networks are convenient, in the case of equal terminations, if you desire to change the topology of the filter without changing the response. It is most often used, as shown in Example 3-7, to eliminate an unnecessary inductor which might have crept into the design through some other transformation process. Inductors are typically more lower-Q devices than capacitors and, therefore, exhibit higher losses. These losses tend to cause insertion loss, in addition to generally degrading the overall performance of the filter. The number of inductors in any network should, therefore, be reduced whenever possible.

A little experimentation with dual networks having unequal terminations will reveal that you can quickly get yourself into trouble if you are not careful. This is especially true if the load and source resistance are a design criteria and cannot be changed to suit the needs of your filter. Remember, when the dual of a network with unequal terminations is taken, then, the terminations *must*, by definition, change value as shown in Fig. 3-26.

BANDPASS FILTER DESIGN

The low-pass prototype circuits and response curves given in this chapter can also be used in the design of bandpass filters. This is done through a simple

Table 3-7A. Chebyshev Low-Pass Prototype Element Values for 1.0-dB Ripple

n	R_s/R_L	C_1	L_2	C_3	L_4
2	3.000	0.572	3.132		
	4.000	0.365	4.600		
	8.000	0.157	9.658		
	∞	1.213	1.109		
3	1.000	2.216	1.088	2.216	
	0.500	4.431	0.817	2.216	
	0.333	6.647	0.726	2.216	
	0.250	8.862	0.680	2.216	
	0.125	17.725	0.612	2.216	
	∞	1.652	1.460	1.108	
4	3.000	0.653	4.411	0.814	2.535
	4.000	0.452	7.083	0.612	2.848
	8.000	0.209	17.164	0.428	3.281
	∞	1.350	2.010	1.488	1.106
n	R_L/R_s	L_1	C_2	L_3	C_4

transformation process similar to what was done in the high-pass case.

The most difficult task awaiting the designer of a bandpass filter, if the design is to be derived from the low-pass prototype, is in specifying the bandpass attenuation characteristics in terms of the low-pass response curves. A method for doing this is shown by the curves in Fig. 3-27. As you can see, when a low-pass design is transformed into a bandpass design, the attenuation bandwidth ratios remain the same. This means that a low-pass filter with a 3-dB cutoff frequency, or a bandwidth of 2 kHz, would transform into a bandpass filter with a 3-dB bandwidth of 2 kHz. If the response of the low-pass network were down 30 dB at a frequency or bandwidth of 4 kHz ($f/f_c = 2$), then the response of the bandpass network would be down 30 dB at a bandwidth of 4 kHz. Thus, the normalized f/f_c axis of the low-pass attenuation curves becomes a ratio of bandwidths rather than frequencies, such that:

$$\frac{BW}{BW_c} = \frac{f}{f_c} \quad (\text{Eq. 3-14})$$

where,

BW = the bandwidth at the required value of attenuation,
 BW_c = the 3-dB bandwidth of the bandpass filter.

Table 3-7B. Chebyshev Low-Pass Prototype Element Values for 1.0-dB Ripple

<i>n</i>	R_S/R_L	C_1	L_2	C_3	L_4	C_5	L_6	C_7
5	1.000	2.207	1.128	3.103	1.128	2.207		
	0.500	4.414	0.565	4.653	1.128	2.207		
	0.333	6.622	0.376	6.205	1.128	2.207		
	0.250	8.829	0.282	7.756	1.128	2.207		
	0.125	17.657	0.141	13.961	1.128	2.207		
	∞	1.721	1.645	2.061	1.493	1.103		
6	3.000	0.679	3.873	0.771	4.711	0.969	2.406	
	4.000	0.481	5.644	0.476	7.351	0.849	2.582	
	8.000	0.227	12.310	0.198	16.740	0.726	2.800	
	∞	1.378	2.097	1.690	2.074	1.494	1.102	
7	1.000	2.204	1.131	3.147	1.194	3.147	1.131	2.204
	0.500	4.408	0.566	6.293	0.895	3.147	1.131	2.204
	0.333	6.612	0.377	9.441	0.796	3.147	1.131	2.204
	0.250	8.815	0.283	12.588	0.747	3.147	1.131	2.204
	0.125	17.631	0.141	25.175	0.671	3.147	1.131	2.204
	∞	1.741	1.677	2.155	1.703	2.079	1.494	1.102
<i>n</i>	R_L/R_S	L_1	C_2	L_3	C_4	L_5	C_6	L_7

Often a bandpass response is not specified, as in Example 3-8. Instead, the requirements are often given as attenuation values at specified frequencies as shown by the curve in Fig. 3-28. In this case, you must transform the stated requirements into information that takes the form of Equation 3-14. As an example, consider Fig. 3-28. How do we convert the data that is given into the bandwidth ratios we need? Before we can answer that, we have to find f_3 . Use the following method.

The frequency response of a bandpass filter exhibits geometric symmetry. That is, it is only symmetric when plotted on a logarithmic scale. The center frequency of a geometrically symmetric filter is given by the formula:

$$f_c = \sqrt{f_a f_b} \quad (\text{Eq. 3-15})$$

where f_a and f_b are any two frequencies (one above and one below the passband) having equal attenuation. Therefore, the center frequency of the response curve shown in Fig. 3-28 must be

$$\begin{aligned} f_c &= \sqrt{(45)(75)} \text{ MHz} \\ &= 58.1 \text{ MHz} \end{aligned}$$

We can use Equation 3-15 again to find f_3 .

$$58.1 = \sqrt{f_3(125)}$$

or,

$$f_3 = 27 \text{ MHz}$$

Now that f_3 is known, the data of Fig. 3-28 can be put into the form of Equation 3-14.

$$\begin{aligned} \frac{\text{BW}_{40 \text{ dB}}}{\text{BW}_{3 \text{ dB}}} &= \frac{125 \text{ MHz} - 27 \text{ MHz}}{75 \text{ MHz} - 45 \text{ MHz}} \\ &= 3.27 \end{aligned}$$

To find a low-pass prototype curve that will satisfy these requirements, simply refer to any of the pertinent graphs presented in this chapter and find a response which will provide 40 dB of attenuation at an f/f_c of 3.27. (A fourth-order or better Butterworth filter will do quite nicely.)

The actual transformation from the low-pass to the bandpass configuration is accomplished by resonating each low-pass element with an element of the opposite type and of the same value. All shunt elements of the low-pass prototype circuit become parallel-resonant

EXAMPLE 3-7

Design an LC high-pass filter with an f_c of 60 MHz and a minimum attenuation of 40 dB at 30 MHz. The source and load resistance are equal at 300 ohms. Assume that a 0.5-dB passband ripple is tolerable.

Solution

First, normalize the attenuation requirements so that the low-pass attenuation curves may be used.

$$\frac{f}{f_c} = \frac{30 \text{ MHz}}{60 \text{ MHz}} = 0.5$$

Inverting, we get:

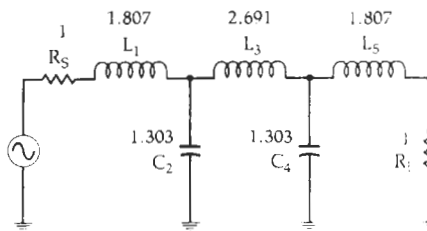
$$\frac{f_c}{f} = 2$$

Now, select a normalized low-pass filter that offers at least 40-dB attenuation at a ratio of $f_c/f = 2$. Reference to Fig. 3.17 (attenuation response of 0.5-dB-ripple Chebyshev filters) indicates that a normalized $n = 5$ Chebyshev will provide the needed attenuation. Table 3-6 contains the element values for the corresponding network. The normalized low-pass prototype circuit is shown in Fig. 3-25A. Note that the schematic below Table 3-6B was chosen as the low-pass prototype circuit rather than the schematic above the table. The reason for doing this will become obvious after the next step. Keep in mind, however, that the ratio of R_s/R_L is the same as the ratio of R_L/R_s , and is unity. Therefore, it does not matter which form is used for the prototype circuit.

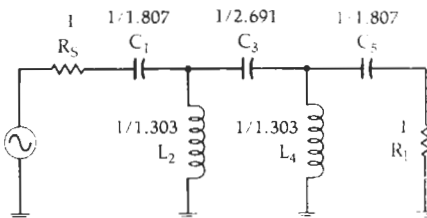
Next, transform the low-pass circuit to a high-pass network by replacing each inductor with a capacitor, and vice-versa, using reciprocal element values as shown in Fig. 3-25B. Note here that had we begun with the low-pass prototype circuit shown above Table 3-6B, this transformation would have yielded a filter containing three inductors rather than the two shown in Fig. 3-25B. The object in any of these filter designs is to reduce the number of inductors in the final design. More on this later.

The final step in the design process is to scale the network in both impedance and frequency using Equations 3-12 and 3-13. The first two calculations are done for you.

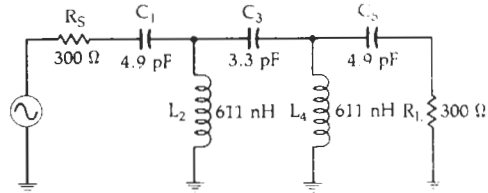
$$C_1 = \frac{1}{\frac{1.807}{2\pi(60 \times 10^6)(300)}} = 4.9 \text{ pF}$$



(A) Normalized low-pass filter circuit.



(B) High-pass transformation.



(C) Frequency and impedance-scaled filter circuit.

Fig. 3-25. High-pass filter design for Example 3-7.

$$L_2 = \frac{300 \left(\frac{1}{1.303} \right)}{2\pi(60 \times 10^6)} = 611 \text{ nH}$$

The remaining values are:

$$\begin{aligned} C_3 &= 3.3 \text{ pF} \\ C_5 &= 4.9 \text{ pF} \\ L_4 &= 611 \text{ nH} \end{aligned}$$

The final filter circuit is given in Fig. 3-25C.

EXAMPLE 3-8

Find the Butterworth low-pass prototype circuit which, when transformed, would satisfy the following bandpass filter requirements:

$$\begin{aligned} BW_{\text{pass}} &= 2 \text{ MHz} \\ BW_{\text{stop}} &= 6 \text{ MHz} \end{aligned}$$

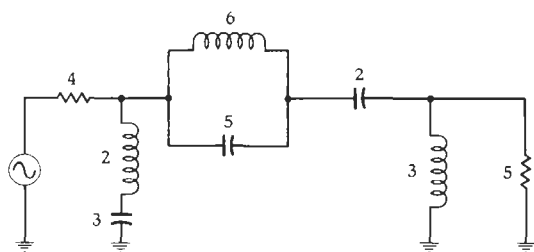
Solution

Note that we are not concerned with the center frequency of the bandpass response just yet. We are only concerned with the relationship between the above requirements and

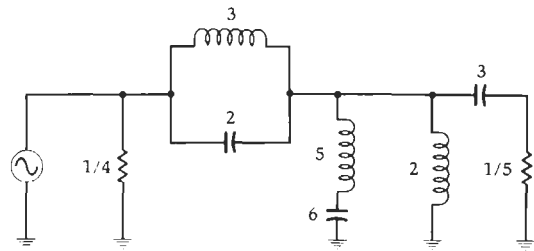
the low-pass response curves. Using Equation 3-14, we have:

$$\begin{aligned} \frac{BW}{BW_c} &= \frac{f}{f_c} = \frac{BW_{\text{stop}}}{BW_{\text{pass}}} \\ &= \frac{6 \text{ MHz}}{2 \text{ MHz}} \\ &= 3 \end{aligned}$$

Therefore, turn to the Butterworth response curves shown in Fig. 3-9 and find a prototype value that will provide 40 dB of attenuation at an $f/f_c = 3$. The curves indicate a 5-element Butterworth filter will provide the needed attenuation.

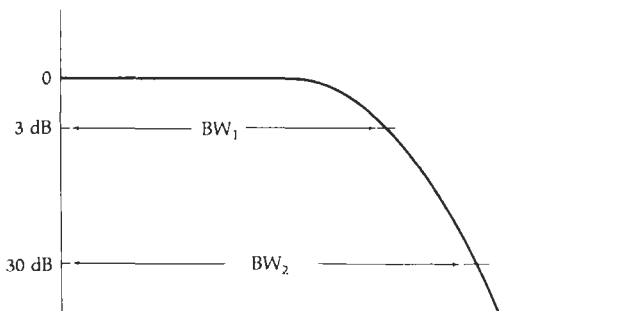


(A) A representative ladder network.

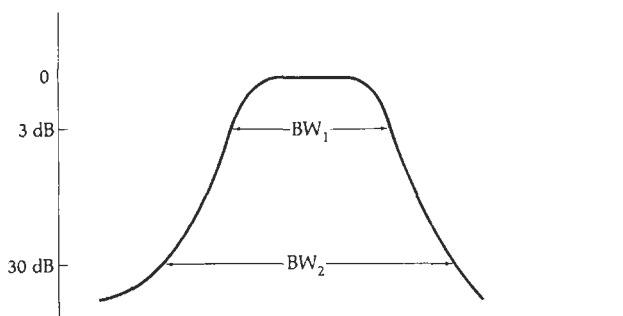


(B) Its dual form.

Fig. 3-26. Duality.



(A) Low-pass prototype response.



(B) Bandpass response.

Fig. 3-27. Low-pass to bandpass transformation bandwidths.

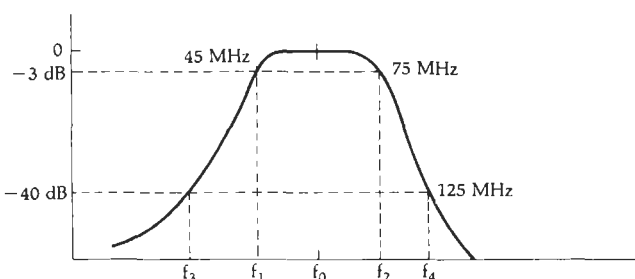


Fig. 3-28. Typical bandpass specifications.

Table 3-8A. Bessel Low-Pass Prototype Element Values

n	R_S/R_L	C_1	L_2	C_3	L_4
2	1.000	0.576	2.148		
	1.111	0.508	2.310		
	1.250	0.443	2.510		
	1.429	0.380	2.764		
	1.667	0.319	3.099		
	2.000	0.260	3.565		
	2.500	0.203	4.258		
	3.333	0.149	5.405		
	5.000	0.097	7.688		
	10.000	0.047	14.510		
	∞	1.362	0.454		
3	1.000	0.337	0.971	2.203	
	0.900	0.371	0.865	2.375	
	0.800	0.412	0.761	2.587	
	0.700	0.466	0.658	2.858	
	0.600	0.537	0.558	3.216	
	0.500	0.635	0.459	3.714	
	0.400	0.783	0.362	4.457	
	0.300	1.028	0.267	5.689	
	0.200	1.518	0.175	8.140	
	0.100	2.983	0.086	15.470	
	∞	1.463	0.843	0.293	
4	1.000	0.233	0.673	1.082	2.240
	1.111	0.209	0.742	0.967	2.414
	1.250	0.184	0.829	0.853	2.630
	1.429	0.160	0.941	0.741	2.907
	1.667	0.136	1.089	0.630	3.273
	2.000	0.112	1.295	0.520	3.782
	2.500	0.089	1.604	0.412	4.543
	3.333	0.066	2.117	0.306	5.805
	5.000	0.043	3.142	0.201	8.319
	10.000	0.021	6.209	0.099	15.837
	∞	1.501	0.978	0.613	0.211
n	R_L/R_S	L_1	C_2	L_3	C_4

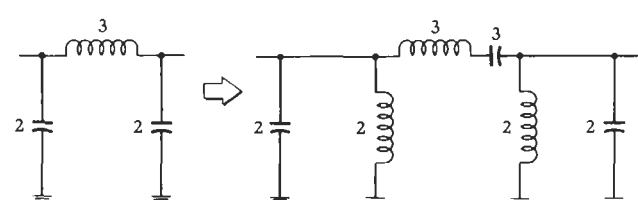
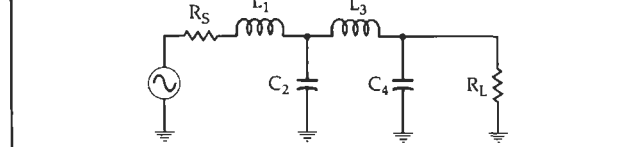


Fig. 3-29. Low-pass to bandpass circuit transformation.

circuits, and all series elements become series-resonant circuits. This process is illustrated in Fig. 3-30.

To complete the design, the transformed filter is

Table 3-8B. Bessel Low-Pass Prototype Element Values

n	R _s · R _L	C ₁	L ₂	C ₃	L ₄	C ₅	L ₆	C ₇
5	1.000	0.174	0.507	0.804	1.111	2.258		
	0.900	0.193	0.454	0.889	0.995	2.433		
	0.800	0.215	0.402	0.996	0.879	2.650		
	0.700	0.245	0.349	1.132	0.764	2.927		
	0.600	0.284	0.298	1.314	0.651	3.295		
	0.500	0.338	0.247	1.567	0.538	3.808		
	0.400	0.419	0.196	1.946	0.427	4.573		
	0.300	0.555	0.146	2.577	0.317	5.843		
	0.200	0.825	0.096	3.835	0.210	8.375		
	0.100	1.635	0.048	7.604	0.104	15.949		
	∞	1.513	1.023	0.753	0.473	0.162		
6	1.000	0.137	0.400	0.639	0.854	1.113	2.265	
	1.111	0.122	0.443	0.573	0.946	0.996	2.439	
	1.250	0.108	0.496	0.508	1.060	0.881	2.655	
	1.429	0.094	0.564	0.442	1.207	0.767	2.933	
	1.667	0.080	0.655	0.378	1.402	0.653	3.300	
	2.000	0.067	0.782	0.313	1.675	0.541	3.812	
	2.500	0.053	0.973	0.249	2.084	0.429	4.577	
	3.333	0.040	1.289	0.186	2.763	0.319	5.847	
	5.000	0.026	1.289	0.123	4.120	0.211	8.378	
	10.000	0.013	3.815	0.061	8.186	0.105	15.951	
	∞	1.512	1.033	0.813	0.607	0.379	0.129	
7	1.000	0.111	0.326	0.525	0.702	0.869	1.105	2.266
	0.900	0.122	0.292	0.582	0.630	0.963	0.990	2.440
	0.800	0.137	0.259	6.652	0.559	1.080	0.875	2.656
	0.700	0.156	0.226	0.743	0.487	1.231	0.762	2.932
	0.600	0.182	0.193	0.863	0.416	1.431	0.649	3.298
	0.500	0.217	0.160	1.032	0.346	1.711	0.537	3.809
	0.400	0.270	0.127	1.285	0.276	2.130	0.427	4.572
	0.300	0.358	0.095	1.705	0.206	2.828	0.318	5.838
	0.200	0.534	0.063	2.545	0.137	4.221	0.210	8.362
	0.100	1.061	0.031	5.062	0.068	8.397	0.104	15.917
	∞	1.509	1.029	0.835	0.675	0.503	0.311	0.105
n	R _L /R _s	L ₁	C ₂	L ₃	C ₄	L ₅	C ₆	L ₇

then frequency- and impedance-scaled using the following formulas. For the parallel-resonant branches,

$$C = \frac{C_n}{2\pi RB} \quad (\text{Eq. 3-16})$$

$$L = \frac{RB}{2\pi f_o^2 L_n} \quad (\text{Eq. 3-17})$$

and, for the series-resonant branches,

$$C = \frac{B}{2\pi f_o^2 C_n R} \quad (\text{Eq. 3-18})$$

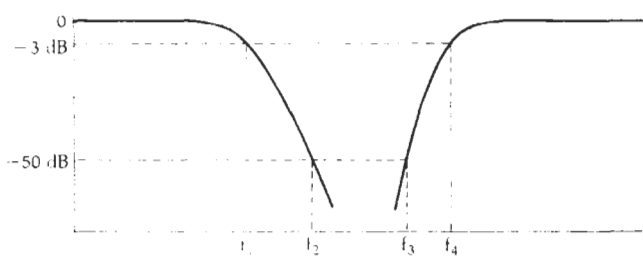


Fig. 3-30. Typical band-rejection filter curves.

$$L = \frac{RL_n}{2\pi B} \quad (\text{Eq. 3-19})$$

where, in all cases,

R = the final load impedance,

B = the 3-dB bandwidth of the final design,

f_o = the geometric center frequency of the final design,

L_n = the normalized inductor *bandpass* element values,

C_n = the normalized capacitor *bandpass* element values.

Example 3-9 furnishes one final example of the procedure for designing a bandpass filter.

SUMMARY OF THE BANDPASS FILTER DESIGN PROCEDURE

1. Transform the bandpass requirements into an equivalent low-pass requirement using Equation 3-14.
2. Refer to the low-pass attenuation curves provided in order to find a response that meets the requirements of Step 1.
3. Find the corresponding low-pass prototype and write it down.
4. Transform the low-pass network into a bandpass configuration.
5. Scale the bandpass configuration in both impedance and frequency using Equations 3-16 through 3-19.

BAND-REJECTION FILTER DESIGN

Band-rejection filters are very similar in design approach to the bandpass filter of the last section. Only, in this case, we want to *reject* a certain group of frequencies as shown by the curves in Fig. 3-30.

The band-reject filter lends itself well to the low-pass prototype design approach using the same procedures as were used for the bandpass design. First, define the bandstop requirements in terms of the low-pass attenuation curves. This is done by using the inverse of Equation 3-14. Thus, referring to Fig. 3-30, we have:

$$\frac{BW_e}{BW} = \frac{f_4 - f_1}{f_3 - f_2}$$

This sets the attenuation characteristic that is needed and allows you to read directly off the low-pass attenuation curves by substituting BW_e/BW for f_e/f on the normalized frequency axis. Once the number of elements that are required in the low-pass prototype circuit is determined, the low-pass network is transformed into a band-reject configuration as follows:

Each shunt element in the low-pass prototype circuit is replaced by a shunt *series-resonant circuit*, and each series-element is replaced by a series *parallel-resonant circuit*.

EXAMPLE 3-9

Design a bandpass filter with the following requirements:

$$f_o = 75 \text{ MHz}$$

$$BW_{3dB} = 7 \text{ MHz}$$

$$BW_{15dB} = 35 \text{ MHz}$$

$$\text{Passband Ripple} = 1 \text{ dB}$$

$$R_s = 50 \text{ ohms}$$

$$R_L = 100 \text{ ohms}$$

Solution

Using Equation 3-14:

$$\frac{BW_{15dB}}{BW_{3dB}} = \frac{35}{7} \\ = 5$$

Substitute this value for f/f_c in the low-pass attenuation curves for the 1-dB-ripple Chebyshev response shown in Fig. 3-18. This reveals that a 3-element filter will provide about 50 dB of attenuation at an $f/f_c = 5$, which is more than adequate. The corresponding element values for this filter can be found in Table 3-7 for an $R_s/R_L = 0.5$ and an $n = 3$. This yields the low-pass prototype circuit of Fig. 3-32A which is transformed into the bandpass prototype circuit of Fig. 3-32B. Finally, using Equations 3-16 through 3-19, we obtain the final circuit that is shown in Fig. 3-32C. The calculations follow. Using Equations 3-16 and 3-17:

$$C_1 = \frac{4.431}{2\pi(100)(7 \times 10^6)} \\ = 1007 \text{ pF}$$

$$L_1 = \frac{(100)(7 \times 10^6)}{2\pi(75 \times 10^6)^2(4.431)} \\ = 4.47 \text{ nH}$$

Using Equations 3-18 and 3-19:

$$C_2 = \frac{7 \times 10^6}{2\pi(75 \times 10^6)^2(0.817)100} \\ = 2.4 \text{ pF}$$

$$L_2 = \frac{(100)(0.817)}{2\pi(7 \times 10^6)} \\ = 1.86 \mu\text{H}$$

Similarly,

$$C_3 = 504 \text{ pF}$$

$$L_3 = 8.93 \text{ nH}$$

This is shown in Fig. 3-31. Note that both elements in each of the resonant circuits have the same normalized value.

Once the prototype circuit has been transformed into its band-reject configuration, it is then scaled in impedance and frequency using the following formulas. For all series-resonant circuits:

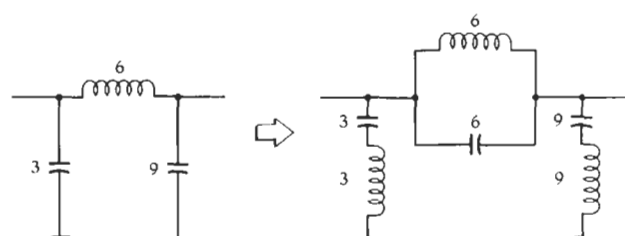


Fig. 3-31. Low-pass to band-reject transformation.

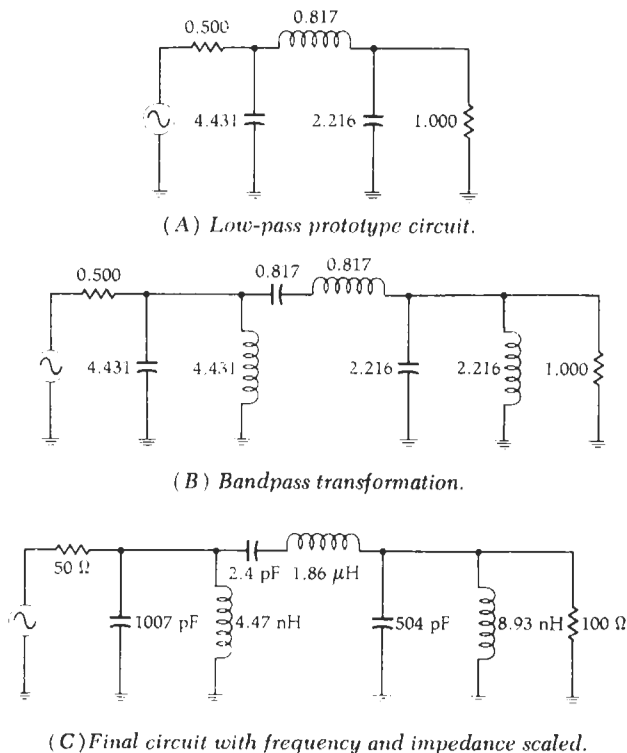


Fig. 3-32. Bandpass filter design for Example 3-9.

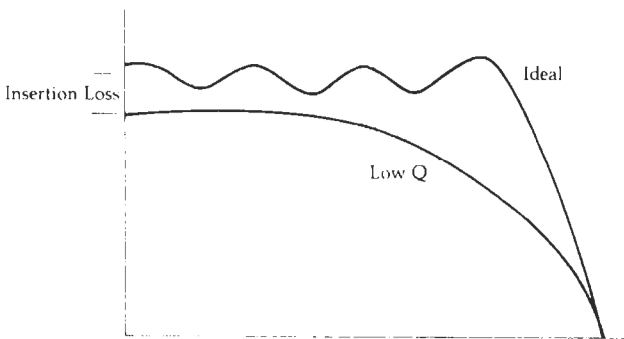


Fig. 3-33. The effect of finite-Q elements on filter response.

$$C = \frac{C_n}{2\pi RB} \quad (\text{Eq. 3-20})$$

$$L = \frac{RB}{2\pi f_o^2 L_n} \quad (\text{Eq. 3-21})$$

For all parallel-resonant circuits:

$$C = \frac{B}{2\pi f_o^2 RC_n} \quad (\text{Eq. 3-22})$$

$$L = \frac{RL_n}{2\pi B} \quad (\text{Eq. 3-23})$$

where, in all cases,

B = the 3-dB bandwidth,

R = the final load resistance,

f_o = the geometric center frequency,

C_n = the normalized capacitor band-reject element value,

L_n = the normalized inductor band-reject element value.

THE EFFECTS OF FINITE Q

Thus far in this chapter, we have assumed the inductors and capacitors used in the designs to be lossless. Indeed, all of the response curves presented in this chapter are based on that assumption. But we know from our previous study of Chapters 1 and 2 that even though capacitors can be approximated as having infinite Q , inductors cannot, and the effects of the finite- Q inductor must be taken into account in any filter design.

The use of finite element Q in a design intended for lossless elements causes the following unwanted effects (refer to Fig. 3-33):

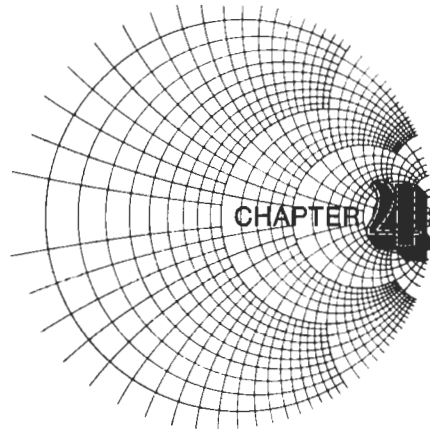
1. Insertion loss of the filter is increased whereas the final stopband attenuation does not change. The relative attenuation between the two is decreased.
2. At frequencies in the vicinity of cutoff (f_c), the response becomes more rounded and usually results in an attenuation greater than the 3 dB that was originally intended.
3. Ripple that was designed into the passband will be reduced. If the element Q is sufficiently low, ripple will be totally eliminated.
4. For band-reject filters, the attenuation in the stopband becomes finite. This, coupled with an increase in *passband* insertion loss, decreases the relative attenuation significantly.

Regardless of the gloomy predictions outlined above, however, it is possible to design filters, using the approach outlined in this chapter, that very closely resemble the ideal response of each network. The key is to use the highest- Q inductors available for the given task. Table 3-9 outlines the recommended minimum element- Q requirements for the filters presented in this chapter. Keep in mind, however, that anytime a low- Q component is used, the actual attenuation response of the network strays from the ideal response to a degree depending upon the element Q . It is, therefore, highly recommended that you make it a habit to use only the highest- Q components available.

Table 3-9. Filter Element-Q Requirements

Filter Type	Minimum Element Q Required
Bessel	3
Butterworth	15
0.01-dB Chebyshev	24
0.1-dB Chebyshev	39
0.5-dB Chebyshev	57
1-dB Chebyshev	75

The insertion loss of the filters presented in this chapter can be calculated in the same manner as was used in Chapter 2. Simply replace each reactive element with resistor values corresponding to the Q of the element and, then, exercise the voltage division rule from source to load.



IMPEDANCE MATCHING

Impedance matching is often necessary in the design of rf circuitry to provide the maximum possible transfer of power between a source and its load. Probably the most vivid example of the need of such a transfer of power occurs in the front end of any sensitive receiver. Obviously, any *unnecessary* loss in a circuit that is already carrying extremely small signal levels simply cannot be tolerated. Therefore, in most instances, extreme care is taken during the initial design of such a front end to make sure that each device in the chain is matched to its load.

In this chapter, then, we will study several methods of matching a given source to a given load. This will be done both numerically and with the aid of the Smith Chart and, in both cases, exact step-by-step procedures will be presented making any calculations as painless as possible.

BACKGROUND

There is a well-known theorem which states that, for *dc circuits*, maximum power will be transferred

from a source to its load if the *load resistance* equals the *source resistance*. A simple proof of this theorem is given by the calculations and the sketches shown in Fig. 4-1. In the calculation, for convenience, the source is normalized for a resistance of one ohm and a source voltage of one volt.

In dealing with ac or time-varying waveforms, however, that same theorem states that the maximum transfer of power, from a source to its load, occurs when the *load impedance* (Z_L) is equal to the *complex conjugate* of the *source impedance*. Complex conjugate simply refers to a complex impedance having the same *real part* with an opposite reactance. Thus, if the source impedance were $Z_s = R + jX$, then its complex conjugate would be $Z_s^* = R - jX$.

If you followed the mathematics associated with Fig. 4-1, then it should be obvious why maximum transfer of power does occur when the load impedance is the complex conjugate of the source. This is shown schematically in Fig. 4-2. The source (Z_s), with a series reactive component of $+jX$ (an inductor), is driving its complex conjugate load impedance con-

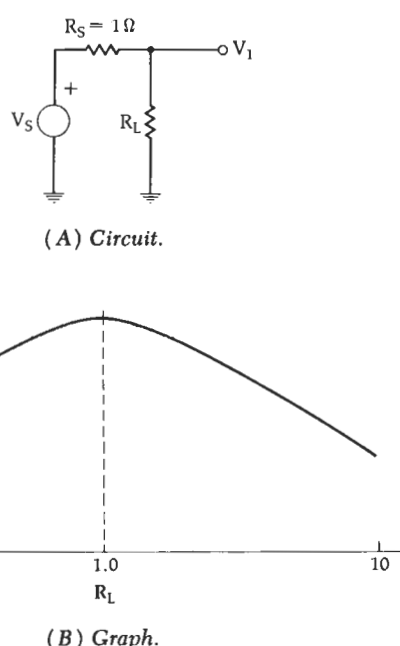


Fig. 4-1. The power theorem.

Proof that $P_{out \ MAX}$ occurs when $R_L = R_s$, in the circuit of Fig. 4-1A, is given by the formula:

$$V_1 = \frac{R_L}{R_s + R_L} (V_s)$$

Set $V_s = 1$ and $R_s = 1$, for convenience. Therefore,

$$V_1 = \frac{R_L}{1 + R_L}$$

Then, the power into R_L is:

$$\begin{aligned} P_1 &= \frac{V_1^2}{R_L} \\ &= \frac{\left(\frac{R_L}{1 + R_L}\right)^2}{R_L} \\ &= \frac{R_L}{(1 + R_L)^2} \end{aligned}$$

If you plot P_1 versus R_L , as in the preceding equation, the result is shown by the curve of the graph in Fig. 4-1B.

sisting of a $-jX$ reactance (capacitor) in series with R_L . The $+jX$ component of the source and the $-jX$ component of the load are in series and, thus, cancel each other, leaving only R_S and R_L , which are equal by definition. Since R_S and R_L are equal, maximum power transfer will occur. So when we speak of a source driving its complex conjugate, we are simply referring to a condition in which any *source* reactance is resonated with an equal and opposite *load* reactance; thus, leaving only equal resistor values for the source and the load terminations.

The primary objective in any impedance *matching* scheme, then, is to force a load impedance to "look like" the complex conjugate of the source impedance so that maximum power may be transferred to the load. This is shown in Fig. 4-3 where a load impedance of $2 - j6$ ohms is transformed by the impedance matching network to a value of $5 + j10$ ohms. Therefore, the source "sees" a load impedance of $5 + j10$ ohms, which just happens to be its complex conjugate. It should be noted here that because we are dealing with *reactances*, which are frequency dependent, the *perfect* impedance match can occur only at one frequency. That is the frequency at which the $+jX$ component exactly equals the $-jX$ component and, thus, cancellation or resonance occurs. At all other frequencies removed from the matching center frequency, the impedance match becomes progressively worse and eventually nonexistent. This can be a problem in broadband circuits where we would ideally like to provide a perfect match everywhere within the broad passband. There are methods, however, of increasing the bandwidth of the match and a few of these methods will be presented later in this chapter.

There are an infinite number of possible networks which could be used to perform the impedance matching function of Fig. 4-3. Something as simple as a 2-element LC network or as elaborate as a 7-element filter, depending on the application, would work equally well. The remainder of this chapter is devoted to providing you with an insight into a few of those infinite possibilities. After studying this chapter, you should be able to match almost any two complex loads with a minimum of effort.

THE L NETWORK

Probably the simplest and most widely used matching circuit is the L network shown in Fig. 4-4. This circuit receives its name because of the component orientation which resembles the shape of an L. As shown in the sketches, there are four possible arrangements of the two L and C components. Two of the arrangements (Figs. 4-4A and 4-4B) are in a low-pass configuration while the other two (Figs. 4-4C and 4-4D) are in a high-pass configuration. Both of these circuits should be recognized from Chapter 3.

Before we introduce equations which can be used to design the matching networks of Fig. 4-4, let's first

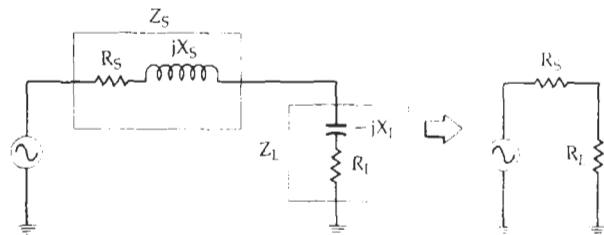


Fig. 4-2. Source impedance driving its complex conjugate and the resulting equivalent circuit.

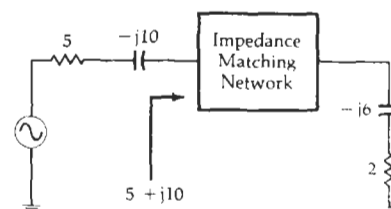
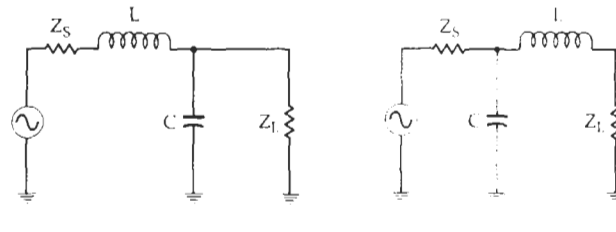
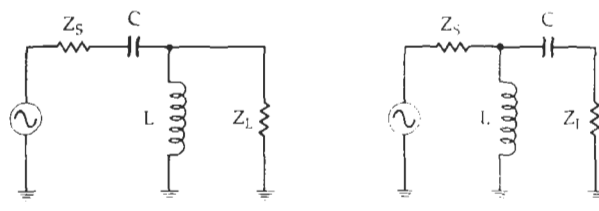


Fig. 4-3. Impedance transformation.



(A) Low-pass.

(B) Low-pass.



(C) High-pass.

(D) High-pass.

Fig. 4-4. The L network.

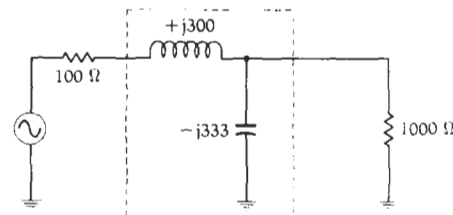


Fig. 4-5. Simple impedance-match network between a 100-ohm source and a 1000-ohm load.

analyze an existing matching network so that we can understand exactly how the impedance match occurs. Once this analysis is made, a little of the "black magic" surrounding impedance matching should subside.

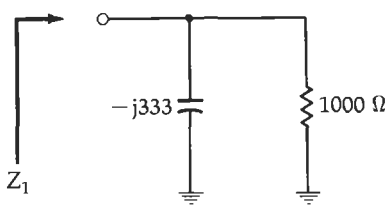


Fig. 4-6. Impedance looking into the parallel combination of R_L and X_c .

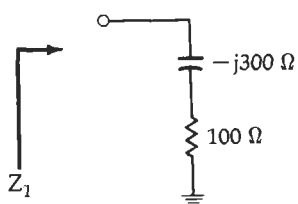


Fig. 4-7. Equivalent circuit of Fig. 4-6.

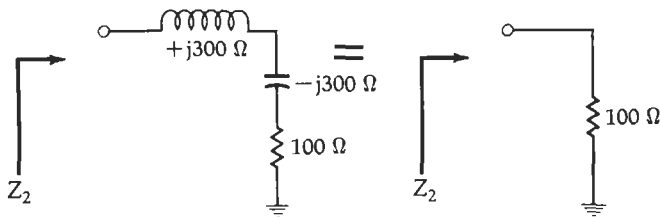


Fig. 4-8. Completing the match.

Fig. 4-5 shows a simple L network impedance-matching circuit between a 100-ohm source and a 1000-ohm load. Without the impedance-matching network installed, and with the 100-ohm source driving the 1000-ohm load directly, about 4.8 dB of the available power from the source would be lost. Thus, roughly one-third of the signal *available* from the source is gone before we even get started. The impedance-matching network eliminates this loss and allows for maximum power transfer to the load. This is done by forcing the 100-ohm source to see 100 ohms when it looks into the impedance-matching network. But how?

If you analyze Fig. 4-5, the simplicity of how the match occurs will amaze you. Take a look at Fig. 4-6. The first step in the analysis is to determine what the load impedance actually looks like when the -j333-ohm capacitor is placed across the 1000-ohm load resistor. This is easily calculated by:

$$\begin{aligned} Z &= \frac{X_c R_L}{X_c + R_L} \\ &= \frac{-j333(1000)}{-j333 + 1000} \\ &= 315 \angle -71.58^\circ \\ &= 100 - j300 \text{ ohms} \end{aligned}$$

Thus, the parallel combination of the -j333-ohm ca-

pacitor and the 1000-ohm resistor *looks like* an impedance of 100 -j300 ohms. This is a *series* combination of a 100-ohm resistor and a -j300-ohm capacitor as shown in Fig. 4-7. Indeed, if you hooked a signal generator up to circuits that are similar to Figs. 4-6 and 4-7, you would not be able to tell the difference between the two as they would exhibit the same characteristics (except at dc, obviously).

Now that we have an *apparent* series 100 -j300-ohm impedance for a load, all we must do to complete the impedance match to the 100-ohm source is to add an equal and opposite (+j300 ohm) reactance in series with the network of Fig. 4-7. The addition of the +j300-ohm inductor causes cancellation of the -j300-ohm capacitor leaving only an apparent 100-ohm load resistor. This is shown in Fig. 4-8. Keep in mind here that the actual network topology of Fig. 4-5 has not changed. All we have done is to analyze small portions of the network so that we can understand the function of each component.

To summarize then, the function of the *shunt* component of the impedance-matching network is to transform a larger impedance down to a smaller value with a real part equal to the real part of the other terminating impedance (in our case, the 100-ohm source). The series impedance-matching element then resonates with or cancels any reactive component present, thus leaving the source driving an apparently equal load for optimum power transfer. So you see, the impedance match isn't "black magic" at all but can be completely explained every step of the way.

Now, back to the *design* of the impedance-matching networks of Fig. 4-4. These circuits can be very easily designed using the following equations:

$$Q_s = Q_p = \sqrt{\frac{R_p}{R_s} - 1} \quad (\text{Eq. 4-1})$$

$$Q_s = \frac{X_p}{R_s} \quad (\text{Eq. 4-2})$$

$$Q_p = \frac{R_p}{X_s} \quad (\text{Eq. 4-3})$$

where, as shown in Fig. 4-9:

Q_s = the Q of the series leg,

Q_p = the Q of the shunt leg,

R_p = the shunt resistance,

X_p = the shunt reactance,

R_s = the series resistance,

X_s = the series reactance.

The quantities X_p and X_s may be either capacitive or inductive reactance but each must be of the opposite type. Once X_p is chosen as a capacitor, for example, X_s must be an inductor, and vice-versa. Example 4-1 illustrates the procedure.

DEALING WITH COMPLEX LOADS

The design of Example 4-1 was used for the simple case of matching two *real* impedances (pure resis-

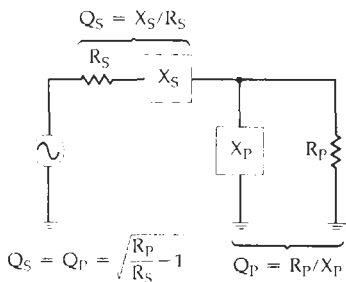


Fig. 4-9. Summary of the L-network design.

EXAMPLE 4-1

Design a circuit to match a 100-ohm source to a 1000-ohm load at 100 MHz. Assume that a dc voltage must also be transferred from the source to the load.

Solution

The need for a dc path between the source and load dictates the need for an inductor in the series leg, as shown in Fig. 4-4A. From Equation 4-1, we have:

$$\begin{aligned} Q_s &= Q_p = \sqrt{\frac{1000}{100} - 1} \\ &= \sqrt{9} \\ &= 3 \end{aligned}$$

From Equation 4-2, we get:

$$\begin{aligned} X_s &= Q_s R_s \\ &= (3)(100) \\ &= 300 \text{ ohms (inductive)} \end{aligned}$$

Then, from Equation 4-3,

$$\begin{aligned} X_p &= \frac{R_p}{Q_p} \\ &= \frac{1000}{3} \\ &= 333 \text{ ohms (capacitive)} \end{aligned}$$

Thus, the component values at 100 MHz are:

$$\begin{aligned} L &= \frac{X_s}{\omega} \\ &= \frac{300}{2\pi(100 \times 10^6)} \\ &= 477 \text{ nH} \\ C &= \frac{1}{\omega X_p} \\ &= \frac{1}{2\pi(100 \times 10^6)(333)} \\ &= 4.8 \text{ pF} \end{aligned}$$

This yields the circuit shown in Fig. 4-10. Notice that what you have done is to design the circuit that was previously given in Fig. 4-5 and, then, analyzed.

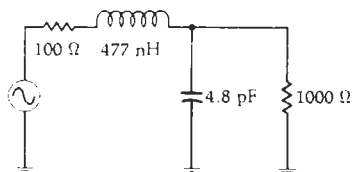


Fig. 4-10. Final circuit for Example 4-1.

tances). It is very rare when such an occurrence actually exists in the real world. Transistor input and output impedances are almost always *complex*; that is they contain both resistive and reactive components ($R \pm jX$). Transmission lines, mixers, antennas, and most other sources and loads are no different in that respect. Most will always have some reactive component which must be dealt with. It is, therefore, necessary to know how to handle these stray reactances and, in some instances, to actually put them to work for you.

There are two basic approaches in handling complex impedances:

1. Absorption—To actually absorb any stray reactances into the impedance-matching network itself. This can be done through prudent placement of each matching element such that element capacitors are placed in parallel with stray capacitances, and element inductors are placed in series with any stray inductances. The *stray* component values are then subtracted from the *calculated* element values leaving new element values (C' , L'), which are smaller than the calculated element values.
2. Resonance—To resonate any stray reactance with an equal and opposite reactance at the frequency of interest. Once this is done the matching network design can proceed as shown for two pure resistances in Example 4-1.

Of course, it is possible to use both of the approaches outlined above at the same time. In fact, the majority of impedance-matching designs probably do utilize a little of both. Let's take a look at two simple examples to help clarify matters.

Notice that nowhere in Example 4-2 was a *conjugate* match even mentioned. However, you can rest assured that if you perform the simple analysis outlined in the previous section of this chapter, the impedance looking into the matching network, as seen by the source, will be $100 - j126$ ohms, which is indeed the complex conjugate of $100 + j126$ ohms.

Obviously, if the *stray* element values are larger than the calculated element values, absorption cannot take place. If, for instance, the *stray* capacitance of Fig. 4-11 were 20 pF, we could not have added a *shunt* element capacitor to give us the total needed shunt capacitance of 4.8 pF. In a situation such as this, when absorption is not possible, the concept of resonance coupled with absorption will often do the trick.

Examples 4-2 and 4-3 detail some very important concepts in the design of impedance-matching networks. With a little planning and preparation, the design of simple impedance-matching networks between complex loads becomes a simple number-crunching task using elementary algebra. Any stray reactances present in the source and load can usually be absorbed in the matching network (Example 4-2), or they can